Russian Original Vol. 34, No. 3, March, 1973

September, 1973

SATEAZ 34(3) 193-304 (1973)

SOVIET ATOMIC ENERGY

АТОМНАЯ ЭНЕРГИЯ
(ATOMNAYA ÉNERGIYA)

TRANSLATED FROM RUSSIAN

CONSULTANTS BUREAU, NEW YORK

SOVIET ATOMIC ENERGY

Soviet Atomic Energy is a cover-to-cover translation of *Atomnaya Énergiya*, a publication of the Academy of Sciences of the USSR.

An arrangement with Mezhdunarodnaya Kniga, the Soviet book export agency, makes available both advance copies of the Russian journal and original glossy photographs and artwork. This serves to decrease the necessary time lag between publication of the original and publication of the translation and helps to improve the quality of the latter. The translation began with the first issue of the Russian journal.

Consultants Bureau journals appear about six months after the publication of the original Russian issue. For bibliographic accuracy, the English issue published by Consultants Bureau carries the same number and date as the original Russian from which it was translated. For example, a Russian issue published in December will appear in a Consultants Bureau English translation about the following June, but the translation issue will carry the December date. When ordering any volume or particular issue of a Consultants Bureau journal, please specify the date and, where applicable, the volume and issue numbers of the original Russian. The material you will receive will be a translation of that Russian volume or issue.

Subscription
$80 per volume (6 Issues)
2 volumes per year
(Add $5 for orders outside the United States and Canada.)

Single Issue: $30
Single Article: $15

CONSULTANTS BUREAU, NEW YORK AND LONDON

227 West 17th Street
New York, New York 10011

Davis House
8 Scrubs Lane
Harlesden, NW10 6SE
England

Published monthly. Second-class postage paid at Jamaica, New York 11431.

SOVIET ATOMIC ENERGY

A translation of *Atomnaya Énergiya*
September, 1973

Volume 34, Number 3 March, 1973

CONTENTS

CONTENTS

(continued)

Engl./Russ.

The Russian press date (podpisano k pechati) of this issue was 3/1/1973. Publication therefore did not occur prior to this date, but must be assumed to have taken place reasonably soon thereafter.

ON THE OCCASION OF THE SIXTIETH BIRTHDAY OF ACADEMICIAN GEORGII NIKOLAEVICH FLEROV

The editorial staff of the periodical Atomnaya Énergiya warmly greets Academician Georgii Nikolaevich Flerov on the occasion of his sixtieth birthday, and wishes him excellent health, long life, and new creative successes.

Translated from Atomnaya Énergiya, Vol. 34, No. 3, p. 145, March, 1973.

ON THE OCCASION OF THE SIXTIETH BIRTHDAY OF IGOR' NIKOLAEVICH GOLOVIN

I. N. Golovin was born in Moscow on March 12, 1913. He graduated from the Physics Department of Moscow State University in 1936. His graduation thesis, The Present Status of the Theory of Nuclear Forces, was recognized as outstanding. In the years 1936-1939, Golovin was a graduate student under the supervision of I. E. Tamm. For his work on the theory of vacuum polarization, he was awarded the learned degree of candidate in physical and mathematical sciences. After completing his graduate work, he took a teaching position at the Moscow Aviation Institute.

During the first years of the war, Golovin was enrolled in the local home guard. He was later assigned to Alma-Ata, where the Aviation Institute had been evacuated. There, in addition to his teaching duties, he carried on scientific work at the Physics and Engineering Institute of the Ukrainian SSR Academy of Sciences, which was also located at Alma-Ata during the period.

In 1944, I. V. Kurchatov invited Golovin to take part in work connected with the production of atomic energy. For the next eight years he served as the first assistant director of the Institute of Atomic Energy. Work on controlled thermonuclear fusion was in progress from the very outset at the Institute, and Golovin became involved in that research, and soon became director of the OGRA thermonuclear division, which was set up under I. V. Kurchatov's instructions.

Translated from Atomnaya Énergiya, Vol. 34, No. 3, p. 146, March, 1973.

Golovin was the initiator of a broad program of research involving storage and confinement of plasma in open-ended magnetic traps, based on the concept put forth by Academician G. I. Budker. Under Golovin's guidance, the large experimental machines OGRA-1, OGRA-2, and OGRA-3 were built, work went forward on ultradeep vacuum in large volumes, and injectors of high-intensity streams of hydrogen ions and atoms were devised.

The experimental and theoretical research carried out under Golovin's supervision played a major role in the development of techniques for generating plasma and controlling high-temperature plasma, and in the understanding of the processes at work, and exerted a substantial influence on the development of thermonuclear reactor concepts and thermonuclear powder-generating station concepts.

High-output injector projects being worked out in Golovin's division are also of great importance in the thermonuclear research program.

The administration of the Institute of Atomic Energy and the editorial staff of the periodical Atomnaya Énergiya warmly greet this fellow-member of the editorial staff, Doctor of Physical and Mathematical Sciences, Professor Igor' Nikolaevich Golovin, on the occasion of his sixtieth birth, and wish him excellent health, long years of life, and new creative successes.

ARTICLES

DEVELOPMENT OF FUEL ELEMENTS FOR FAST POWER REACTORS

I. S. Golovnin, Yu. K. Bibilashvili, and T. S. Men'shikova

UDC 621.039.54

The main stages in the development of sodium-cooled fast power reactors in the USSR are: the successful operation of the BR-5 reactor, reconstructed now into the BR-10 reactor; the development and start-up of the BOR-60 reactor, reaching nominal power in 1971; the completion of the construction of the BN-350 experimental industrial reactor; the construction of the BN-600 reactor [1-4]. The experimental data accumulated in the course of this program permit the development and construction of large-scale industrial installations with fast reactors. Scientists in many countries have estimated that the optimum electric power per unit lies in the 1000-2000 MW range. Practically all sodium-cooled fast reactor subassemblies were difficult to complete because of technical innovations and lack of adequate experience in related fields of technology. This kind of installation requires heavy-duty sodium pumps and heat exchangers, steam generators, strong large-scale reactor vessels, turbogenerators, etc.

The development of fuel elements for fast reactors requires serious efforts. Studies of the nuclear physics, chemical–metallurgical, and technological characteristics of a number of fuel materials and possible structural materials have sufficed to determine the direction of development of fuel elements for the core and breeding blanket of sodium-cooled fast reactors for the next 10-15 years. Austenitic stainless steel is the most suitable material for fuel-element cladding and will be the basic structural material during the next decade.

Fast reactors use uranium oxide and uranium–plutonium fuel because of its good compatibility with structural materials and the sodium coolant, its good radiation resistance, and the simplicity of its production technology. It is appropriate to note that the development of oxide fuel elements for fast reactors started in the Soviet Union on the basis of the experimental work on the BR-5 reactor, and has been taken as basic by all European countries including France, England, and Italy, and at the present time the USA also. The use of oxide fuel avoids a number of difficulties connected with the production of reliably operating fuel elements, and accelerates the accumulation of fast reactor operating experience and data on which the design of large-scale power systems can be based. This facilitates a possible subsequent shift to carbide, nitride, or carbonitride fuel, and finally to the most alluring – metallic fuel – if favorable scientific solutions are found.

The development of oxide fuel element designs permitting a burnup of up to 10% of the heavy atoms for linear specific loadings up to 600 W/cm and cladding operating temperature of the order of 700°C is itself a difficult problem. The lack of experimental arrangements permitting the production of actual operating conditions of the fuel elements (irradiation by an integrated flux of more than 10^{23} fast neutrons/cm^2, dynamics of burnup, etc.) led to a somewhat belated discovery of such phenomena as the iodine–cesium interaction of the core with the cladding, and the embrittlement and swelling of steel under high radiation doses. These phenomena have still not been adequately investigated quantitatively and so far there is no possibility of completely correcting earlier designs. However, there existence has not stopped the development of oxide-fueled sodium-cooled reactors started earlier. Studies have enabled us to understand the processes occurring in cores of oxide fuel elements at high burnups and huge temperature gradients, including the mechanical interaction of the core and cladding, and to produce a dynamic model of these processes serving as a basis for fuel-element calculations.

Translated from Atomnaya Énergiya, Vol. 34, No. 3, pp. 147-153, March, 1973. Original article submitted September 14, 1972.

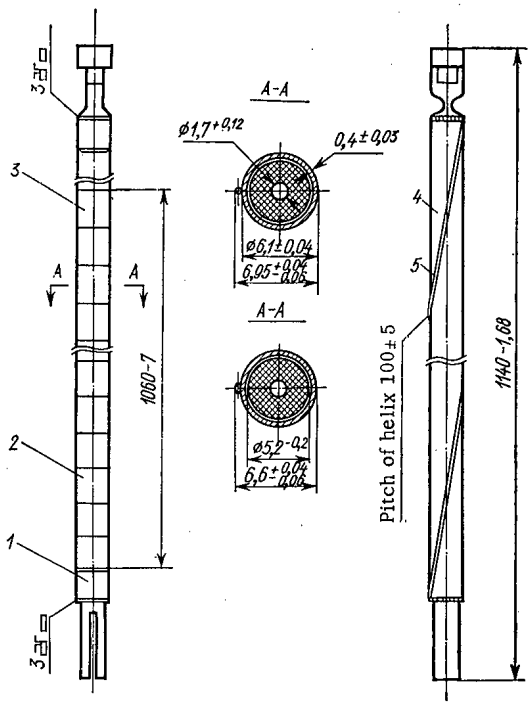

Fig. 1. Core fuel element design for loading of BN-350 reactor: 1) lower cap; 2) sleeve; 3) upper cap; 4) cladding; 5) wire.

Our basic ideas consist of the following [5-7]:

1. After a burnup of more than 3% of the heavy atoms oxide fuel elements with loadings of 500-600 W/cm are practically completely (more than 80-90%) free of gaseous fission products. Thus swelling is a minimum as compared with other forms of fuel. The volume of uranium dioxide and mixed uranium and plutonium oxides increases 1% on the average for 1% burnup, while for loadings of ~ 200-250 W/cm plutonium dioxide swells 1.5% for 1% burnup.

2. Oxide fuel softens at temperatures above 900°C, its plasticity increasing sharply with temperature. Radiation intensifies this process. In the compact oxide core of a thin fuel rod operating at high linear loadings only the outer 0.15-0.2 mm layer remains rigid and exerts the main mechanical action on the cladding.

3. The high temperature gradients which arise during a change in reactor power cause radial cracks in a compact core. For loadings above ~350 W/cm these cracks are "healed" during steady-state operation by an evaporation—condensation mechanism with mass transfer into the colder part of the core. As a result of radial mass transfer the initial gap between the cladding and core is rather rapidly eliminated under operating conditions until the mechanism of "fragment" swelling is brought into play. In the cold state the gap is determined by the difference in thermal expansions of the materials.

4. During operation an oxide core undergoes structural changes leading to the formation of several characteristic zones: an outer zone with the original structure, an equiaxed grain zone, and a columnar grain zone. The zone boundaries correspond to the radial temperature distribution determining the radial variation of mechanical properties of the core material. The structural changes in the core occur as a result of the formation and migration of mostly large pores inward into the high-temperature zone, forming a central hole or increasing the size of the existing hole during the initial period of irradiation if the fuel element was constructed with a central void. The accumulation of solid fragments has a relatively small effect on structural changes up to 10% burnup.

5. The outer rigid layer of an oxide core must have a uniformly distributed initial porosity to compensate for the swelling of this layer during the accumulation of fission fragments. The mechanism of this process can be explained by the production and diffusion of vacancies in the microscopic regions of the thermal spikes produced in the slowing down of fission fragments. The minimum value of the initial porosity is determined by the required burnup. It is assumed that the increase in volume due to the accumulation of solid fission fragments does not exceed 0.4% for 1% burnup.

6. The mean effective fuel density in a cross section of a fuel element, computed by taking account of the internal porosity of the pellets, the central hole in the core, and the gaps, must be limited to a value, depending on the construction, which prevents melting of the inner portions of the core with subsequent axial mass transfer.

7. The power density in a fuel element is limited to a value which does not cause melting of the central part of the core during the operating period. In this case the contraction of the central hole in the core toward the end of the operating period as swelling occurs under the restrictive action of the cladding is taken into account, as is the lowering of the melting point of the dioxide with poisoning by fission products.

8. The swelling of steel in a neutron field significantly changes the pattern of stress and strain in the fuel element cladding. Estimates based on a design model which assumes that the rate of swelling of the core is independent of the extent of its mechanical interaction with the cladding shows that the swelling of steel has a favorable effect on the efficiency of the central fuel elements of an assembly. The jackets of these fuel elements "escape" from the core, as it were, and the mechanical loadings decrease. Because

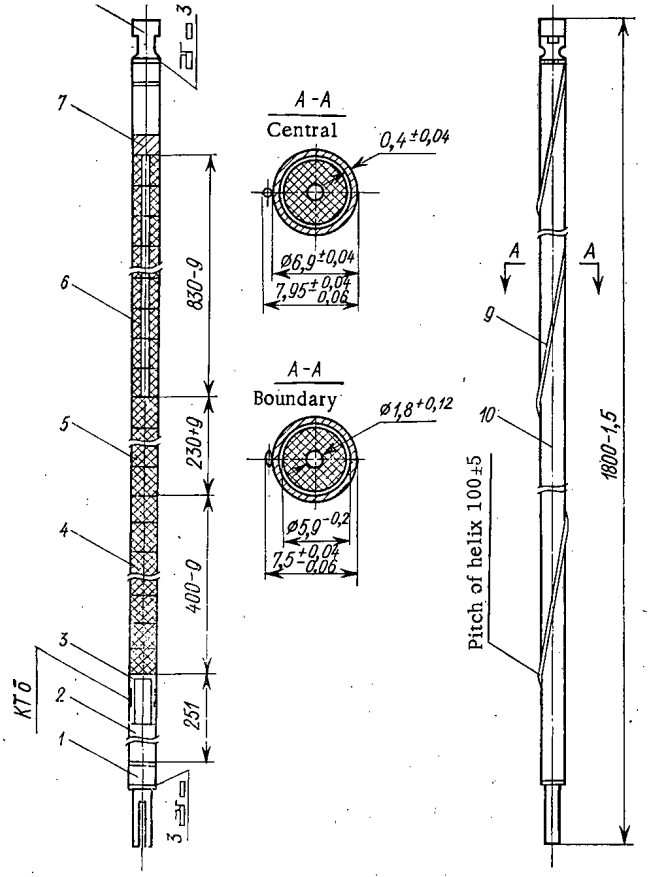

Fig. 2. Core fuel element design for the second loading of the BN-350 reactor: 1) lower cap; 2) gas space; 3) can; 4) lower end shield briquet; 5) core briquet; 6) sleeve; 7) porous plug; 8) upper cap; 9) spacing wire (tape); 10) cladding.

of the nonuniformity of the temperature around the perimeter of the cladding of a fuel element on the periphery of an assembly further stresses arise as a result of the nonuniform swelling of steel. The magnitude of these stresses depends on the temperature of the "rosette." Therefore it is desirable to take measures to decrease the nonuniformity of the temperature around the perimeter of the peripheral fuel elements. In Soviet reactors displacers [6] are introduced into the peripheral cells of an assembly to accomplish this [6].

The ideas presented above can be carried over completely to the operation of a fuel element with a vibrocompacted core of powdered dioxide fuel. The only difference is in the initial period of irradiation during which the powder is sintered into a compact rod with a central hole. For such fuel elements the initial operation of the reactor at power must follow a special program to ensure the solidification of the hollow core without melting.

The safety factor of the cladding was calculated by taking account of the thermal and mechanical stresses from the gas pressure and the swelling of the core. The long-term strength and long-term plasticity were also taken into account, as was the relaxation of stresses [6].

The design of fuel elements for the core of the BN-350 reactor, intended for the first loading, was developed before the calculational and design methods for oxide fuel elements were in final form. However, the ability to operate up to 5% burnup was verified by direct experiment in a sodium loop of the MIR-2 reactor and in the BR-5. The fuel element design is shown in Fig. 1. It consists of a stainless steel tube 6.1 mm in diameter with a wall thickness of 0.55 mm filled with sleeves of sintered uranium dioxide forming a core 1060 mm long. The average effective density in a cross section of the fuel element is 8 g/cm^3. The nominal initial diametral gap between the cladding and the core is 0.3 mm. The ends of the cladding are closed by argon arc welds. There is practically no gas collector. The empty volume in

TABLE 1. Comparative Characteristics of Fuel Element Designs

Characteristics	BN-350 fuel element		BN-600 fuel element
	basic	II variant	
Diameter, mm	6,1	6,9	6,9
Length of active portion, mm	1060	230+830 =1060	90+660=750
Maximum cladding temperature, °C*	680	700	710
Maximum fuel temperature, °C*	1800	2500	2500
Maximum heat loading, W/cm	450	530	530
Maximum burnup,%	5	10	10
Gas pressure at end of operating period, atm	140	100	40
Maximum† tangential strain of cladding,%	0,25	1,8	1,6
Safety factor of cladding (with respect to tension)at end of operating period	1,4	1,37 (1,05 ‡	1,55(1,06 ‡)

*Temperatures indicated for hot spots.
†Calculations performed without taking account of the effect of reactor radiation on material properties.
‡Time to rupture decreased by a factor of 100 in comparison with the properties of steel without taking account of the effect of reactor radiation on them.

the fuel element is made up of the central hole of the core, the gap between the cladding and the core, and the small space in the upper part of the element (20-25 mm) which compensates for the thermal expansion, taking account of the allowance for the height of the core. The spacing of the fuel elements in an assembly is maintained by a helically wound wire.

The design pressure of gases in the fuel element at the end of the operating period is 140 atm, but the safety factor of the cladding remains above one for a maximum cladding temperature of about 680°C at the beginning of the operating period and 650°C at the end. Hexagonal assemblies are formed of 169 fuel elements.

In the second loading of the BN-350 reactor it is proposed to use the more refined core fuel element design shown in Fig. 2. The diameter of the fuel element here is increased to 6.9 mm, and 127 of them can be placed in a hexagonal assembly of the same size, maintaining the loading of the fissionable isotope. A gas space is provided in the lower colder part of the fuel element, and the lower end reflector is combined with the fuel core in a single jacket. This permits a decrease in the pressure of fission product gases inside the cladding to a maximum of 100 atm for 10% burnup of the heavy nuclei. A certain increase in the average temperature of the core decreases its mechanical action on the cladding during swelling. Since this was confirmed on experimental samples irradiated in the SM-2 reactor, the fuel element design developed turned out to be operable to a burnup of 100,000 MW days/ton of UO_2.

It should be noted that the lower 230 mm of the fuel core directly adjoining the end reflector (Fig. 2) is made of solid rather than hollow briquets. The increase in effective fuel density in the cross section of the fuel element achieved in this way leads to an increase in the surface temperature of the briquets and to a decrease in the mechanical action of the core on the cladding in this part. Figure 3 shows the longitudinal distribution of the tangential strain of the fuel element cladding for the second loading. The increase in effective fuel density in the lower part of the fuel element from 75 to 86% of theoretical decreases the strain of the cladding toward the end of the operating period from 2.3 to 1.8%, which significantly increases its operating reserve [7, 8].

An alternative fuel element design provided for the incorporation of both the lower and upper end reflectors into a single jacket. This design was not successful in the BN-350 reactor, however, because of a significant increase in the hydraulic resistance of the assembly. This idea has been employed in the design of a BN-600 fuel element now being developed. One version of this fuel element is shown in Fig. 4. The fuel element was designed for a 10% burnup of heavy nuclei, and can use a fuel core of both uranium dioxide and a $(UPu)O_2$ mixture. The jacket has a large gas space (800 mm) and a "heating" region of the fuel core (90 mm) for decreasing the tangential strain of the cladding. Samples of fuel elements close to the design described are being tested in the BOR-60 reactor at the present time. Table 1 lists the comparative characteristics of the fuel element designs described.

The quality of manufacture of the fuel core has an appreciable effect on the efficiency and operating characteristics of fuel elements. Pelletization is an accepted production process in fuel core manufacture in the USSR and other countries. Rather efficient automatic presses ensuring low production losses have been developed [5, 6, 9]. Although the charging material intended for processing by an automatic press requires more careful preparation to ensure constancy of the bulk density and the duplication of sizes and properties of the individual pellets, the amount of plasticizer acceptable in it is significantly less than in

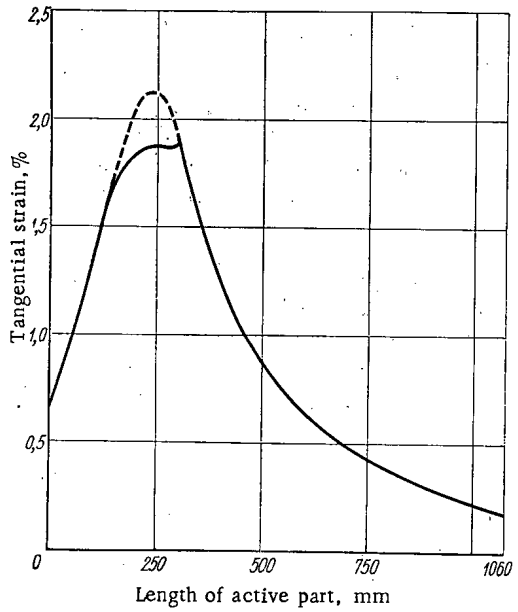

Fig. 3. Tangential strain of cladding along the length of a core fuel element of the BN-350 reactor in which the effective density along a length of 230 mm from the lower end of the active part of the fuel element is: – – – – –) 75% of theoretical; ———) 86% of theoretical.

powders used in other methods of forming oxide cores. This ensures higher quality of the product after sintering: uniform density, correct geometric shape, smaller deviations of dimensions from nominal. The latter permits the omission of the grinding process except to correct pellets rejected, for example, as the result of wear of the pressing device.

A point in favor of the pelletization process is the possibility of using automatic presses with a lubricated pressing device to form "damp" pellets of powder practically without the addition of a plasticizer. This further improves the accuracy of the pellet manufacture and their quality, and permits an increase in the fuel charge in the fuel elements. The optimum technology uses a starting powder with a minimum amount of materials which are eliminated in the sintering process.

Some remarks on the purity of the starting material are in order. In choosing the condition of the uranium dioxide the developer and user generally start from the possibilities of the supplier but try to use the purest product. In principle the supplier can produce a product of any degree of purity, and a high degree of purity may turn out to be economically advantageous to him. An increased contamination of the initial uranium dioxide, particularly by highly volatile admixtures, can affect the quality of the pellets produced, the capacity of the fuel with respect to heavy atoms, and the efficiency of the fuel elements. Not all impurities worsen the working capacity of fuel element cores, however, and the presence of impurities below a certain level has a negligible effect on the fuel element properties. There has been little research on the dependence of the technological properties and radiation stability of fuel elements on the purity of the starting material, yet it is one way of reducing the cost of the fuel cycle.

Another aspect of the problem of quality and economy of the production of ceramic cores is the choice of plasticizer. In our practice the most widely used binders are aqueous solutions of high-molecular alcohols. Plasticizers of this type permit the use of simple technological equipment. However, they are not optimum in at least two respects: first, they require the selection of rather narrow pressure limits in forming pellets; second, they prolong the sintering process because of the difficulty of eliminating moisture.

Anhydrous plasticizers are more suitable: high-molecular fatty acids, their salts (stearates and behanates), particularly if there is a problem of obtaining a given uniform initial porosity in the sintered material [10]. The binding properties of these substances are manifested even for small additions to the charge, and can improve the quality of the production.

The sintering process is the most important technological operation for obtaining products of compact uranium dioxide. It can be performed in a vacuum or in various atmospheres. The most common is sintering in a hydrogeneous atmosphere. This ensures adequate stability of pellet size and properties (density, stoichiometric composition) and guarantees a low carbon content in the product.

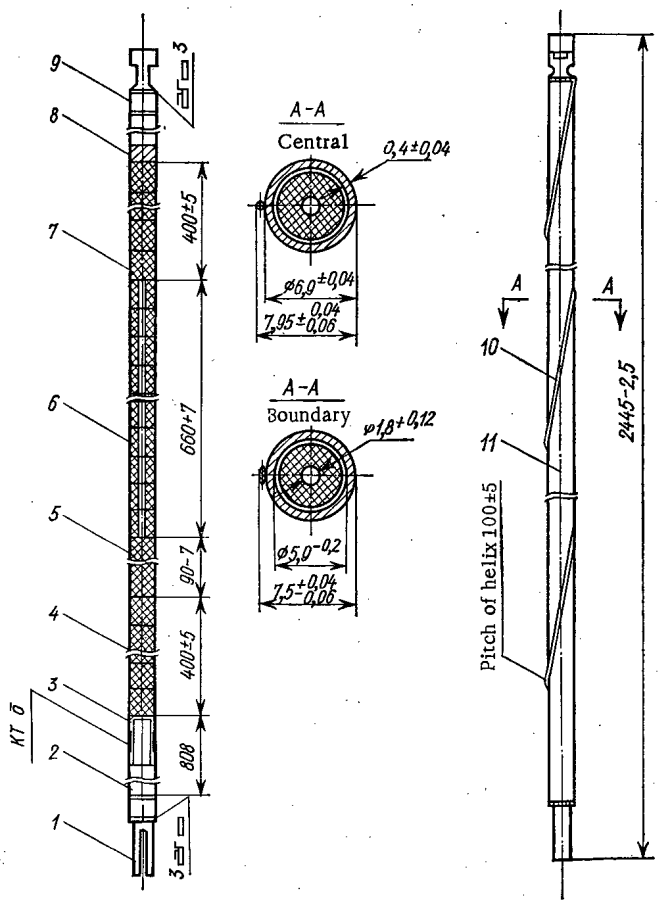

Fig. 4. Alternative design of a fuel element for the core of the BN-600 reactor: 1) lower cap; 2) gas space; 3) can; 4) lower and shield briquet; 5) core briquet; 6) sleeve; 7) upper end shield briquet; 8) porous plug; 9) upper cap; 10) spacing wire (tape); 11) cladding.

Uranium dioxide will be used as core fuel in the first loadings of the BN-350 and BN-600 fast power reactors. After reactors of this type have been mastered the fuel will be mixed oxides (UO_2 + 15-20% PuO_2). It is proposed to make fuel elements of this type by pressing pellets.

The technological process of making fuel elements with cores of mixed-oxide fuel involves certain special features. The first feature has to do with the method of making the original powder. This powder can be obtained either by mechanical mixing of powdered uranium and plutonium oxides, or by coprecipitating them from solutions [11]. Choosing one or the other method requires taking account of the necessity of a uniform distribution of plutonium in the fuel core. A solid solution of plutonium dioxide in uranium dioxide formed by sintering pellets pressed from mechanically mixed powders may have significant nonuniformities in the distribution of components in small volumes, which leads to a large Doppler coefficient of reactivity of the system. Further technological operations to equalize the distribution of concentrations in such fuel may increase the cost of the process. The coprecipitation process and the subsequent firing lead to the formation of crystals of a solid solution of oxides, and the distribution of the fissionable component in such powders is very uniform. It should be kept in mind that the use of coprecipitated mixtures does not require the complete separation of uranium and plutonium in the reprocessing of spent fuel elements, and this may reduce the cost of the external fuel cycle. Of course in the initial phase of production the choice of the method of manufacture of mixed-oxide fuel may be determined by the current possibilities of the manufacturing plants in the country, but for a stabilized process of multiple reprocessing of fuel the method of chemical coprecipitation appears to be preferable.

A second feature of the process of manufacturing pellets of mixed-oxide fuel is the difference in affinities of uranium and plutonium for oxygen and hydrogen. This leads to a significant effect of the atmosphere on the sintering process. In sintering in a reducing atmosphere a two-phase structure of solid solutions is formed in the core with the phase concentrations depending on the sintering regime. A single-phase structure can be obtained by sintering in an oxidizing atmosphere, but the necessity of such a process to improve the radiation stability of the fuel must be confirmed experimentally.

A third feature of the production of mixed oxides is the high toxicity of the product. The presently existing areas for the manufacture of fuel elements with cores containing plutonium dioxide [10] are equipped with glove boxes and provide for carrying out the process manually. However, for large-scale industrial production of plutonium fuel the safety requirements may demand significant corrections and necessitate partial or complete remote control, particularly for multiple reprocessing of fuel. Remote control ordinarily involves an increase in production costs. From our point of view a reasonable mechanization and automation of technological processes will be advantageous in the large scale production of plutonium fuel and for sufficiently developed equipment will permit the elimination of hand work except for brief manual operations to correct faults or replace equipment. This decreases the requirements for high reliability, durability, and dependability of operation which can be demanded of a remote control system reprocessing materials with a biologically dangerous radiation level.

LITERATURE CITED

1. A. I. Leipunskii et al., (USSR) SMEA Symposium on the State and Prospects of Construction of Fast Reactor Power Plants [in Russian], Vol. 1, Obninsk (1967), p. 249.
2. A. I. Leipunskii et al., ibid., p. 123.
3. A. I. Leipunskii et al., Atomnaya Énergiya, 30, No. 2, 165 (1971).
4. A. I. Leipunskii et al., Atomnaya Énergiya, 25, No. 5, 380 (1968).
5. I. S. Golovnin et al., Paper at the Franco-Soviet Symposium on the Development of Fuel Elements for the BOR-60 Reactor [in Russian], Kadarash (1970).
6. A. I. Leipunskii et al., Paper 49/P/460 at the Fourth Geneva Conference [in Russian] (1971).
7. I. S. Golovnin et al., Atomnaya Énergiya, 30, No. 2, 216 (1971).
8. R. Klipot and A. Smolders, Powder Metallurgy, 12, 24, 305 (1969).
9. M. Batler et al., Paper M 88/33 at a Symposium on the Use of Plutonium as a Reactor Fuel [in Russian], Brussels (1967).
10. E. A. Evans et al, Paper P/236 (USA) at the Third Geneva Conference (1964).
11. C. Sory et al., J. Nuclear Mat., 35, 267 (1970).

THE SYSTEM $MoO_3 - UO_3$

O. A. Ustinov, M. A. Andrianov,
N. T. Chebotarev, and G. P. Novoselov

UDC 548.736

An x-ray analysis [1] of the system $UO_2 - UO_3 - MoO_3$, performed on specimens obtained by sintering stoichiometric amounts of uranous–uranic oxide and molybdenum trioxide in vacuum at 750°C, revealed that the reaction of these oxides leads to the formation of $UMoO_6$ and U_2MoO_8. Sintering of uranous–uranic oxide with molybdenum trioxide in air at 750°C leads to the formation of uranyl molybdate UO_2MoO_4 [2]. This compound has a monoclinic structure [3] with the following unit cell constants: a = 7.200 Å, b = 5.480 Å, c = 13.59 Å; β = 104°36'; the space group is $p2_1/c$; the unit cell of this compound contains four formula units.

We have investigated the reaction of MoO_3 and U_3O_8 in air in the range from room temperature to 1000°C in order to construct the phase diagram $MoO_3 - UO_3$. We used x-ray and thermographic analysis for this purpose. Thermographic analysis was performed in an NTR-64 thermorecorder. The standard was MgO. Weighed amounts (0.5 g) of the mixtures were placed in quartz crucibles and heated at a rate of 20°C /min. No reaction of the crucible material with the melt was observed. The temperature was measured by Pt–Pt/Rh thermocouples to within ±5°C. The specimens for x-ray analysis were obtained by heating mixtures of the powdered initial oxides for 4 h at 700°C, after which the sintered mixtures were ground and then reheated under the same conditions. The temperature was measured to within ±10°C by a Chromel–Alumel thermocouple. The x-ray diffraction patterns of the powders thus obtained were recorded in RKU-86 cameras in Co- and Cr-radiation.

We used uranous–uranic oxide (U_3O_8), obtained by heating uranium dioxide in air at 600°C for 10 h, and molybdenum trioxide (MoO_3) of cp grade. The x-ray diffraction patterns of the initial U_3O_8 and MoO_3 powders exhibit only lines of the corresponding phases.

TABLE 1. Temperature of Thermal Effects Recorded on Differential Heating Curves of Mixtures of U_3O_8 and MoO_3

U_3O_8 content of $MoO_3 - U_3O_8$ mixture		Temperature of effects, °C			
wt.%	mole % (in terms of $UO_{2.67}$)	I	II	III	IV
0	0	—	—	800	—
10	5,4	600	740	780	—
17	9,5	610	740	760	—
20	11,4	610	740	760	—
30	18,0	610	740	780	—
40	25,4	610	740	830	—
45	29,5	600	740	860	—
60	43,4	610	740	930	—
70	54,4	600	—	—	980
80	67,2	600	—	—	980
90	82,1	610	—	—	980
100	100	—	—	—	—

TABLE 2. Phase Composition of Mixtures of MoO_3 and U_2O_8 after Heating to 700°C*

U_3O_8 content of $MoO_3 - U_3O_8$ mixture		Phase composition (from x-ray analysis data)
wt. %	mole % (in terms of $UO_{2.67}$)	
10	5,4	MoO_3
20	11,4	MoO_3
30	18,0	$MoO_3 \gg UO_2MoO_4$
40	25,4	$MoO_3 \gg UO_2MoO_4$
50	33,8	$UO_2MoO_4 \gg MoO_3$
60	43,4	UO_2MoO_4 + traces of MoO_3
70	54,4	UO_2MoO_4
80	67,2	$UO_2MoO_4 + U_3O_8$
90	82,1	$U_3O_8 + UO_2MoO_4$
100	100	U_3O_8

*Residence time 8 h.

Translated from Atomnaya Énergiya, Vol. 34, No. 3, pp. 155-157, March, 1973. Original article submitted May 15, 1972.

TABLE 3. Comparison of Interplanar Spacings in the Structures of the Molybdate Investigated by the Authors and UO_2MoO_4 [3]

Indices hkl	Interplanar spacings: authors' data		[3]		Indices hkl	Interplanar spacings: authors' data		[3]	
	I_{vis}*	d, Å	I_{rel}†	d, Å		I_{vis}*	d, Å	I_{rel}†	d, Å
$\bar{1}02$	w	5,53	14	5,51	300	m. w.	2,308	5	2,321
110, $\bar{1}11$	m	4,30	19	4,30	122			7	2,305
012	s	4,20	100	4,20	$\bar{3}12$	m. w.	2,178	4	2,188
111	m	3,921	24	3,915	$\bar{3}04$			1	2,172
200	m	3,471	20	3,480	$\bar{3}13$	m	2,118	10	2,122
$\bar{2}02$			18	3,457	123				
112	m	3,351	11	3,367	311	m	2,030	8	2,036
$\bar{1}13$			12	3,341	302, 016				
004	m	3,288	31	3,286	$\bar{2}14$	w	1,986	4	1,992
210	m	2,927	11	2,933	$\bar{2}16$	m. w.	1,962	4	1,969
$\bar{2}12$					222			2	1,958
$\bar{1}14$	v. w.	2,827	5	2,833	312	w	1,912	4	1,909
014			4	2,820	025	w	1,897	4	1,899
202	v. w.	2,790	5	2,801	$\bar{3}06$, 116	m	1,838	6	1,841
$\bar{2}04$	w	2,753	7	2,762	223	w	1,821	4	1,823
020			2	2,739	031	m	1,793	4	1,809
104	v. w.	2,715	5	2,721	$\bar{4}02$			6	1,800
$\bar{1}21$, 120	m	2,544	10	2,548	017	av.(d)	1,763	1	1,777
$\bar{2}14$	m. w.	2,453	3	2,465	320			5	1,771
$\bar{1}22$			6	2,455	130, 313, $\bar{1}31$			5	1,767

* In this column the following abbreviations are used: w weak, av average, s strong, v. w very weak, and d diffuse.

†Juenke and Bartram [3] determined the reflection intensity I from diffractometric data.

RESULTS

When mixtures of U_3O_8 and MoO_3 are heated in air to 600-1000°C, bright yellow powders or cakes are formed. The differential heating curves of mixtures of the initial oxides exhibit an exoeffect I at approximately 600°C in all cases (Table 1). This effect is not observed on the thermograms after reheating. For sintered mixtures containing up to 60 wt. % U_3O_8 we observe a constant endoeffect II (740°C) and a variable endoeffect III. Effects II and III are also observed when the thermograms of these mixtures are recorded again. Between the compositions of mixtures corresponding to 60 and 70 wt. % U_3O_8 the effect at 740°C disappears and effect IV appears at 980°C.

X-ray analysis revealed formation of a molybdate (Table 2) with a complex structure in this system.

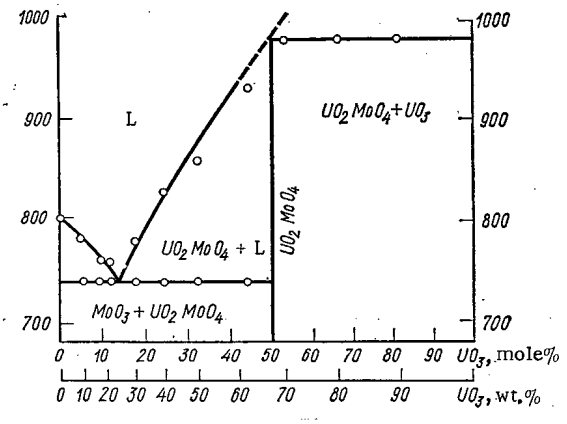

Fig. 1. Phase diagram of the system MoO $-UO_3$.

X-ray analysis showed that this compound is uranyl molybdate UO_2MoO_4, the crystal structure of which was established by Juenke and Bartram [3]. Table 3 gives the interplanar spacings in the molybdate structure, calculated from several leading lines of the x-ray diffraction pattern obtained in Cr-radiation, together with the interplanar spacings in the structure of UO_2MoO_4, taken from [3], for comparison.

DISCUSSION OF RESULTS

According to the x-ray data and visual observations on the change in color of the mixtures during heating, exoeffect I at 600-610°C corresponds to the onset of the reaction of U_3O_8 and MoO_3. When mixtures containing up to 65 wt. % U_3O_8 were heated to 740°C or above, they partly or completely melted. Therefore endoeffect II at 740°C is due to eutectic melting of the mixtures. Endoeffect III is

observed when the mixtures pass completely into the liquid state, i.e., it characterizes the liquidus line of the system. Endoeffect IV at a constant temperature of 980°C is due to peritectic decomposition of UO_2MoO_4, formation of which was established by x-ray analysis. When UO_2MoO_4 is heated in vacuum to 1000°C it decomposes with formation of U_3O_8 and MoO_3. Since the composition UO_2MoO_4 ($UO_3 \cdot MoO_3$) corresponds in the ternary system U–Mo–O to the cross section UO_3-MoO_3, not the cross section $U_3O_8-MoO_3$, we may assume that during the reaction of U_3O_8 and MoO_3 (taken as the initial materials) in air, U_3O_8 is oxidized to UO_3. Therefore our data must be regarded as the result of the reaction of MoO_3 with UO_3.

The phase diagram of the system MoO_3-UO_3 (Fig. 1) was constructed from the thermographic and x-ray data. The diagram exhibits a compound UO_2MoO_4 which melts incongruently at ~980°C; together with MoO_3, this compound gives a eutectic containing ~14.6 wt. % UO_3, the melting point being 740°C. After our experimental work was completed, Serezhkin et al. [4] published their results; these confirmed the data in [3] on the structure of UO_2MoO_4 and agreed with our results.

LITERATURE CITED

1. V. K. Trunov et al., Zh. Neorgan. Khimii, 10, No. 11, 2576 (1965).
2. V. K. Trunov et al., Dokl. Akad. Nauk SSSR, 141, No. 1, 114 (1961).
3. E. Juenke and S. Bartram, Acta Crystal., 17, 618 (1964).
4. V. N. Serezhkin et al., Radiokhimiya, 13, No. 4, 659 (1971).

BUILDUP OF TRANSURANIUM ELEMENTS IN VK-50 REACTOR FUEL

V. Ya. Gabeskiriya, V. S. Belokopytov,
Yu. B. Novikov, V. G. Polyukhov,
V. M. Sarychev, G. A. Simakin,
and A. P. Chetverikov

UDC 621.039.524.4-97:
621.311.25:621.039

In order to find the isotopic composition of irradiated fuel of a water-moderated water-cooled boiling reactor we have experimentally investigated the isotopic composition of irradiated fuel in samples cut from VK-50 reactor fuel elements. We have sought to determine: a) the isotopic composition of uranium, plutonium, and americium after irradiation; b) the amount of plutonium, americium, and curium isotopes produced by irradiation; c) the dependence of buildup of transuranium elements on burnup.

Preparation and Dissolution of Samples

The assembly out of which the fuel element was extracted has been irradiated for 657 effective days and held up for more than a year. The fuel was 2%-enriched uranium dioxide.

Irradiation did not cause any significant structural changes in fuel. The fact that no temperature domains (fusing, formation of acicular or equiaxial grains) have been observed indicates that the temperature of uranium dioxide at the center of the pellet did not exceed 1600°C (Fig. 1). Four samples were cut at different length of the fuel element (Fig. 2) in order to obtain information about the variation of isotopic composition and buildup of transuranium elements with burnup. The weight of the samples was 0.6 to 1 g. The samples were then dissolved in a mixture of concentrated perchloric and nitric acids (heated). The solution was brought up to 100 ml by adding 8 N nitric acid.

EXPERIMENTAL METHOD

Radiometric Analysis. Without chemically separating the transuranium elements, aliquots were taken from the investigated solution and made into targets from which the alpha spectra and total alpha activity were determined. The content of Cm^{242} and Cm^{244} was calculated from the results of alpha spectrometric analysis taking into account the data of absolute alpha count.

The measurements were carried out with the aid of an alpha spectrometer with a silicon semiconductor detector. The Am^{241} line (5486 keV) resolution of the spectrometer was ~40 keV. The absolute activity of targets with alpha emitters was measured with a proportional flow counter of 4π geometry. The accuracy of alpha activity measurements was ±2%. The accuracy of the final results of the determination of Cm^{242} and Cm^{244} content was ±20%.

The fission product content was determined from gamma activity of Cs^{137} and Ce^{144} isotopes using a gamma spectrometer with a coaxial Ge(Li) detector having a volume of 21.7 cm^3 and an active surface area of 6.76 cm^2.

The Ba^{137} line (662 keV) resolution of the gamma spectrometer was ~6.5 keV. The accuracy of determination of Cs^{137} and Ce^{144} content in the samples was not less than 15%.

Determination of Isotopic Content of Uranium, Plutonium, and Americium. To find the isotopic composition of uranium a small amount of the starting solution was deposited on the evaporator of the three-strand ion source of the mass spectrometer.

Translated from Atomnaya Énergiya, Vol. 34, No. 3, pp. 159-162, March, 1973. Original article submitted April 20, 1972.

Fig. 1. Macro- and microstructure of fuel.

For isotopic analysis of plutonium the latter was separated out from the solution and decontaminated of fission elements. Separation and decontamination was done by extraction using a 0.5 M solution of D-2 EHPA [1]. Plutonium was first stabilized in a tetravalent state by a 30% solution of hydrogen peroxide in the presence of 8 N nitric acid by heating in a water bath. Extraction was carried out at a ratio $V_{water} : V_{org} = 1 : 1$ for 2-3 min followed by phase separation.

The water phase containing americium, curium, and fission products was poured off, concentrated to two-three drops by evaporation, and prepared for subsequent americium analysis.

The remaining organic phase was rinsed with 7 N hydrochloric acid to remove any trace of iron. For reextraction we used a 10% solution of ammonium carbonate. The reextract was rinsed with decane and calcinated to remove ammonium salts. The dry residue was dissolved in 1 ml of 8 N nitric acid while heating.

The isotopic composition of uranium, plutonium, and americium was determined using an MI-1311 and a modified MI-1305 mass spectrometers. A three-strand ion source was added to the latter to produce the ion beam. A type SI-01 ion counter was used to record the ion current. A rhenium foil served as an ionizer. The analytic technique was similar to that described in [2].

Determination of the Content of Uranium, Plutonium, and Americium Isotopes. The amount of uranium in the analyzed sample was determined by the Sakhorov method [3], and the content of plutonium and americium isotopes was determined by the method of isotopic dilution. Reference tracers of Pu^{242} and Am^{243} were added to aliquot parts of the analyzed solution. Plutonium and americium were separated chemically after careful mixing. The technique described in [5] was used in further analysis. The content of plutonium and americium was determined in two or more parallel analyses.

RESULTS

Isotope Composition of Uranium, Plutonium, and Americium. The content of uranium, plutonium, and americium in the investigated samples is listed in Table 1, together with the data of radiometric analysis of the content of Cm^{242}, Cm^{244}, Cs^{137}, and Ce^{144}. As seen in Table 1, heavy plutonium isotopes constitute 39% of sample 2.

The error in determination of uranium by the Sakhorov method was ±5%. The accuracy of determination of plutonium by the isotopic dilution method was ±3% and that of americium better than ±5%. The amount of americium in sample No. 4 was estimated from the results of radiometric analysis. The content of transuranium and fission elements was referred to the time the fuel assembly was unloaded from the reactor.

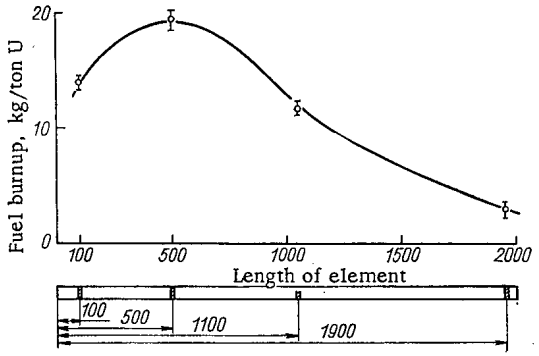

Fig. 2. Burnup distribution along fuel element.

Dependence of Isotopic Composition of Uranium, Plutonium, and Americium on Burnup. The amount of fission products of U^{235}, Pu^{239}, and P^{241} was calculated from the experimental results listed in Table 1. Burnup X due to U^{235} fission was calculated from

$$X = 1000\left[\gamma_0^5 - (\gamma_t^5 + \gamma_t^6)\frac{\gamma_0^8}{\gamma_t^8 + z\omega}\right] \text{kg/ton U}, \quad (1)$$

where γ_0^i and γ_t^i is the relative content of the i-th isotope before and after irradiation (i being the last digit of the mass number of the given isotope), and z is the measured ratio of plutonium to uranium content in the sample.

TABLE 1. Isotopic Content of Transuranium Elements and Fission Fragments in Investigated Samples

Sample No.	Uranium content, mg	Content of uranium isotopes, %				Plutonium content, mg	Content of plutonium isotopes, %					Americium content, µg	Content of americium isotopes, %		Content of other isotopes, µg			
		U235	U236	U238	U238		Pu239	Pu240	Pu241	Pu242			Am241	Am243	Cm242	Cm244	Cs137	Ce144
1	660	0,86±0,01	0,18±0,01	98,96±0,02		2,972	68,37±0,22	23,14±0,19	6,93±0,11	1,56±0,01		29,29	91,04±0,11	8,96±0,11	1,44	0,43	262	86
2	715	0,64±0,01	0,22±0,01	99,14±0,02		4,511	60,71±0,17	26,30±0,14	9,68±0,08	3,31±0,03		50,34	75,87±0,35	24,13±0,35	3,28	1,62	457	154
3	570	0,94±0,02	0,18±0,01	98,89±0,02		1,924	69,92±0,12	20,81±0,11	7,68±0,03	1,59±0,02		33,60	87,58±0,19	12,42±0,19	1,66	—	295	139
4	780	1,70±0,02	0,069±0,004	98,23±0,02		0,757	92,34±0,02	6,77±0,15	0,89±0,02	<1		~4	≫90	≪10	0,013	—	66	28

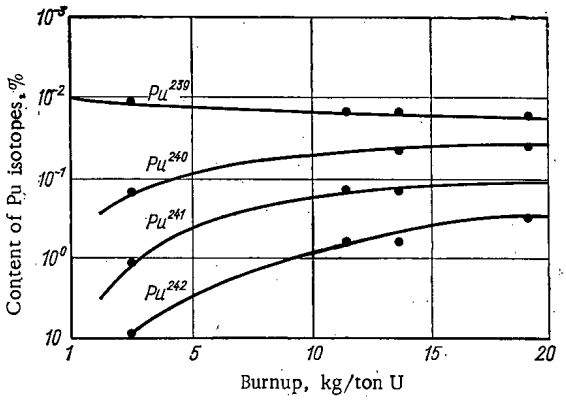

Fig. 3. Isotopic composition of plutonium as a function of burnup.

The factor ω in (1) is found from

$$\omega = \gamma_i^9 + \frac{1+\alpha^9}{\alpha^9}\left(\gamma_i^0 + \gamma_i^1 + \frac{1+\alpha^1}{\alpha^1}\gamma_i^2\right), \qquad (2)$$

where α^i is the ratio of the effective radiative capture cross section to the fission cross section of the i-th isotope.

The values of α^9 and α^1 for Pu^{239} and Pu^{241} isotopes were adopted from [6].

The contribution of plutonium isotopes in total burnup Y was calculated from

$$Y = \frac{z(1000-X)(\omega-1)}{1+z\omega}\ \text{kg/ton U}. \qquad (3)$$

The calculated results of burnup in the samples and data on the content of plutonium, americium, and curium per ton of starting uranium are listed in Table 2 and represented by the curves in Figs. 2-4.

The error in the determination of U^{235} burnup is due first of all to the error in isotopic analysis and decreases with increasing burnup. The error in burnup in samples with low and high burnup was ±8% and ±3% respectively.

The contribution of plutonium into total burnup was determined to within ±(12-15)% since α^9 and α^1 are known to within ±(5-10)% and the error in z is ±6%.

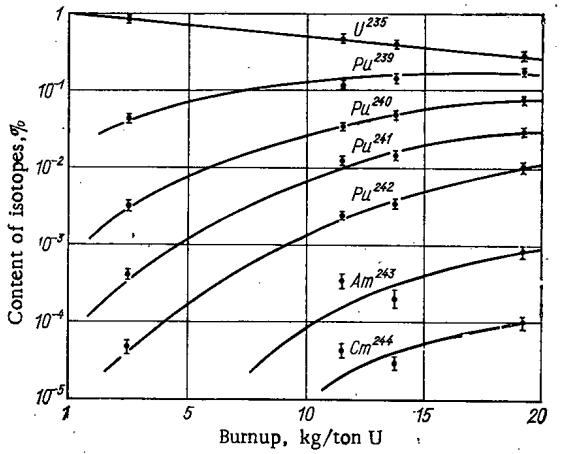

Fig. 4. Content of uranium, plutonium, americium, and curium isotopes as a function of burnup.

TABLE 2. Content of Uranium, Plutonium, Americium, and Curium Isotopes (kg/ton U)

Isotopes	Sample No.			
	1	2	3	4
U^{235}	8,34±0,10	6,16±0,10	9,14±0,19	16,73±0,20
U^{236}	1,75±0,09	2,12±0,11	1,76±0,09	0,68±0,03
U^{238}	971,70±0,97	966,26±0,97	974,15±0,97	979,05±0,98
Pu^{239}	3,02±0,18	3,72±0,22	2,34±0,14	0,892±0,054
Pu^{240}	1,02±0,06	1,62±0,10	0,70±0,04	0,0657±0,0039
Pu^{241}	0,31±0,02	0,60±0,04	0,26±0,02	0,0087±0,0005
Pu^{242}	0,07±0,01	0,21±0,01	0,06±0,01	$< 0,0001$
Am^{241} ($\times 10^3$)	40,0±2,9	52,4±3,8	50,8±2,3	$< 0,45 \cdot 10^{-3}$
Am^{243} ($\times 10^3$)	3,95±0,79	16,6±3,8	7,2±1,4	$< 5 \cdot 10^{-5}$
Cm^{244} ($\times 10^3$)	0,63±0,13	2,05±0,41	0,890±0,178	—
Uranium fission products	9,79±0,29	11,62±0,35	8,68±0,28	2,37±0,19
Plutonium fission products	3,96±0,48	7,62±0,91	2,87±0,34	0,18±0,02
Total burnup	13,75±0,55	19,24±0,97	11,55±0,45	2,55±0,19

As seen in Table 2, the highest burnup, equal to 19.24 ± 0.97 kg of poison per 1 ton uranium, has been obtained in sample No. 2 taken at 500 mm from the bottom end of the fuel element. This sample also shows a significant contribution of plutonium into total burnup which amounts to 39%. The distribution of burnup along the fuel element was determined from the amount of poisons found in mass spectrometric analysis and from the content of Cs^{137} and Ce^{144} fragments. No significant Cs^{137} migration has been observed within the experimental error.

LITERATURE CITED

1. Yu. I. Gryzin et al., Techniques of Radiochemical Determination of Plutonium, Americium, Curium, Californium, Berkelium, and Fission Products in Irradiated Materials [in Russian], Preprint NIIAR, P-81 (1970).
2. H. Palmer, in: Advances in Mass Spectrometry [Russian translation], IL, Moscow (1963), p. 35.
3. V. K. Markov et al., Uranium and Methods of Its Determination [in Russian], Atomizdat, Moscow (1965).
4. Webster, in: Advances in Mass Spectroscopy [Russian translation], IL, Moscow (1963), p. 107.
5. V. Ya. Gabeskiriya et al., Investigation of Buildup of Plutonium Isotopes in VVÉR-1 Reactor Fuel at the Novo-Voronezh Atomic Power Plant [in Russian], Preprint NIIAR, P-66 (1970).
6. Neutron Cross Sections, BNL-325, Second Edition Suppl. No. 2, Vol. 3 (1965).

REGULAR SYSTEM OF CLOSELY SPACED NEUTRON ABSORBERS

I. L. Chikhladze and Ya. V. Shevelev

UDC 621.039.51

In [1] a calculational method was proposed for a reactor with a regular lattice of widely spaced absorbers. It is necessary to ask what the precise meaning of "widely spaced" is, and whether it is impossible to use the method when the distance between the absorbers is equal to their diameter. This question is considered in the present work, in which the previously used method is generalized to a closely spaced lattice and it is shown that in a series of cases the corrections to the zeroth approximation used earlier are small, even if the absorbers are close to each other (formally, with the simultaneous tending of the transport mean free path to zero). This paper clarifies the magnitude of the error which arises when the same effective boundary conditions on the absorber are used for different distributions of neutrons on its surface.

We look at a linear lattice of thick, cylindrical, thermal-neutron-absorbing blocks of radius ρ. The blocks are situated in a nonabsorbing moderator at some distance from the core boundary. The centers of the blocks are located at the points $\mathbf{r} = m\mathbf{a}$ (Fig. 1).* We shall first solve the homogeneous problem (later, an absorbing medium with a slowing-down source of neutrons will be considered).

The thermal neutron flux $\Phi(\mathbf{r})$ is determined everywhere except those regions adjacent to the absorbing blocks by the diffusion equation

$$\nabla^2\Phi(\mathbf{r}) = 0 \tag{1}$$

together with the condition of periodicity

$$\Phi(\mathbf{r}+\mathbf{a}) = \Phi(\mathbf{r}).$$

We direct y axis along $\mathbf{a}$ and denote the two-dimensional radius vector by the complex variable $z = y + ix$. Then the solution of Eq. (1) can be written in the following form†:

$$\Phi(z) = \operatorname{Re}\left\{A_0 \ln \sin\frac{\pi z}{a} + \sum_{k=1}^{\infty}\sum_{m=-\infty}^{\infty}\frac{A_k}{(z-ma)^k} + \sum_{l=0}^{1} B_l z^l\right\}. \tag{2}$$

Solutions with $k = -\infty, \ldots, -1$ also satisfy Eq. (1). However, we discard them, inasmuch as the sum over m of such terms diverges. Terms of the type $B_l z^l$ with $l > 1$ do not satisfy the condition of periodicity of the solution along the y axis. The term with $l = 1$ satisfies the condition of periodicity along the y axis, provided that $\operatorname{Re} B_1 = 0$. For the same reason $\operatorname{Im} A_0 = 0$.

Using the method of [1], we find the averaged asymptotic neutron flux far from the lattice. Averaging is not required for the term

$$\operatorname{Re}\sum_{l=0}^{1} B_l z^l = B_0 - \operatorname{Im} B_1 x \tag{3}$$

*Here $\mathbf{r}$ is a two-dimensional radius vector.

†By excluding the imaginary part of $\Phi(z)$ we are making the class of those sets of coefficients A and B for which $\Phi(z)$ is a harmonic function narrower. However, the desired set of coefficients for which the boundary conditions are satisfied belongs to precisely this "narrow" class.

Translated from Atomnaya Énergiya, Vol. 34, No. 3, pp. 163-169, March, 1973. Original article submitted April 30, 1972.

The term

$$\operatorname{Re}\ln\sin\frac{\pi z}{a}=\frac{\pi|x|}{a}-\ln 2 \tag{4}$$

also does not depend on y.

Continuing, we write

$$\left\langle \operatorname{Re}\sum_{k=1}^{\infty}\sum_{m=-\infty}^{\infty}\frac{A_k}{(z-ma)^k}\right\rangle_y=\operatorname{Re}\sum_{k=1}^{\infty}\sum_{m=-\infty}^{\infty}\frac{A_k}{a}\int_0^a\frac{dy}{(ix-ma+y)^k}=\operatorname{Re}\sum_{k=1}^{\infty}\sum_{m=-\infty}^{\infty}\frac{A_k}{a}\int_{ix-ma}^{ix-a(m+1)}\frac{dw}{w^k}$$

$$=\operatorname{Re}\frac{A_1}{a}\int_{ix-\infty}^{ix+\infty}\frac{dw}{w}=\operatorname{Re}\frac{A_1}{a}\lim_{w^*\to\infty}\ln\frac{ix+w^*}{ix-w^*}=\begin{cases}\frac{\pi}{a}\operatorname{Im}A_1 & \text{for } x>0,\\ -\frac{\pi}{a}\operatorname{Im}A_1 & \text{for } x<0.\end{cases} \tag{5}$$

With the help of expressions (3) to (5) one can obtain the averaged neutron fluxes on the two different sides of the lattice and their limiting values on the line x = 0:

$$\left.\begin{aligned}\Phi_+(x)&=A_0\frac{\pi x}{a}-A_0\ln 2+B_0\\ &-\operatorname{Im}B_1x+\frac{\pi}{a}\operatorname{Im}A_1;\\ \Phi_-(x)&=-A_0\frac{\pi x}{a}-A_0\ln 2\\ &+B_0-\operatorname{Im}B_1x-\frac{\pi}{a}\operatorname{Im}A_1;\end{aligned}\right\} \tag{6}$$

$$\left.\begin{aligned}\Phi_{+0}&=-A_0\ln 2+B_0+\frac{\pi}{a}\operatorname{Im}A_1;\\ \Phi_{-0}&=-A_0\ln 2+B_0-\frac{\pi}{a}\operatorname{Im}A_1.\end{aligned}\right\} \tag{7}$$

Differentiating (6), we obtain the values of the derivatives of the average fluxes:

$$\left.\begin{aligned}\frac{d\Phi_+}{dx}&=\frac{d\Phi_{+0}}{dx}=A_0\frac{\pi}{a}-\operatorname{Im}B_1;\\ \frac{d\Phi_-}{dx}&=\frac{d\Phi_{-0}}{dx}=-A_0\frac{\pi}{a}-\operatorname{Im}B_1.\end{aligned}\right\} \tag{8}$$

In order to obtain the remaining 2n + 1 equations (in the n-th approximation), it is necessary to set up, for each harmonic, the boundary conditions at the surface of the absorber:

$$\left(\frac{\Phi_n}{\gamma_n\lambda_{tr}}-\frac{\partial\Phi_n}{\partial r}\right)_{r=\rho}=0, \tag{9}$$

where the γ_n is determined from independent considerations for each azimuthal harmonic $\Phi_n(r)$. In order to use expression (9) it is necessary to represent the solution (2) as a function of the angle φ_n associated with some one of the absorbers (e.g., the central one with m = 0). For the first term one can use the expansion [2]

$$\ln\sin u=\ln u+\sum_{l=1}^{\infty}\frac{(-1)^l 2^{2l-1}B'_{2l}u^{2l}}{l(2l)!}, \tag{10}$$

where the B'_{2l} are Bernoulli numbers.

We shall use Taylor's formula to expand the second term of Eq. (2) (for m ≠ 0). For m > 0 we have

$$\sum_{m=1}^{\infty}\frac{1}{(z-ma)^k}=\sum_{m=1}^{\infty}\sum_{n=0}^{\infty}\frac{z^n}{n!}\left[\frac{d^n}{dz^n}(z-ma)^{-k}\right]_{z=0}=\sum_{m=1}^{\infty}\sum_{n=0}^{\infty}\frac{z^n}{n!}(-1)^k\frac{(k+n-1)!}{(k-1)!}\cdot\frac{1}{(ma)^{k+n}}, \tag{11}$$

and analogously for m < 0

$$\sum_{m=1}^{\infty}\frac{1}{(z+ma)^k}=\sum_{m=1}^{\infty}\sum_{n=0}^{\infty}\frac{z^n}{n!}\left[\frac{d^n}{dz^n}(z+ma)^{-k}\right]=\sum_{m=1}^{\infty}\sum_{n=0}^{\infty}\frac{z^n}{n!}(-1)^n\frac{(k+n-1)!}{(k-1)!}\cdot\frac{1}{(ma)^{k+n}}. \tag{12}$$

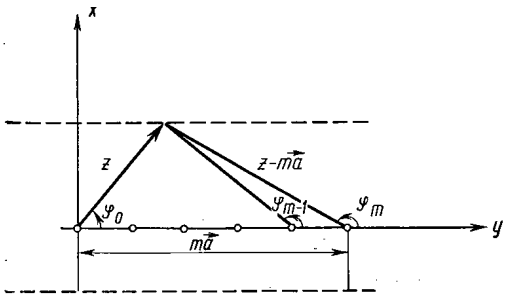

Fig. 1. Homogeneous regular lattice.

Using Eqs. (10) to (12) we write Eq. (2) in the form

$$\Phi(z)=A_0\ln\frac{\pi|z|}{a}+\mathrm{Re}\Big[\sum_{n=1}^{\infty}\frac{A_n}{z^n}+A_0\sum_{n=1}^{\infty}\frac{(-1)^n 2^{2n-1}B'_{2n}}{n(2n)!}\times\Big(\frac{\pi z}{a}\Big)^{2n}+\sum_{n=0}^{\infty}\Big(\frac{\pi z}{a}\Big)^n\sum_{k=1}^{\infty}A_k d_{nk}+\sum_{n=0}^{1}B_n z^n\Big]. \tag{13}$$

Here A_0, B'_{2n}, B_0, and d_{nk} are real numbers, B_1 is an imaginary number, and the A_k are complex numbers,

$$d_{nk}=\sum_{m=1}^{\infty}[(-1)^n+(-1)^k]\Big(\frac{a}{\pi}\Big)^n\frac{(k+n-1)!}{(k-1)!}\cdot\frac{1}{(ma)^{k+n}}. \tag{14}$$

It follows from Eq. (14) that $d_{nk}\neq 0$ only if n and k have the same parity.

We write the solution (13) in the form

$$\Phi(r,\varphi)=A_0\ln\frac{\pi r}{a}+\sum_{n=1}^{\infty}(\cos n\varphi\cdot\mathrm{Re}\,A_n+\sin n\varphi\cdot\mathrm{Im}\,A_n)\frac{1}{r^n}+A_0\sum_{n=1}^{\infty}\frac{(-1)^n 2^{2n-1}B'_{2n}}{n(2n)!}\Big(\frac{\pi r}{a}\Big)^{2n}$$
$$\times\cos 2n\varphi+\sum_{n=1}^{\infty}\Big(\frac{\pi r}{a}\Big)^n\Big[\cos n\varphi\sum_{k=1}^{\infty}d_{nk}\,\mathrm{Re}\,A_k-\sin n\varphi\sum_{k=1}^{\infty}d_{nk}\,\mathrm{Im}\,A_k\Big]+\sum_{k=1}^{\infty}d_{0k}\,\mathrm{Re}\,A_k+B_0-\mathrm{Im}\,B_1\cdot r\sin\varphi. \tag{15}$$

Then, using Eq. (9), we obtain the equations

$$A_0\Big(\ln\frac{\pi\varphi}{a}-\frac{\gamma_0\lambda_{tr}}{\rho}\Big)+\sum_{k=2,4,\ldots}^{\infty}\frac{2g_k}{a^k}\mathrm{Re}\,A_k+B_0=0; \tag{16}$$

$$g_k=\sum_{m=1}^{\infty}\frac{1}{2m^k};\quad n=0; \tag{17}$$

$$\mathrm{Im}\,B_1\delta_{1n}(\gamma_n\lambda_{tr}-\rho)=\Big(\frac{n\gamma_n\lambda_{tr}}{\rho}+1\Big)\frac{\mathrm{Im}\,A_n}{\rho}+\Big(1-\frac{n\gamma_n\lambda_t}{\rho}\Big)\rho^n\sum_{k=1,3,5,\ldots}^{\infty}\frac{g_{k+n}}{a^{k+n}}\frac{(k+n-1)!}{(k-1)!}\mathrm{Im}\,A_k; \tag{18}$$

$$\mathrm{Re}\,A_k=0,$$

where δ_{1n} is the Kronecker delta. In Eqs. (17) and (18) n and k are odd. In the following two equations n and k are even:

$$\Big(1+\frac{\gamma_n\lambda_{tr}n}{\rho}\Big)\frac{\mathrm{Re}\,A_n}{\rho^n}+\rho^n\Big(1-\frac{n\gamma_n\lambda_{tr}}{\rho}\Big)\sum_{k=2,4,\ldots}^{\infty}\frac{(k+n-1)!}{(k-n)!\,n!}\cdot\frac{2g_{k+n}}{a^{k+n}}\mathrm{Re}\,A_k+A_0B'_n$$
$$\times\frac{(-1)^{\frac{n}{2}}2^n}{n(n)!}\Big(1-\frac{n\gamma_n\lambda_{tr}}{\rho}\Big)=0; \tag{19}$$

$$\mathrm{Im}\,A_k=0. \tag{20}$$

The system of Eqs. (7), (8), and (16) to (20) give the solution of the problem in closed form for an arbitrary approximation. One must remark that Eqs. (17) and (19) contain either only $\mathrm{Im}\,A_k$, or only $\mathrm{Re}\,A_k$, of the same parity. This makes the solution of the system of equations much easier. After truncation (that is, in the n-th approximation), the system contains 2n + 5 equations with 2n + 3 unknowns. After elimination of these unknowns, two boundary conditions are obtained instead of the two usual equations of continuity. We look at different approximations.

Zeroth Approximation: $\mathrm{Re}\,A_k=\mathrm{Im}\,A_k=0$; $k=n=1,2,\ldots\infty$. One can easily obtain from the system of equations the equations:

$$\left.\begin{aligned}&\Phi_{+0}=\Phi_{-0};\\ &\frac{d\Phi_{+0}}{dx}=\frac{d\Phi_{-0}}{dx}=\frac{\pi}{av_0}(\Phi_{+0}+\Phi_{-0});\\ &v_0=\ln\frac{a}{2\pi\rho}+\frac{\gamma_0\lambda_{tr}}{\rho}.\end{aligned}\right\} \tag{21}$$

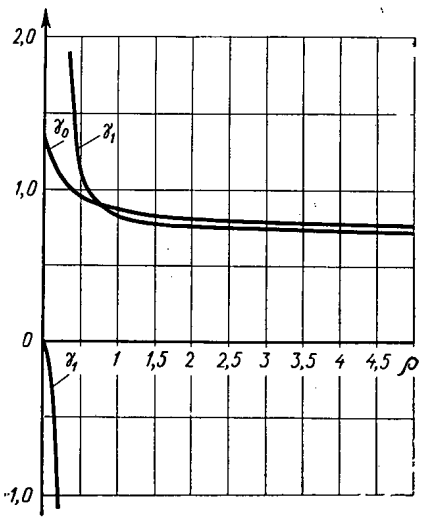

Fig. 2. Dependence of γ_0 and γ_1 on the relative radius ρ.

The system (21) coincides with the system obtained in [1]. The approximation we are considering is valid when the absorbers are at large distances from each other ($a/d \gg 1$).

First Approximation. $\mathrm{Re}\,A_k = \mathrm{Im}\,A_k = 0$; $k = n = 2, 3, \ldots, \infty$. The use of some simple transformations results in:

$$\frac{d\Phi_{+0}}{dx} - \frac{d\Phi_{-0}}{dx} = \frac{\pi}{a\nu_0}(\Phi_{+0} + \Phi_{-0});$$
$$\Phi_{+0} - \Phi_{-0} = \frac{\pi a}{\nu_1}\left(\frac{d\Phi_{+0}}{dx} + \frac{d\Phi_{-0}}{dx}\right);$$
$$\nu_1 = \frac{1 + \frac{\rho}{\gamma_1\lambda_{tr}}}{1 - \frac{\rho}{\gamma_1\lambda_{tr}}}\left(\frac{a}{\rho}\right)^2 - 2g_2; \qquad (22)$$
$$g_2 = \sum_{m=1}^{\infty}\frac{1}{m^2} = \frac{\pi^2}{6}.$$

Second Approximation. $\mathrm{Re}\,A_k = \mathrm{Im}\,A_k = 0$; $k = n = 3, 4, \ldots, \infty$. In an analogous fashion we write

$$\Phi_{+0} - \Phi_{-0} = \frac{\pi a}{\nu_1}\left(\frac{d\Phi_{+0}}{dx} + \frac{d\Phi_{-0}}{dx}\right);$$
$$\frac{d\Phi_{+0}}{dx} - \frac{d\Phi_{-0}}{dx} = \frac{\pi}{a(\nu_0 + \Delta)}(\Phi_{+0} + \Phi_{-0});$$
$$\Delta = \frac{2g_2}{\left(\frac{a}{\rho}\right)^4}\cdot\frac{1}{6\frac{g_4}{\left(\frac{a}{\rho}\right)^4} + \frac{1 + \frac{2\gamma_2\lambda_{tr}}{\rho}}{1 - \frac{2\gamma_2\lambda_{tr}}{\rho}}}; \qquad (23)$$
$$g_4 = \sum_{m=1}^{\infty}\frac{1}{m^4} = \frac{\pi^4}{90}.$$

From these results it is easy to induce a general law: in each succeeding approximation one of the boundary conditions remains unchanged (this is a result of the separation of the equations into equations with coefficients with even indices and with odd indices), while the second boundary condition contains a correction of order $(\rho/a)^4$ relative to the preceeding approximation. This guarantees the fast convergence of the approximation.

We now look at a lattice in which the absorbers are located in an absorbing medium and are close to each other. In this case the thermal neutron flux is described by the equation

$$-\nabla^2\Phi(\mathbf{r}) + \frac{1}{L^2}\Phi(\mathbf{r}) = \frac{q}{L^2\Sigma}. \qquad (24)$$

The solution of Eq. (24) for the geometry of Fig. 1 (not as yet assuming that a/L and ρ/a are small) must be sought in the form

$$\Phi(\mathbf{r}) = \Phi_{\mathrm{reg}}(\mathbf{r}) + \sum_{n=-\infty}^{\infty} A_n \sum_{m=-\infty}^{\infty} e^{in\varphi_m} K_n\left(\frac{|\mathbf{r} - m\mathbf{a}|}{L}\right). \qquad (25)$$

The regular solution corresponding to Eq. (24) must have the form

$$\Phi_{\mathrm{reg}}(\mathbf{r}) = \Phi_{\mathrm{reg}}(x) = C_+ e^{\frac{x}{L}} + C_- e^{-\frac{x}{L}} + \frac{q}{\Sigma}. \qquad (26)$$

Consequently the asymptotic flux averaged over a lattice spacing is determined according to Eq. (25) as

$$\Phi(x) = \Phi_{\mathrm{reg}}(x) + \sum_{n=-\infty}^{\infty} A_n \sum_{m=-\infty}^{\infty}\frac{1}{a}\int_0^a e^{in\varphi_m(y)} K_n\left(\sqrt{\frac{x^2 + (y - ma)^2}{L}}\right) dy. \qquad (27)$$

One can obtain, after lengthy calculation from Eq. (27),

$$\Phi(x) = \Phi_{\mathrm{reg}}(x) + \sum_{n=2\nu=-\infty}^{\infty}\frac{A_n}{a}|x|\sum_{k=0}^{E\left(\frac{n}{2}\right)}(-1)^k\binom{|n|}{2k}\Gamma\left(\frac{|n|+1}{2} - k\right)2^{\frac{|n|+1}{2} - k}\left(\frac{|x|}{L}\right)^{-\frac{|n|}{2}+k} K_{\frac{n-1}{2}+k}\left(\frac{|x|}{L}\right)$$

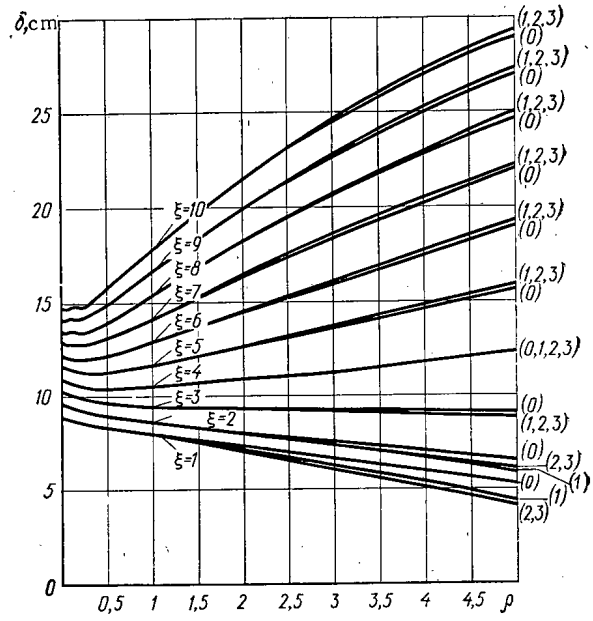

Fig. 3. The dependence of the effective extrapolation distance δ on ρ and ξ for the reactor IGR in the case $\gamma_0 = \gamma_0(\rho)$ and in the case $\gamma_1 = \gamma_1 \cdot (\rho)$ (the order of the approximation is presented in parenthesis).

$$+\sum_{n=2\nu+1=-\infty}^{\infty} A_n \frac{i}{a} x \operatorname{sign}(n) \sum_{k=0}^{E\left(\frac{|n|-1}{2}\right)} (-1)^k \binom{|n|}{2k+1} \Gamma\left(\frac{|n|}{2}-k\right) 2^{\frac{|n|}{2}-k} \left(\frac{|x|}{L}\right)^{-\frac{|n|}{2}+k} K_{\frac{|n|}{2}+k}\left(\frac{|x|}{L}\right), \qquad (28)$$

where Γ is the gamma function of Euler, E is the integral part, $\binom{|n|}{2k}$ is the number of combinations of |n| things taken 2k at a time. After using representations of these functions, and of the McDonald function K, and after summing, one can obtain the relatively simple expression

$$\Phi(x) = \Phi_{reg}(x) + \frac{\pi L}{a} A_0 e^{-\frac{|x|}{L}} + 2\frac{\pi L}{a} A_1 \frac{x}{|x|} e^{-\frac{|x|}{L}} - 2\frac{\pi L}{a} A_2 e^{-\frac{|x|}{L}} - 2\frac{\pi L}{a} A_3 \frac{x}{|x|} e^{-\frac{|x|}{L}} + 2\frac{\pi L}{a} A_4 e^{-\frac{|x|}{L}} + \dots . \qquad (29)$$

All harmonics enter into Eq. (29), in contrast to Eq. (6), which contains only A_0 and A_1 (for the case $L = \infty$). However, as calculation demonstrates, A_n decreases as the power $(a/L)^n$, and in the limit $L \to \infty$ only the two terms $\sim A_0$ and $\sim A_1$ remain in the equation, and the equation itself takes the form of Eq. (6). On the basis of Eq. (29) and their derivatives one can easily find four equations for the fluxes and their derivatives on the two different sides of the band.

In order to obtain the boundary conditions on the surface of the absorber, it is necessary to represent the solution (25) in such a way as to display its dependence on the azimuthal angle measured, for example, from the central absorber. We make use of the theory of complex Bessel functions for the right and left half-planes and rewrite expression (25) as

$$\Phi(r) = \Phi_{reg}(r) + \sum_{n=-\infty}^{\infty} A_n \sum_{k=-\infty}^{\infty} I_k\left(\frac{r}{L}\right) [(-1)^n + (-1)^k] \sum_{m=1}^{\infty} K_{-n+k}\left(\frac{ma}{L}\right) e^{ik\varphi_0} + \sum_{k=-\infty}^{\infty} A_k K_k\left(\frac{r}{L}\right) e^{ik\varphi_0}. \qquad (30)$$

It follows from Eq. (30) that the middle term differs from zero only when the numbers n and k are of the same parity. An analogous situation took place for the expansion of the function $\sum_{m=-\infty}^{\infty} (1/(z-ma)^k)$ in the case $L = \infty$ (the coefficients d_{nk}). As one would expect, in the limit $L \to \infty$ the quantities

$$[(-1)^n + (-1)^k] \sum_{m=1}^{\infty} K_{-n+k}\left(\frac{ma}{L}\right)$$

go over (with an accuracy of up to an insignificant multiplier) to the coefficients d_{nk}. In order to use the boundary condition (9) it is necessary to make a transformation of the regular solution (26). We substitute $x = r \sin \varphi_0$ in this solution and use the generating function for Bessel functions [2]

TABLE 1. Dependence of the Effective Extrapolation Distance δ on the Absorber Radius ρ for $\xi = 1$ and for Different Choices of γ_n and Different Approximations

ρ	$\gamma_0 = \gamma_0(\rho)$	$\gamma_1(\rho) = \gamma_2(\rho)_1 = \gamma_3(\rho) = \gamma_1(\rho)$ as in [4]			$\gamma_1(\rho) = \gamma_2(\rho) = \gamma_3(\rho) = \gamma_0(\rho)$ as in [5]		
	zeroth approximation	approximation			approximation		
		I	II	III	I	II	III
0,01	8,860	8,857	8,857	8,857	8,869	8,868	8,868
0,05	8,804	8,791	8,790	8,790	8,837	8,835	8,835
0,10	8,747	8,711	8,708	8,709	8,795	8,792	8,792
0,15	8,691	8,603	8,599	8,601	8,745	8,742	8,742
0,20	8,627	8,611	8,605	8,624	8,683	8,678	8,678
0,30	8,523	8,696	8,689	8,693	8,577	8,570	8,570
0,40	8,440	8,525	8,515	8,516	8,489	8,479	8,479
0,50	8,361	8,416	8,404	8,404	8,401	8,390	8,389
0,60	8,284	8,321	8,307	8,307	8,315	8,301	8,301
0,70	8,210	8,232	8,216	8,216	8,231	8,215	8,215
0,80	8,138	8,146	8,129	8,129	8,147	8,130	8,130
0,90	8,067	8,062	8,044	8,044	8,065	8,047	8,047
1,00	7,998	7,981	7,962	7,962	7,985	7,966	7,966
1,25	7,822	7,772	7,755	7,755	7,777	7,759	7,759
1,50	7,651	7,565	7,559	7,559	7,571	7,560	7,560
1,75	7,483	7,360	7,393	7,393	7,366	7,380	7,380
2,00	7,315	7,152	7,425	7,425	7,158	7,277	7,277
2,50	6,980	6,728	6,484	6,485	6,735	6,424	6,424
3,75	6,141	5,611	5,402	5,406	5,620	5,404	5,404
5,00	5,296	4,400	4,139	5,149	4,413	4,147	4,147

$$\exp\frac{1}{2}\left(t-\frac{1}{t}\right)z=\sum_{k=-\infty}^{\infty}I_k(z)\,t^k.$$

We put $t = e^{i\varphi_0}$, and then after some little transformations we obtain:

$$\Phi_{reg}(r)=\sum_{k=-\infty}^{\infty}\left[I_k\left(\frac{r}{L}\right)\{C_+(-i)^k + C_-(-i)^{-k}\}e^{ik\varphi_0}+C_0\delta_{k0}\right]$$

$$=\sum_{k=-\infty}^{\infty}\left[D_kI_k\left(\frac{r}{L}\right)+C_0\delta_{k0}\right]e^{ik\varphi_0}; \qquad (31)$$

$$D_k=[C_+(-i)^k+C_-(-i)^{-k}]. \qquad (32)$$

After substituting Eq. (31) into (30) we obtain the result

$$\Phi(r)=\sum_{k=-\infty}^{\infty}\left\{D_kI_k\left(\frac{r}{L}\right)+C_0\delta_{k0}\right.$$

$$+\sum_{n=-\infty}^{\infty}I_k\left(\frac{r}{L}\right)[(1)^n+(-1)^k]\,A_n$$

$$\left.\times\sum_{m=1}^{\infty}K_{-n+k}\left(\frac{ma}{L}\right)+A_kK_k\left(\frac{r}{L}\right)\right\}e^{ik\varphi_0}. \qquad (33)$$

By substituting Eq. (33) into the boundary conditions (9) we obtain equations for each of the $2n + 1$ harmonics:

$$\left[I_{k-1}\left(\frac{\rho}{L}\right)-\frac{2L}{\gamma_k\lambda_{tr}}I_k\left(\frac{\rho}{L}\right)+I_{k+1}\left(\frac{\rho}{L}\right)\right]\left\{D_k+\sum_{n=-\infty}^{\infty}[(-1)^n+(-1)^k]\,A_n\right.$$

$$\left.\times\sum_{m=1}^{\infty}K_{-n+k}\left(\frac{ma}{L}\right)\right\}-A_k\left[K_{k-1}\left(\frac{\rho}{L}\right)+\frac{2L}{\gamma_k\lambda_{tr}}K_k\left(\frac{\rho}{L}\right)+K_{k+1}\left(\frac{\rho}{L}\right)\right]-\frac{2L}{\gamma_k\lambda_{tr}}C_0\delta_{k0}=0; \quad -n\leqslant k\leqslant n. \qquad (34)$$

Equation (34) and the four equations obtained with the help of Eq. (29) solve the problem is closed form.

The above method was used for the determination of the effective extrapolation distance in a two group approximation for a homogeneous lattice of absorbers located on the core-reflector boundary of the reactor IGR [3]. The calculation was performed in different approximations up to and including the third, with the help of a program written for the M-220 computer. The magnitude of L was taken as infinitely large. The magnitude of γ_1 in these calculations was determined with the help of the polarization coefficient of a black block β_r, obtained in [4]:

$$\gamma_1=\rho\frac{1+\frac{\beta_r}{2}}{1-\frac{\beta_r}{2}}. \qquad (35)$$

Here ρ is expressed in mean free paths, and β_r is given, according to [4], by

$$\beta_r=-\frac{3}{2}\cdot\frac{\rho-\frac{3}{4\rho}}{\left[1+\frac{3\rho}{4}+u(\rho)\right]};$$

$$u(\rho)=\frac{3\rho}{\pi}\int_0^{\infty}dx K_{i3}(\rho x)\operatorname{arctg}x;$$

$$K_{i3}(x)=\int_0^{\infty}e^{-x\operatorname{ch}u}\frac{du}{\operatorname{ch}^3u}.$$

The dependence of γ_1 on the radius is shown in Fig. 2. The effective extrapolation distance was calculated for the values of ρ presented in Table 1, and for values of the relative distance $a/2\rho = \xi = 1, 2, \ldots, 10$. For the values of n ranging from one to three the calculation was carried out for the case $\gamma_1 = \gamma_2 = \gamma_3$ (γ_1 determined according to Eq. (35)) and the case $\gamma_0 = \gamma_1 = \gamma_2 = \gamma_3 = \gamma_0(\rho)$, as in [5]. Almost all authors use the approximation $\gamma_1(\rho) = \gamma_0(\rho)$, and consequently in the present situation there is considerable interest in the comparison of the results of the calculation of a critical reactor with the accurately computed $\gamma_1 = y_1(\rho)$ having a discontinuity for ρ between 0.2 and 0.3 (see Fig. 2) and with the inaccurate $\gamma_1(\rho) = \gamma_0(\rho)$, which is a quite smooth function of ρ.

The results of the calculation for $\xi = 1$ are presented in Table 1. The dependence of the effective extrapolation distance on the radius is shown in Fig. 3 for different ρ and different approximations. It is apparent from the graphs that the various approximations converge rapidly (the third approximation coincides with the second to four significant figures), and that within the entire range of variation of ρ the zeroth approximation is satisfactory (accuracy ±1%). Moreover, in spite of the discontinuity in γ_1, the solution is continuous in ρ, and the differences from the solution in the case $\gamma_1(\rho) = \gamma_0(\rho)$ are completely insignificant.

LITERATURE CITED

1. Ya. V. Shevelev and I. L. Chikhladze, Atomnaya Énergiya, 32, No. 1 (1972).
2. I. S. Gradshtein and I. M. Ryzhik, Tables of Integrals, Sums, Series, and Products [in Russian], Gostekhizdat, Moscow (1962).
3. I. V. Kurchatov et al., Third Geneva Conference (1964), paper 322a.
4. B. P. Kochurov, Computation of the Dipole Moment of a Cylindrical Block [in Russian], Preprint ITÉF (1964).
5. A. D. Galanin, Theory of Thermal Nuclear Reactors [in Russian], Atomizdat, Moscow (1957).

BIBLIOGRAPHY

NEW BOOKS

A. I. Baz', V. I. Gol'denskii, V. Z. Gol'dberg, and Ya. B. Zel'dovich, Light and Intermediate Nuclides near Nucleon Stability Boundaries*

The book deals with the existence and properties of nuclides near the boundaries of nucleon stability, and related problems referable to analogous states.

The text reviews the available experimental data on "borderline" nuclides, and goes into detail on the possibility of predicting the masses and other properties of nuclides yet to be detected. Basic experimental techniques useful in the search for new nuclides and investigation of analogous states are outlined.

The prospects for detecting new modes of radioactive decay of nuclides near the nucleon stability boundaries, proton radioactivity, and two-proton radioactivity, are analyzed. Possible existence of nuclides with a marked neutron excess and even purely neutron nuclides are discussed from a theoretical vantage point.

This text is written for physicists in research work, and for graduate and undergraduate students concerned with current problems in the physics of the atomic nucleus.

* * *

Plasma Theory Proceedings of the P. N. Lebedev Institute of Physics†

This compendium of articles contains review papers on plasma physics. Interactions between relativistic electron beams and plasma and the problem of critical currents, the theory of equilibrium and stability of a high-current discharge in a high-density plasma, the theory of oscillations and stability of a semiconducting plasma with a small number of charge carriers in a strong electric field, and plasma hydrodynamics in a strong radio-frequency field, are all discussed.

The articles are aimed at research scientists interested in topics in plasma physics.

* * *

Nuclear Reactions and Interactions between Neutrons and Matter, Proceedings of the P. N. Lebedev Institute of Physics‡

The basic content of the collection of articles consists of papers devoted to the study of nuclear reactions induced by neutrons, and nonstationary transport of neutrons traversing moderating media. Some experimental research techniques for probing nuclear reactions are also discussed.

*Nauka, Moscow, 1972.
†Nauka, Moscow, 1972.
‡Nauka, Moscow, 1972.

Translated from Atomnaya Énergiya, Vol. 34, No. 3, pp. 169-170, March, 1973.

The articles are written for physicists working in the field of nuclear physics, but may also prove useful to research scientists specializing in other areas where nuclear physics techniques can be applied in research.

* * *

Cosmic Rays, No. 3*

Papers on a very broad range of topics concerning cosmic ray variations at the earth and in the earth's space environs, in research based on the use of artificial earth satellites and lunar satellites, are published in this collection. Some of the articles deal with improvements in equipment devised for the study of the composition and spectrum of cosmic rays, secular variations, and the azimuthal effect.

This collection of papers will be of interest to a broad range of specialists on the physics of cosmic rays and related branches of science.

* * *

B. V. Myasoedov, L. I. Guseva, I. A. Lebedev, et al., Analytical Chemistry of the Transplutonium Elements†

This monograph is devoted to a rounded discussion of topics in the analytical chemistry of ten elements in the periodic table, from americium (Z = 95) to kurchatovium (Z = 104). The combined treatment of these elements in a single book is based on much that is in common in their physical and chemical properties (radioactivity, behavior in aqueous solutions), and also on the methods applicable in the isolation and investigation of these elements. Extensive literature material bearing on all aspects of the problem is amassed.

The book, which contains a wealth of useful information and valuable recommendations, is of great interest to a broad range of research scientists interested in various aspects and realms of the chemistry of the transplutonium elements.

* * *

A. F. Belyaev, P. F. Pokhil, A. I. Korotkov, et al., Combustion of Powdery Metals in Active Media‡

This books deals with important and timely problems pertaining to ignition and combustion of such metals as aluminum, beryllium, magnesium, boron, lithium, etc., which are widely used in modern industry and engineering: they make it possible, for instance, to significantly improve the physicochemical characteristics of rocket propellants. The text cites, and reviews for the first time, a generous amount of experimental and theoretical material amassed by Soviet and foreign authors over the past 10 to 15 years. Modern research techniques and basic regularities of ignition and combustion of metals are also presented, light is shed on the effect of additives in metals on the physical and energetic parameters of powders and explosives.

The book is written for research scientists and engineers engaged in the field of combustion, and also for instructors, graduate and undergraduate students, specializing in this field.

* * *

*Nauka, Moscow, 1972.
†Nauka, Moscow, 1972.
‡Nauka, Moscow, 1972.

Uranium and Thorium in Magmatic and Metamorphic Rocks of the Central Portion of the Altai-Sayan Folded Region, Proceedings of the Institute of Geology and Geophysics of the Siberian Branch of the Division of the USSR Academy of Sciences, No. 142*

Data on the content of uranium and thorium are cited in the monograph. Their distribution in magmatic and metamorphic rock is demonstrated. Forms of occurrence of uranium in intrusive, effusive, and metamorphic rock, and the behavior of uranium and thorium in their formation processes, come under discussion. A relationship is established between the concentration of uranium and thorium and the geological conditions governing the formation of the uranium and thorium, and the geochemical history of the radioactive elements is discussed. The monograph comprises the first major review of the radiogeochemistry of rock species over an extensive portion of Siberia.

The book is written for geologists, geochemists, and mineralogists.

* * *

V. V. Cherdyntsev, Nuclear Vulcanology†

This is the first book in the worldwide literature to undertake a review of nuclear volcanology, the study of the behavior of radioactive isotopes and their decay products in volcanic processes as matter is ejected from the interior of the earth. Radioactive isotopes are of expectional importance in the solution of this problem, since it is well known that they exist in a rigorously determinate state of radioactive equilibrium at great depths below the surface.

Extensive experimental material amassed in recent years (in large part by Soviet scientists) pave the way for deriving some regularities of significance not only for volcanology but also for the study of the properties of the upper mantle and the formation of the Earth's crust, and for the study of volcanogenic deposits in the continents and oceans.

The book is written for broad range of readers, first of all research scientists, engineers, and students interested in Earth science and in space science.

* * *

Physical Metallurgy of Nonferrous Metals and Alloys‡

This compendium of articles devoted to the memory of the outstanding Soviet metallurgical scientist A. M. Bochvar covers a broad range of topics relating to the physical metallurgy, general metallurgy, and machining of alloys of aluminum, magnesium, copper, and titanium. Results of research undertaken with the object of developing new alloys, studying phase equilibria in systems of the above nonferrous metals, the nature of hardening and methods of processing, processes of melting, casting, heat treatment, and deformation of those alloys are published in this text. Some of the articles deal with improvements and advances in technological production conditions for diverse semifinished products made from nonferrous alloys. Individual articles point out ways of utilizing new elements in the alloying of these metals and alloys.

This publication is intended for research scientists, metals scientists, metallurgists, experts in machining and metals processing, machinery manufacture technologists, and also for instructors and students in metallurgical and machinery design colleges.

*Nauka, Moscow, 1972.
†Nauka, Moscow, 1972.
‡Nauka, Moscow, 1972.

D. L. Broder et al. (editors)

MANUAL ON RADIATION SHIELDING FOR ENGINEERS, VOL. I*

Reviewed by U. Ya. Margulis

The appearance in Russian of the first volume of the Manual on Radiation Shielding for Engineers is a highly important and helpful development. In connection with the vigorous development of the nuclear power industry and the widespread ultilization of sources of ionizing radiations in the national economy, the contingent of engineering and technical workers interested in the design and calculations of biological shielding has been on the increase. This three-volume manual was published in response to an IAEA initiative. Leading specialists in the field of radiation shielding, Soviet scientists included, took part in the preparation of the publication.

The translation editors (most of whom took part in writing sections of the manual) proceeded in what, in our view, is an entirely correct manner in abridging some of the sections which are covered quite amply in the Soviet literature. Since the first English-language volume of the manual appeared back in 1968, the initiative of the editors of the Russian-language edition in supplementing the manual text with some new material (descriptions of detailed characteristics of radiation flux and calculation design techniques) is also to be commended.

The first volume contains exhaustive material on the attenuation of narrow and broad beams of γ-radiation. Specifically, values of interaction cross sections of γ-radiation, attenuation coefficients and energy absorption coefficients, and buildup factors for various materials, are listed and tabulated. Appropriate computational formulas for estimating attenuation of broad and narrow beams of γ-radiation are presented. The data cited on techniques for calculating multilayer shielding and backscattering of γ-radiation may prove highly useful in calculations.

The complete and painstaking descriptions of neutron attenuation and scattering in matter, and methods for calculating and design of antineutron shielding, are to be noted.

The first chapter, dealing with methods for calculating attenuation of radiation, and in particular a program for computing attenuation of radiation by the Monte Carlo method, is highly useful; methods for solving the transport equation are cited. Methods for integrating the function of a point source, etc. are described in some detail.

One outstanding merit of the manual is the ample number of examples on solution of various radiation shielding problems. All of these features render the manual accessible to a broad range of practical workers.

In conclusion, we should take note of the excellence of the translation, the high scientific and literary level of the editorial work, and the excellent format of the book.

*Atomizdat, Moscow, 1972.

Translated from Atomnaya Énergiya, Vol. 34, No. 3, p. 170, March, 1973.

ARTICLES

TEST OF NEUTRON DIFFUSION THEORY IN A MEDIUM WITH CHANNELS BY THE PULSED SOURCE METHOD (SINGLE CHANNEL IN A MODERATING BLOCK)

I. F. Zhezherun

UDC 539.125.5.17.52

One measures, by the pulsed-neutron-source method (see [1]), three diffusion parameters of the moderator: the absorption cross section Σ_0 of the product of velocity and absorption cross section $v\Sigma_0$, the diffusion coefficient D_0, and the coefficient of diffusion cooling C_0. These parameters are usually determined from the relationship

$$\alpha_0 = v\Sigma_0 + D_0B^2 - C_0B^4, \tag{1}$$

α_0 is a quantity directly measured by experiment, and represents the logarithmic decrement (decay constant) for neutrons in a block of moderator with geometric parameter B^2. For a block in the form of a rectangular parallelopiped with dimensions (to the extrapolated endpoints) x_e, y_e, z_e, along the coordinate axes, one has

$$B^2 = \pi^2(x_e^{-2} + y_e^{-2} + z_e^{-2}).$$

If the medium is anisotropic and consists of a lattice of empty channels in a moderator, with the channels directed along the z axis, then Eq. (1) takes the more complex form [2, 3]

$$\alpha = v\Sigma + D_\perp B_\perp^2 + D_\parallel B_\parallel^2 - C_\perp B_\perp^4 - C_\parallel B_\parallel^4 - C_\times B_\perp^2 B_\parallel^2. \tag{2}$$

The coefficients with subscripts "$\parallel$" and "$\perp$" correspond to directions along the transverse to the channels, while

$$B_\perp^2 = \pi^2(x_e^{-2} + y_e^{-2}),\ B_\parallel^2 = \pi^2 z_e^{-2}.$$

Reference [3] gives

$$C_\times = C_\perp + C_\parallel, \tag{3}$$

and in the case where the transport mean free path λ does not depend on energy one also has

$$\frac{C_\parallel}{C_\perp} = \frac{D_\parallel^2}{D_\perp^2}. \tag{4}$$

Laletin [4] showed that in this case the following relationships are also valid:

$$\frac{C_\perp}{C_0} = \frac{D_\perp^2}{D_0^2};\quad \frac{C_\parallel}{C_0} = \frac{D_\parallel^2}{D_0^2};\quad \frac{C_\times}{C_0} = 2\frac{D_\perp D_\parallel}{D_0^2}. \tag{5}$$

The quantity $D_\parallel$ in Eq. (2) depends on the channel length z. If the interaction of the channels can be neglected then [5]:

$$\frac{D_\parallel(z)}{D_0} = 1 + \frac{p}{1+p}\left[1 + \frac{3}{2}Q\frac{R}{\lambda} - \frac{3}{2}Q\frac{R}{\lambda}\frac{\varepsilon R}{2z}\right] = \frac{D_\parallel^\infty}{D_0}\left\{1 - \frac{\frac{R}{1+p}\frac{3}{2}Q\frac{Q}{\lambda}\varepsilon\frac{R}{2z}}{D_\parallel^\infty/D_0}\right\} = \frac{D_\parallel^\infty}{D_0}\{1 - \Delta(z)\}, \tag{6}$$

where p is the ratio of the volume of the cavity to the volume of the continuous material in the lattice cell, R is the hydraulic radius of the channel, $Q = (\bar{l})^2/\overline{l^2}$ is a coefficient depending on the shape of the channel

Translated from Atomnaya Énergiya, Vol. 34, No. 3, pp. 171-175, March, 1973. Original article submitted December 9, 1971.

(the ratio of the square of the mean chord $(\bar{l})^2$ to the mean squared chord $\overline{l^2}$), $\varepsilon = 7.2$; $D_{\parallel}^{\infty}$ is the diffusion coefficient for an infinitely long channel.

Taking into account the dependence on z of $D_{\parallel}$ leads to the change in Eq. (2) of the term $D_{\parallel}(z)B_{\parallel}^2$ to $D_{\parallel}^{\infty}B_{\parallel}^2 - GB_{\parallel}^3$, where

$$G = 1.725 \frac{p}{1+p} Q \frac{R^2}{\lambda} D_0. \quad (7)$$

As is shown in [6], the analysis of the results of measurements by the pulsed-source method according to Eq. (2), with the term $GB_{\parallel}^3$ included, gives values of $D_{\perp}$ and $D_{\parallel}^{\infty}$ which are found to be in excellent agreement with theoretical calculations, even including the case of strongly anisotropic media, such as a lattice of channels of diameter 15 cm in graphite with a lattice spacing of 20 cm. Thus the pulsed neutron source method in this situation, just as in the study of homogeneous media, gives the capability of reliably measuring the diffusion parameters even for anisotropic media.

However, in the case of anisotropic media with hollow channels, the amount of data which must be measured increases considerably, and the difficulties in obtaining adequate accuracy in the measurement of the decay constant α increase considerably, inasmuch as Eqs. (5) are not always satisfied. It is therefore desirable to find another form of the pulsed-source experiment, free of the above-mentioned inadequacies, for the study of such media.

The present paper attempts to describe such an experiment. The paper gives the results of a study of anisotropic media in a system consisting of a single hollow channel in a block of moderator.

Experimental Setup and Experimental Results

Moderating blocks were constructed in the form of rectangular parallelepipeds from slabs of beryllium or bricks of beryllium oxide, and placed in the neutron beam from the linear accelerator at the I. V. Kurchatov IAÉ. In some of the measurements a portable pulsed-neutron source with an energy of 14 MeV was used, instead of the accelerator beam. The block was covered on all sides by cadmium sheets of thickness 0.5-1.0 mm and by boron carbide of thickness 5 g/cm^2. The locations of the source and the neutron dedector were selected in such a way as to maximize the suppression of higher harmonics. In the majority of measurements four BF-3 counters, with B^{10} enrichments of up to 85%, and with diameters of 2 cm and lengths of 25 cm, were used, joined in parallel. The monitoring apparatus consisted of a nonoverloading amplifier and a twenty channel time analyzer. The apparatus is described in more detail in [7] to [9], where the results of diffusion parameter measurements using beryllium and beryllium oxide are given. Empty channels with square cross sections passed through the blocks along their vertical axes.

The decay constant α was determined for blocks of different dimensions by applying the method of least squares [10] to the experimentally measured decay of the neutron density. In applying this method, the well-known procedure of rejection of the initial points of the decay curve was used, in order to definitely isolate the fundamental harmonic. In all cases the asymptotic decay was exponential, independent of the location of the detector. In controlled measurements for some blocks, neutron detectors of diameters 2 cm and lengths 5 and 50 cm were used, the detectors being placed on the surface of the block parallel to one of its faces, and situated either directly over the channel or else at various distances from the channel. The cadmium shield on the counter permitted only those neutrons to pass through which left the block from directly under the counter. Therefore the integrand counter readings represented a quantity proportional to the neutron leakage from the block at the location of the counter. Figure 2 gives the integrated readings of counters of lengths 5 and 50 cm placed on the end surface of a block of beryllium oxide of diameters 75 × 75 × 70 cm with a channel of dimension 15 × 15 cm, for different locations of the counters.

Table 1 presents the results of measurements of the decay constant α in various blocks having channels. The measurement errors are everywhere 0.5 to 0.7%. For blocks of the same dimensions but without channels the decay constant α_0 was calculated from Eq. (1) using the following parameters [9]:

for beryllium (density 1.79 g/cm^3)

$$v\Sigma_0 = 261.3 \pm 6.9 \text{ sec}^{-1};$$

$$D_0 = (1.233 \pm 0.007) \cdot 10^5 \text{ cm}^2/\text{sec};$$
$$C_0 = (3.13 \pm 0.08) \cdot 10^5 \text{ cm}^4/\text{sec};$$

for beryllium oxide (density 2.79 g/cm^3)

$$v\Sigma_0 = 185 \pm 5.8 \text{ sec}^{-1}; D_0 = (1.548 \pm 0.009) \text{ cm}^2/\text{sec};$$
$$C_0 = (4.63 \pm 0.24) \cdot 10^5 \text{ cm}^4/\text{sec}.$$

Control measurements of the decay constant α_0 were made for several blocks without channels and gave results coinciding, within the limits of experimental error, with the calculated values.

Discussion of Experimental Results

We remark that Eq. (6) was obtained for a flat (i.e., constant) neutron distribution in the cell in directions perpendicular to the channel, and must be modified for application to the conditions of this experiment. In a block without channels the neutron density distribution is cosine-shaped in all three of the principal directions. The presence of a channel results in some deviation of the distribution from cosinusoidal, expecially in directions transverse to the channel. The distribution in the block itself was not measured, but inferences concerning this distribution can be drawn from the distribution of leakage on the block surface.

Thus, in the leakage term $D_\perp B_\perp^{*2}$ for transverse directions, the parameter $B_\perp^{*2}$ is, strictly speaking, not equal to the geometric parameter $B_\perp^2$. It is shown in [4] that $B_\perp^{*2} = B_\perp^2 \beta$, where $\beta = 1 + 0.5\,p$. In our measurements $p \leq 0.06$. One can therefore consider the neutron density distribution to be close to cosinusoidal even for the transverse directions. Then the term in square brackets in Eq. (6) should be multiplied by the quantity

$$\eta = \frac{\pi^2}{4}, \tag{8}$$

which is the usual coefficient arising from neutron density balance, or importance balancing.

In [4] this coefficient is obtained for the extrapolated dimensions of a block. If one takes into consideration the fact that for, small blocks, the true dimensions x, y, and z of the block can be significantly different from the extrapolated dimensions x_e, y_e, and z_e, then one obtains for η

$$\eta = \frac{\pi^2}{4} \cdot \frac{x}{x_e \sin \frac{\pi x}{2x_e}} \cdot \frac{y}{y_e \sin \frac{\pi y}{2y_e}} \cos^2 B_\perp R. \tag{8a}$$

Consequently, for the conditions of our experiment, instead of Eq. (6) one has for the quantity $D_\parallel/D_0$ the expression

$$\frac{D_\parallel(z)}{D_0} = 1 + \frac{p}{1+p}\left[1 + \frac{3}{2} Q \frac{R}{\lambda}\left(1 - \varepsilon \frac{R}{2z}\right)\right]\eta = \frac{D_\parallel^\infty}{D_0}\{1 - \Delta(z)\,\eta\}. \tag{6a}$$

The decay constant for the neutron density in a block is given [4] by the equation

$$\alpha = v\Sigma + D_0 B_\perp^2 \beta + D_0 B_\parallel^2 \frac{D_\parallel}{D_0} - G B_\parallel^2 \eta - C_0 B_\perp^4 \beta^2 - C_0 B_\parallel^4 \left(\frac{D_\parallel}{D_0}\right)^2 - 2 C_0 B_\perp^2 \beta B_\parallel^2 \frac{D_\parallel}{D_0}. \tag{9}$$

Here Eq. (5) has been used, $B_\perp^{*2}$ has been replaced by $B_\perp^2 \beta$, and

$$v\Sigma = \frac{1}{1+p}(v\Sigma_0 + p v\Sigma_B \eta), \tag{10}$$

where Σ_0 and Σ_B are macroscopic absorption cross sections for the block material and for the air filling the channel, respectively.

Equation (9) is an equation of the second degree with respect to the quantity $D_\parallel/D_0$, and relates it to the experimentally measured decay constant α, the geometric parameters of the block, and the diffusion parameters of the material composing the block. Solving this equation with the term $GB_\parallel^3 \eta$ present and also with this term deleted we obtain the experimental values of $D_\parallel(z)/D_0$ and $D_\parallel^\infty/D_0$ for blocks of finite length and of infinite length (see columns 11 and 14 in Table 1).

The extrapolation distance for the calculation of B^2 is determined by the transport mean free path λ for the continuous medium.

Equations (5), as well as $B_\perp^{*2} = B_\perp^2(1 + 0.5p)$, are satisfied only approximately for beryllium and beryllium oxide, and consequently the values of $D_\parallel(z)/D_0$ and $D_\parallel^\infty/D_0$ obtained contain a certain systematic error. We estimate this error in the following fashion.

TABLE 1. Results of Measurements for Blocks with Channels and Comparison to Calculation

Block material	Block dimensions, cm			Transverse channel dimensions		p	α, sec^{-1}	$\alpha - \alpha_0$, sec^{-1}	$\frac{D_\parallel(z)}{D_0}$ for a block with a single channel		
	x	y	z	cm	$\frac{R}{\lambda}$				calc. Eq. (6a)	experiment: from Eq. (12)	experiment: from Eq. (9)
Beryllium (density 1.79 g/cm² λ = 1.49 cm)	52,4	52,4	47,9	4×4	1,34	0,0059	1560,6	24,0±11,0	1,046	1,052±0,023	1,088±0,023
	52,4	52,4	47,9	8×8	2,68	0,0239	1662,9	126,3±11,6	1,252	1,270±0,032	1,291±0,032
	52,4	52,4	47,9	12×12	5,33	0,0555	1793,7	257,1±12,5	1,570	1,555±0,045	1,566±0,045
Beryllium oxide (density 2.79 g/cm³, λ = 1.87 cm)	65,0	65,0	60,0	5×5	1,34	0,0060	1238,9	18,4±8,7	1,047	1,048±0,022	1,048±0,022
	65,0	65,0	70,0	5×5	1,34	0,0060	1137,4	12,7±8,0	1,048	1,047±0,028	1,044±0,028
	65,0	65,0	80,0	5×5	1,34	0,0060	1069,0	9,8±7,5	1,048	1,046±0,034	1,038±0,034
	75,0	75,0	70,0	5×5	1,34	0,0045	983,5	14,2±6,8	1,036	1,051±0,025	1,049±0,025
	70,0	70,0	60,0	10×10	2,68	0,0208	1211,7	76,4±8,4	1,224	1,204±0,021	1,197±0,021
	70,0	70,0	70,0	10×10	2,68	0,0208	1100,1	61,0±7,7	1,234	1,222±0,026	1,208±0,026
	70,0	70,0	80,0	10×10	2,68	0,0208	1026,6	51,2±7,2	1,242	1,243±0,032	1,224±0,032
	65,0	65,0	60,0	15×15	4,02	0,0562	1435,2	214,6±10,0	1,577	1,572±0,024	1,551±0,024
	65,0	65,0	70,0	15×15	4,02	0,0562	1301,2	176,5±9,1	1,627	1,638±0,030	1,668±0,030
	65,0	65,0	80,0	15×15	4,02	0,0562	1200,3	140,3±8,4	1,665	1,665±0,036	1,600±0,036
	75,0	75,0	70	15×15	4,02	0,0419	1099,3	130,1±7,7	1,429	1,472±0,025	1,450±0,025
	75,0	75,0	80	15×15	4,02	0,0419	1006,0	100,7±7,0	1,460	1,477±0,030	1,445±0,030

TABLE 1 (continued)

Block material	$\frac{D_\parallel^\infty}{D_0}$ for a block with a single channel				η from Eq. (8)	$\frac{D_\parallel^\infty}{D_0}$ for a block with a single channel	
	calc. Eq. (6a)	experiment: from Eq. (12)	experiment: from Eq. (9)	experiment: from Eq. (16)		calc. Eq. (6)	experiment
Beryllium (density 1.79 g/cm² λ = 1.49 cm)	1,052	1,056±0,023	1,094±0,023	—	2,228	1,024	1,025±0,010
	1,335	1,354±0,034	1,378±0,034	—	2,053	1,163	1,172±0,017
	1,932	1,911±0,055	2,085±0,055	—	1,777	1,525	1,513±0,031
Beryllium oxide (density 2.79 g/cm³, λ = 1.87 cm)	1,053	1,053±0,015	1,050±0,015	1,062±0,032	2,229	1,025	1,024±0,007
	1,040	1,055±0,025	1,053±0,025	—	2,257	1,018	1,024±0,011
	1,297	1,284±0,015	1,275±0,015	1,246±0,037	2,091	1,142	1,136±0,007
	1,942	1,947±0,017	1,928±0,017	2,008±0,060	1,778	1,530	1,533±0,010
	1,760	1,800±0,020	1,697±0,020	1,634±0,107	1,910	1,398	1,419±0,011

Declassified and Approved For Release 2013/09/15 : CIA-RDP10-02196R000400010003-7

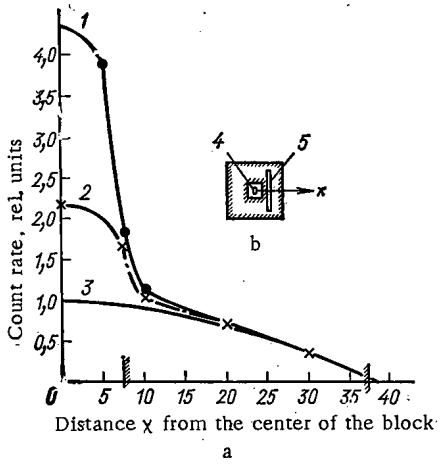

Fig. 1. Integrated readings of counters of length 5 cm (1) and 50 cm (2) on the surface of a block. Curve 3 represents the cosine distribution of neutrons in the absence of a channel (calculated curve). Diagram b gives a location of the counters (4, 5).

Consider the increase in the logarithmic decrement $\Delta\alpha = \alpha - \alpha_0$ which is measured in experiment for two equally-sized blocks one of which contains a channel. This increase can be written, according to Eqs. (2) and (1), as

$$\alpha - \alpha_0 = v\Sigma - v\Sigma_0 + (D_\perp B_\perp^{*2} - D_0 B_\perp^2) + [D_\parallel(z) - D_0] B_\parallel^2 - (C_\perp B_\perp^{*4} - C_0 B_\perp^4) - (C_\parallel - C_0) B_\parallel^4 - [(C_\perp + C_\parallel) B_\perp^{*2} - 2C_0 B_\perp^2] B_\parallel^2. \quad (11)$$

One obtains from this equation

$$\frac{D_\parallel(z)}{D_0} = 1 + \frac{\alpha - \alpha_0}{D_0 B_\parallel^2} + \delta_1 - \delta_2 + \delta_3, \quad (12)$$

where δ_1, δ_2, and δ_3 are quantities of higher order of smallness.

$$\delta_1 = \frac{v\Sigma - v\Sigma_0}{D_0 B_\parallel^2} = \frac{1}{D_0 B_\parallel^2}(\eta v\Sigma_B - v\Sigma_0)\frac{p}{1+p}; \quad (13)$$

$$\delta_2 = \frac{D_\perp B_\perp^{*2} - D_0 B_\perp^2}{D_0 B_\parallel^2}; \quad (14)$$

$$\delta_3 = \frac{(C_1 B_\perp^{*4} - C_0 B_\perp^4) + (C_\parallel - C_0) B_\parallel^4 + [(C_\perp + C_\parallel) B_\perp^{*2} - 2C_0 B_\perp^2] B_\parallel^2}{D_0 B_\parallel^2}. \quad (15)$$

If one now computes $D_\parallel(z)/D_0$ and $D_\parallel^\infty/D_0$ according to Eq. (12), assuming $-\delta_2 + \delta_3 = 0$ (see columns 10 and 13 in Table 1), then the values obtained for these quantities from the experiment are somewhat larger than the true values, inasmuch as $\delta_2 > \delta_3$.

From measurements of the decay constant α in blocks of different lengths but of the same transverse dimensions, one obtains without use of Eq. (12),

$$\frac{D_\parallel^\infty}{D_0} = \left[1 - \frac{\Delta(z_i)\eta_i {}_iB_\parallel^2 - \Delta(z_k)\eta_k {}_kB_\parallel^2}{{}_iB_\parallel^2 - {}_kB_\parallel^2}\right]^{-1}\left\{\frac{\alpha_i - \alpha_k}{D_0({}_iB_\parallel^2 - {}_kB_\parallel^2)} + \delta_4\right\}, \quad (16)$$

where the small quantity δ_4 is equal to

$$\delta_4 = \frac{C_\parallel({}_iB_\parallel^2 + {}_kB_\parallel^2) + (C_\perp + C_\parallel) B_\perp^{*2}}{D_0}. \quad (17)$$

Now we determine, taking into account Eq. (6), the experimental values of $D_\parallel^\infty/D_0$ according to Eq. (16), computing δ_4 with the approximations $C_\perp B_\perp^{*2} = C_0 B_\perp^2$ and $C_\parallel = C_0(1+p)^3 = C_\perp$ (see column 15 of Table 1). Because of these approximations δ_4 will be underestimated, and consequently these values will be somewhat less than the true values.

Comparing now the values of $D_\parallel^\infty/D_0$, obtained by Eqs. (12) and (16), and averaging the results for blocks of different lengths (columns 13 and 15 in Table 1), we see that these values are equal to each other, within the limits of experimental error, and are also equal (within experimental error) to the values in column 14. This indicates that the corrections δ_2, δ_3, and δ_4 are small, and that the systematic errors in $D_\parallel/D_0$ are smaller than the experimental errors shown in Table 1 – these experimental errors everywhere include only the uncertainity in the measurement of the decay constant α. Consequently the values of $D_\parallel/D_0$ in columns 10 and 13 of Table 1 are evidently no less accurate than the values in columns 11 and 14.

Columns 17 and 18 present the calculated and experimental values of $D_{\parallel}^{\infty}/D_0$ for corresponding (square) lattices of channels with a lattice spacing equal to the transverse dimension of a block. The latter values were obtained by division of the quantity $[(D_{\parallel}^{\infty}/D_0)-1]$ (and its error) from column 13 by the quantity η from column 16.

It is apparent from Table 1 that the experimental and calculated values of the longitudinal diffusion coefficient are in good agreement for all the systems studied. These systems had ratios R/λ of the hydraulic radius to the transport mean free path which ranged from 1.34 to 5.33.

CONCLUSIONS

The proposed method using a pulsed neutron source for the study of neutron diffusion in heterogeneous systems consisting of blocks of moderator with a single channel gives the capability of accurately measuring the longitudinal diffusion coefficient $D_{\parallel}$ and its dependence on the channel length. The measured diffusion coefficient is easily converted to the case of a lattice of channels, inasmuch as the system studied can be viewed as an elementary cell of a lattice.

However, in comparison to the usual pulsed-source experiment for the study of diffusion in lattices of channels, the method has some advantages, including:

economy of materials, since a lattice of channels must have significantly larger dimensions;

economy of the measurement time, since for one block geometry one must measure only the logarithmic decrement α of one block with a channel, while for a lattice of channels one must measure twenty or thirty values of α;

increased sensitivity of the method, because the influence of the separated central channel on α is increased almost by a factor of two, as a consequence of the fact that the neutron density attains its maximum at the center of the block.

The inadequacies of the method evidently include:

capability of measuring only the longitudinal diffusion coefficient $D_{\parallel}$;

restriction of the application of the method to the measurement of the diffusion coefficient of lattices with a sufficiently large lattice spacing (in comparison to λ).

The latter restriction is not fundamental and relates only to the described experiment of one central channel in a block. Moreover, if, in a block with transverse dimensions equal to several cells (e.g., four or nine), one successively measures the value of $\Delta\alpha$ associated with one channel, two channels, etc., then one can determine not only $D_{\parallel}$, but also the effect of interaction of the channels. When $D_{\perp}$ of the lattice is known, in the determination of $D_{\parallel}$ by the measurement of $\Delta\alpha$ [Eqs. (12) to (16)], the number of channels (i.e., cells) in a block can be unlimited (the more the number of channels, the more accurately are the corrections δ_i obtained).

LITERATURE CITED

1. Proc. Symp. on Pulsed Neutron Research, Vol. 1, IAEA, Vienna (1965).
2. V. Deniz, J. Ge Ho, and M. Sagot, Nucl. Sci. Eng., 32, 201 (1968).
3. A. V. Stepanov, Preprint of the Physics Institute of the Academy of Sciences of the USSR, Moscow (1969).
4. N. I. Laletin, Atomnaya Énergiya, 32, No. 4 (1972).
5. N. I. Laletin, Atomnaya Énergiya, 7, 18 (1959).
6. I. F. Zhezherun, Atomnaya Énergiya, 34, No. 2, 143 (1972).
7. I. F. Zhezhurun, Atomnaya Énergiya, 14, No. 2, 193 (1963).
8. I. F. Zhezhurun, Atomnaya Énergiya, 16, No. 3, 224 (1964).
9. I. Zhezhurun, Proc. Symp. on Neutron Thermalization and Reactor Spectra, IAEA, Vienna (1968), No. 2, p. 449.
10. I. S. Silin, Preprint No. 11-3363, DIYaI, Dubna (1967).

PRODUCTION OF GAMMA-ACTIVE ISOTOPES IN SOIL BY NEUTRONS WITH ENERGIES UP TO 1 GeV

A. A. Aleksandrov, E. K. Gel'fand,
B. V. Man'ko, Yu. T. Mironov,
B. S. Sychev, and S. I. Ushakov

UDC 551.510.72:614.876

The problem of induced radioactivity is characteristic of high-current accelerators. Accelerators a few hundred meters and more in size frequently employ earth as a shielding material. The radioactivity induced in the soil requires particularly careful study since it cannot be determined a priori what part of this activity will remain at the accelerator site and what part will be leached out by atmospheric precipitation and ground waters, giving rise to a potential danger of contamination of the water supply system.

We investigated the activation of soil samples irradiated in the neutron flux generated by 1 GeV protons at the LIYaF synchrocyclotron of the Academy of Sciences of the USSR. We measured the amounts of various radioactive isotopes leached out of irradiated soil samples.

EXPERIMENTAL METHOD

The soil samples were irradiated for 49 days. The container with the samples was placed between the accelerator vacuum chamber and the external proton beam channel. The main source of neutrons was the first section of the external channel. The angle between the proton beam and the direction from the effective source to the container was approximately 5°. The high-energy neutron spectrum for similar geometric conditions is given in [1]. The container was a box (20 × 40 × 40 cm) made of sheet metal 0.5 mm thick. The soil samples weighing 2-3 kg each were placed in individual polyethylene bags. The samples occupied about 80% of the container. Protons and pions as well as neutrons were present in the irradiation region. The high-energy hadron flux was monitored with the widely used [2] Al^{27} (x, x2p, 3n)Na^{22} reaction having a threshold of ~25 MeV. In accordance with data in [3] the reaction cross section was considered weakly dependent on the kind of primary particles. The thermal neutron flux was monitored with the Co^{59} (n, γ)Co^{60} reaction. The high-energy particle flux averaged over time and the volume of the containers was $1.15 \pm 0.28 \cdot 10^6$ particles/cm^2 sec, and the thermal neutron flux was $5.2 \pm 0.9 \cdot 10^5$ neutrons/cm^2 sec.

After irradiation the soil samples were stored for two months. During this time the short-lived isotopes with $T_{1/2} \ll 1$ month almost completely decay. They are of no particular interest since estimates of possible velocities of ground waters [4] indicate that the activity leached out of the soil does not spread an appreciable distance from the accelerator in less than a month.

The activity was measured with a scintillation gamma-ray spectrometer having a 40 × 40 mm NaI(Tl) crystal, and with a 20 cm^3 Ge (Li) detector.

The gamma spectra were taken for 17 soil samples. Table 1 shows the results of measuring the gamma spectrum of one of the samples two months after irradiation. Six lines were clearly distinguished in the gamma spectra corresponding to the isotopes Be^7, Na^{22}, Sc^{46}, and Mn^{54}.

In addition to the experimental data Table 1 lists the calculated values of the gamma yields. The calculations were made by using the well-known formula

$$q_{kj} = E\varepsilon_{kj}\left(1-\exp\left[-\frac{\tau \ln 2}{T_k}\right]\right)\exp\left[-\frac{t \ln 2}{T_k}\right]\sum_{(i)}\frac{\sigma_{ik}\cdot 6.02\cdot 10^{23}}{A_i}\eta_i,$$

where q_{kj} (photons/g · sec^{-1} is the yield of gamma photons of the j-th energy in the decay of the k-th isotope in 1 g of soil per sec; F (particles/cm^2 sec) is the flux density of particles producing the nuclear reaction

Translated from Atomnaya Énergiya, Vol. 34, No. 3, pp. 177-179, March, 1973. Original article submitted April 17, 1972; revision submitted July 27, 1972.

TABLE 1. Relative Gamma Yields of Various Isotopes Produced in Soil

Parent isotope	Reaction cross section, mb	Radioactive isotope	Half-life, days	Gamma energy, MeV	Number of gamma photons per decay	Specific yield of gamma photons, photons/g sec		Specific yield of gamma photons at stauration,* quantum/g·sec
						calc.	expt.	
C^{12} O^{16} Al^{27} Si^{28}	10 7 9,1 9,1	Be^{7}	53,6	0,477	0,123	6,2	6,2±0,1	29
Na^{23} Mg^{24} Al^{27} Si^{28}	36,6 28,2 14,5 14,5	Na^{22}	950	0,511 1,275	1,80 1,00	8,7 4,8	7,6±0,2 4,3±1,6	260 144
Fe^{56}	27,6	Cr^{51}	27,8	0,325	0,09	0,29	†	1,82
Fe^{56}	6,84	Sc^{46}	84	0,887 1,119	1,00 1,00	1,05 1,05	1,3±0,1 1,4±0,1	5,2 5,2
Fe^{56}	54,1	Mn^{54}	291	0,835	1,00	4,00	4,8±0,1	41
Fe^{58}	1 b	Fe^{56}	45	1,098 1,289	0,56 0,44	0,115 0,091	$<0,2$ $<0,2$	0,55 0,43

*Calculated by Eq. (1), $t = 0$, $\tau \to \infty$.
†Not reliably indentified.

under consideration; ε_{kj} is the number of photons of the j-th energy per decay of the k-th isotope; τ is the time of irradiation; T_k is the half-life of the k-th isotope; t is the time after cessation of irradiation; σ_{ik} (cm^2) is the cross section for the formation of the k-th isotope from the i-th isotope, averaged over the primary particle spectrum, A_i is the atomic weight of the i-th isotope; η_i is the weight fraction of the i-th isotope in the soil.

The change in the container itself of the spectrum of the high-energy particles incident on it was not taken into account in the calculation. The values of the reaction cross sections were taken from [2, 3, 5-9].

The average chemical composition of all soil samples, and the chemical composition of sample No. 10 are listed in Table 2.

The experimental values of the yields of isotopes for various samples vary within limits corresponding to the change in chemical composition of the soil.

In addition to the specific activity of the soil measurements were made of the degree of leaching of the various isotopes, defined as the ratio of the specific activity of the isotope in question leached out by water, to the specific activity in the soil, for a mixture of equal masses of soil and water. The measurements were performed in the following way. Equal masses of soil and water were thoroughly mixed, and the mixture allowed to stand. The water above the sediment, appearing completely transparent, was poured off into a container to be placed on the detector. Then the specific activity of the substances dissolved in water was measured one day, two months, and four months after mixing. Table 3 shows the ratios of the gamma yields of radioactive isotopes dissolved in water to the specific gamma yield from radioactive isotopes in irradiated soil. These ratios, expressed in percent, are called the leaching factors. It is clear from Table 3 that the isotope Na^{22} has the largest leaching factor, with the isotope apparently reaching its maximum concentration in water in a few days. An insignificant amount of leaching of Mn^{52} was detected with the semiconductor detector. Leaching of the other isotopes was not detected. Very similar results for the degree of leaching of radioactive isotopes were reported in [10].

In addition to isotopes emitting gamma rays, pure beta emitters are also formed in soil. Estimates show that the most active isotope of this type will be Ca^{45}. The saturated specific activity of Ca^{45} (Table 1) is estimated as 4.2 decays/g·sec for our experimental conditions. This value is only about one fortieth of the specific activity of Na^{22}.

TABLE 2. Chemical Composition of Soils (wt. %).

Sample	H	C	O	Na	Mg	Al	Si	S	K	Ca	Fe
Soil*	0,98	0,89	50,7	†	1,23	16,3	20,5	0,5	†	3,95	4,95
Sample No. 10	0,40	0,80	50,0	†	1,46	12,0	24,8	0,44	†	4,0	6,1

*Average over 17 samples.
†Within the limits of acuracy of the chemical analysis the element was not detected.

TABLE 3. Values of Leaching Factors of Radioactive Isotopes.

Isotope	Time after mixing		
	24 h	2 months	4 months
Be^7	<1	<1	<1
Na^{22}	12 ± 3	17 ± 2	18 ± 3
Sc^{46}	<7	<10	<7
Mn^{54}	<5	5 ± 3	<5

The following conclusions can be drawn from our experiments:

1) The measured values of the gamma yields of various isotopes in soil are in satisfactory agreement with the calculated values if account is taken of the error in the reaction cross sections for spallation, which apparently is not less than 15%.

2) The largest saturated specific activity corresponds to the isotope Na^{22} which experiences the greatest leaching from the soil, up to 20 wt. %.

3) Pure beta emitters do not contribute significantly to the total specific activity of an earthen shield around a high-energy accelerator.

The authors thank I. R. Zolotykh and V. S. Frolov for help in the selection of the soil samples, D. I. Berezhnov and A. G. Khramtsovaya for performing the chemical analyses, and P. P. Vaishnisyi for placing the Ge(Li) detector at our disposal.

LITERATURE CITED

1. B. V. Man'ko and B. S. Sychev, Trudy Radiotekhnicheskogo Instituta, No. 9, RTI, Moscow (1971), p. 117.
2. N. A. Perfilov, O. V. Lozhkin, and V. I. Ostroumov, Nuclear Reactions Induced by High-Energy Particles [in Russian], AN SSSR, Moscow–Leningrad (1962).
3. G. Rudstam, Z. Naturf., 21A, 1027 (1966).
4. G. Higgins, J. Geophys. Res., 64, 1509 (1959).
5. E. Bruninx, High-Energy Nuclear Reaction Cross Sections, CERN 61-1 (1961); CERN 62-9 (1964).
6. S. Charalambus and A. Rindi, Nucl. Instrum. Methods, 56, 125 (1967).
7. J. Cline, Nucl. Phys., A169, 437 (1971).
8. I. V. Gordeev, D. A. Kardashev, and A. V. Malyshev, Nuclear Physics Constants [in Russian], Gosatomizdat, Moscow (1963).
9. D. Hughes and R. Schwartz, Neutron Cross Sections, Second Edition BNI, New York (1958).
10. M. Awschalom et al., IEEE Trans. Nucl. Sci., 18, 739 (1971).

ACCELERATION OF ELECTRONS IN THE SLOW-WAVE FIELD OF A PLASMA WAVEGUIDE

A. M. Egorov, Ya. B. Fainberg,
V. I. Kurilko, A. F. Kivshik,
L. I. Bolotin, and A. F. Bats

UDC 533.9

Experimental investigations carried out at low signal levels have confirmed the existence of slow waves in a plasma waveguide and have verified the dispersion relationships predicted by theory [1-3]. Further investigations [4] showed that the slowing-down properties of a plasma waveguide are preserved up to power values of the order of several megawatts.

Previous experimental investigations [4] were confined to the study of the dispersion properties of the plasma waveguide and the topography of the electromagnetic fields. The present study is devoted to an experimental investigation of the interaction between an electron beam and the field of a slow wave of finite amplitude in an anisotropic plasma waveguide. The purpose of the study is to detect the capture of the particles of an injected beam by the slow wave of such a waveguide; to measure the variation of the main parameters of the beam of captured particles as functions of the characteristics of the plasma, the external magnetic field, and the level of superhigh-frequency (SHF) power; and to verify how closely these functional relationships agree with the basic laws predicted by theory.

A block diagram of the experimental installation is shown in Fig. 1. The plasma waveguide consisted of a plasma-beam discharge device in a glass tube 50 mm in diameter and 200 cm long. The waveguide diameter was 20 mm. The ionization was effected by an electron beam with an energy of 6-10 keV and a current of 5 A. The waveguide was placed inside a copper shield 100 mm in diameter and in a constant magnetic field. The SHF power was fed from a KIU-12 klystron amplifier (P_u = 1-16 MW, τ_u = 2.5 μsec, f = 2800 MHz). The plasma density was measured by means of SHF probing with a 3 cm signal.

The SHF energy introduced into the plasma waveguide is propagated along the waveguide in the form of a slow wave whose phase velocity v_{ph} is determined by the density of the plasma, the intensity of the magnetic field, the geometry of the plasma, and the amplitude of the wave [1, 6]. For sufficiently large values of the amplitude of the longitudinal field of this wave (E_0) and the energy of the beam of injected particles, $W_{inj} = mv_0^2/2$, the condition for capture of beam particles by the wave field may be satisfied [8]

$$\left(1-\frac{v_0}{v_{ph}}\right)^2 < \frac{2eE_0\lambda}{m_0c^2\beta_{ph}}, \quad \beta_{ph}=\frac{v_{ph}}{c}. \tag{1}$$

Under the conditions of the experiment the phase velocity of the wave in the plasma waveguide varied over the range $0.45c < v_{ph} < 0.6c$. Substituting into (1) the minimum value of injection energy and the minimum value of wave phase velocity (W_{inj} = 6 keV, β_{ph} = 0.45), we obtain for the threshold value of the wave-field voltage $E_{0\,thresh}$ = 5 kV/cm. The beam particles captured by the waves will move along the waveguide with an average velocity equal to v_{ph}, the phase velocity of the wave. The presence of a potential well of the wave leads to the appearance of an oscillatory motion of the captured particles – phase oscillations with a frequency $\Omega^2 \equiv eE_0k_{11}/m$ – which determines (for sufficiently large fields E_0) the width of the energy spectrum of the accelerated beam:

$$W_{\substack{\max\\\min}} = \frac{m}{2}(v_{ph}\pm v_{\Omega max})^2; \quad v_{\Omega max} = v_{ph}\sqrt{\frac{2eE_0\lambda}{m_0c^2\beta_{ph}}}. \tag{2}$$

Translated from Atomnaya Énergiya, Vol. 34, No. 3, pp. 181-184, March, 1973. Original article submitted March 24, 1972.

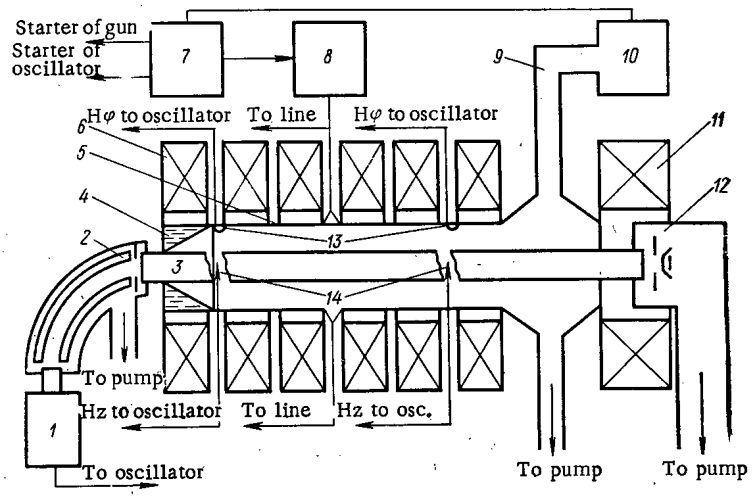

Fig. 1. Block diagram of the installation. 1) Photomultiplier with scintillator (Faraday cylinder); 2) electrostatic analyzer; 3) discharge tubes; 4) load-absorber of SHF power; 5) external shield; 6) solenoid of external magnetic field; 7) starter; 8) measuring SHF generator, $\lambda = 3.2$ cm; 9) regular waveguide; 10) klystron amplifier, $\lambda = 10$ cm; 11) solenoid of injector magnetic field; 12) electron injector; 13), 14) SHF probes.

The current of this beam is proportional to the density of captured particles, and the maximum value of the density can be estimated from the relation $\omega_b^2 = \Omega^2$ [5] ($\omega_b^2 = 4\pi n_b e^2/m$ is the Langmuir frequency of the beam):

$$I = n_b(E_0)\, S v_{ph} \Delta\varphi\,(E_0), \tag{3}$$

where S is the cross section of the beam; $\Delta\varphi$ is the phase width of the capture region.

In the general case the last value is determined by several parameters: the amount by which the field amplitude exceeds the threshold level, the energy spread of the injected beam, the degree of homogeneity of the plasma waveguide, etc. [8]. It is difficult to measure these parameters quantitatively and to take them into consideration, and therefore in what follows we shall measure only the variation of the current as a function of the input power level, and the value of $\Delta\varphi$ will be estimated from experimental data.

The accelerated electrons were observed by means of a photomultiplier on the basis of the luminescence of a scintillator placed at the outlet of an electrostatic analyzer, as well as directly with a Faraday cylinder. Figure 2 shows the oscillograms of the energy spectra of accelerated electrons corresponding to different plasma densities in the waveguide (horizontal scale) and different SHF input power levels (vertical scale). The left-end peak on each oscillogram corresponds to the injected beam, the peak to the right corresponds to the accelerated electrons. These oscillograms show that for a fixed input power level, the accelerated electrons appear only in a particular region of values of plasma density.*

The absence of any particles captured by the wave for low values ($n_0 \leq 10^{11}$ cm^{-3}) and high values ($n_0 \geq 10^{13}$ cm^{-3}) of plasma density is due to the fact that under these conditions the amplitude of the accelerating field is small because the plasma waveguide is not consistent with the regular waveguide [4]. In addition, as the plasma density increases, we observe a decrease in the shunt resistance of the plasma waveguide. As can be seen from the oscillograms (Fig. 2), the amplitude of the current of injected electrons decreases as the accelerated electrons appear, since it is the high-velocity part of the injected beam that is captured first of all when there is acceleration. As a result, the position of the maximum for uncaptured electrons is displaced toward the low-energy end. Calculations based on the obtained spectra indicate that the value of the total current of accelerated and injected electrons remains the same to within 20%. Figure 3 shows

*An increase in the current of injected particles leads to similar results, since changing the current changes the plasma density.

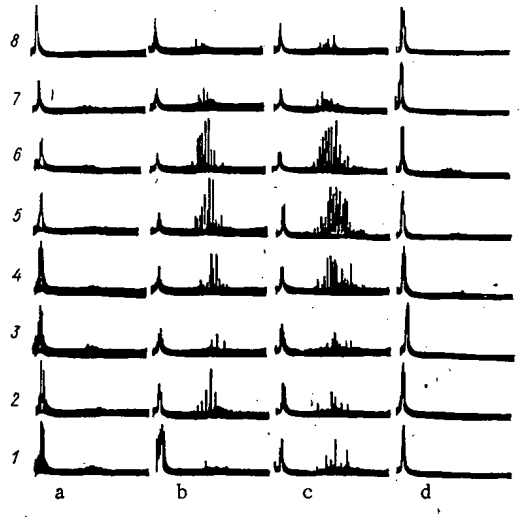

Fig. 2. Oscillograms of electron spectra with variation of plasma density: a) $(0.2\text{-}0.5)\cdot10^{12}$ cm^{-3}; b) $(2\text{-}4)\cdot10^{12}$ cm^{-3}; c) $(5\text{-}7)\cdot10^{12}$ cm^{-3}; d) $(8\text{-}10)\cdot10^{12}$ cm^{-3}; for different SHF power input levels: 1) 5.8 MW; 3) 3.1 MW; 4) 2.3 MW; 5) 1.7 MW; 6) 1.3 MW; 7) 0.9 MW; 8) 0.67 MW. Full scale on the oscillograph beam scan corresponds to an energy of 160 keV.

the variation of the current of captured and uncaptured particles, as well as the energy spectra of accelerated (captured) electrons, as functions of injection energy. From the graphs in Fig. 3 it is clear that as the injection energy increases, the current of accelerated electrons increases more rapidly than the injection current. This is attributable to the fact that for a fixed wave-field amplitude the capture conditions improve with increasing injection energy (as $v_{inj} \to v_{ph}$). The half-width of the accelerated-particle spectrum, determined by the intensity of the accelerating field and the phase velocity of the wave, remains unchanged. The phase velocity of the electromagnetic wave in our experiments was (0.45-0.6)c. These values of phase velocity were obtained for direct measurements of the field distribution [4], which were in satisfactory agreement with the theory and with the results obtained by measuring the position of the current maximum in the spectrum of accelerated electrons. Figure 4 shows how the spectrum of captured electrons varies with the intensity of the magnetic field. It can be seen that as the magnetic field intensity increases, the position of the current maximum in the spectrum of accelerated electrons, determined by the phase velocity, is displaced toward the high-energy end. The increase in phase velocity as the magnetic field

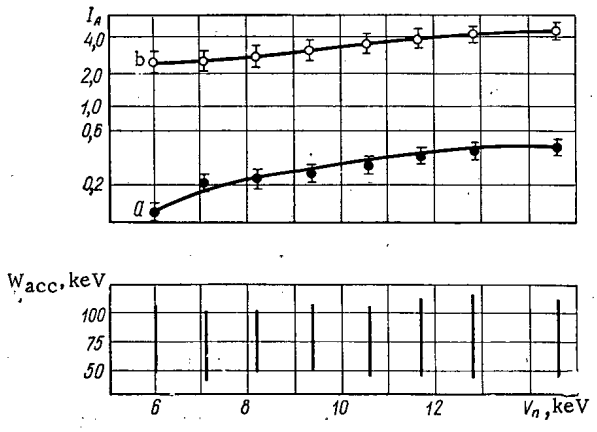

Fig. 3

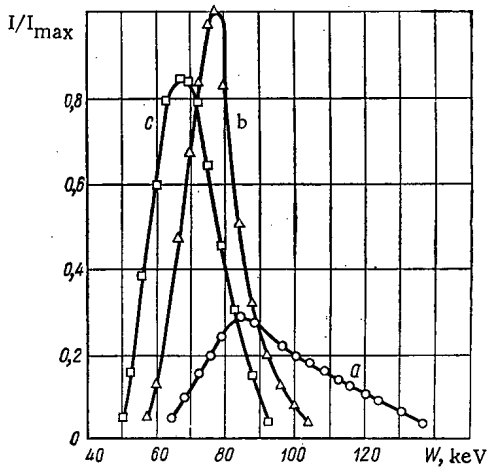

Fig. 4

Fig. 3. Current of injected electrons (b) and accelerated electrons (a) (top graph) and half-widths of the accelerated-electron spectrum (bottom graph) as functions of injection energy: $P_{SHF} = 2.5$ MW; $\omega_H = 2.04\cdot10^{10}$; $\omega_0 = 1.13\cdot10^{10}$.

Fig. 4. Spectra of current of accelerated electrons as functions of the intensity of the external magnetic field for $W_{inj} = 11.7$ keV; $\omega_0 = 1.13\cdot10^{10}$; $P_{SHF} = 3$ MW; a) $\omega_H = 2.29\cdot10^{10}$; b) $\omega_H = 2.11\cdot10^{10}$; c) $\omega_H = 1.94\cdot10^{10}$.

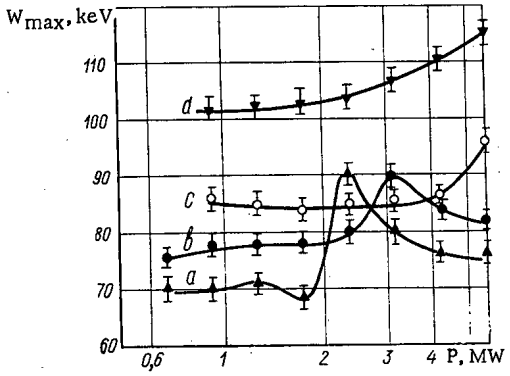

Fig. 5

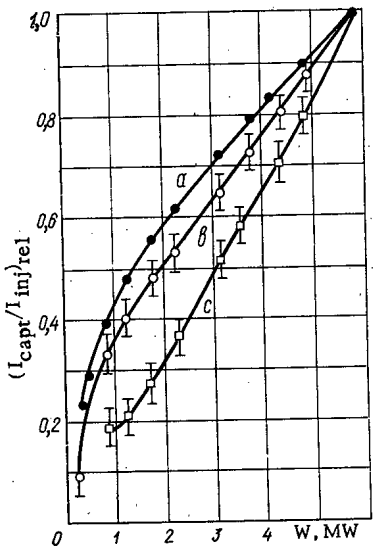

Fig. 6

Fig. 5. Energy at the maximum value of the accelerated current, as a function to the SHF power input for various values of the external magnetic field: a) $\omega_H = 1.88 \cdot 10^{10}$; b) $\omega_H = 2.04 \cdot 10^{10}$; c) $\omega_H = 2.18 \cdot 10^{10}$; d) $\omega_H = 2.33 \cdot 10^{10}$.

Fig. 6. Coefficient of capture as a function of the SHF power input: a) calculated coefficient; b), c) experimental values for $\omega_H = 1.88 \cdot 10^{10}$ and $\omega_H = 2.18 \cdot 10^{10}$, respectively.

increases is a consequence of the theory of propagation of electromagnetic waves in a plasma waveguide [1]. Independent measurements of the phase velocity of the wave also confirm this theoretical deduction. The differences in the shapes of the spectra can be explained by the following: for a magnetic field intensity of $H_0 = 1100$ Oe (curve c) there is an increase in energy losses, since in this case the working frequency is close to the cyclotronic electron frequency, and the amplitude of the accelerating field of the wave is relatively small. The maximum value of the accelerated-particle current in this case is also less for $H_0 = 1200$ Oe (curve b). The widening of the spectrum for $H_0 = 1300$ Oe (curve a) is attributable to the fact that in this case the amplitude of the field, which determines the energy spread of the captured particles, is relatively high. An increase in the power input in Fig. 5 leads to a widening of the accelerated-electron spectrum and a displacement of the current maximum in the spectrum toward the high-energy end. The latter result is due to the fact that as the SHF power level increases, the phase velocity of the wave increases as a result of nonlinear effects [6].

An estimate of the accelerating-field intensity can be obtained from measurements of maximum and minimum energy values in the spectra of accelerated electrons. For $W_{max} = 160$ keV, $W_{min} = 6$ keV, and $\beta_{ph} = 0.5$, the field intensity E_0 is 10 kV/cm.

Figure 6 shows the experimentally measured curves and the calculated curve for the coefficient of capture (the ratio of accelerated-electron current to injection current) as a function of the SHF power level. To determine the experimental value of the effective phase width of the cluster $(\Delta\varphi)_{eff}$ in (3), we defined the theoretical and experimental capture-coefficient values at maximum input power level, $P_{SHF} = 5.8$ MW, to be equal. It was found that $(\Delta\varphi)_{eff} \cong 0.2$.*

Thus, the above results found by experimental measurement of the parameters of the beam of accelerated electrons confirm the electron-capture mechanism assumed for the slow wave of a plasma waveguide. The variation of accelerated-particle current as a function of wave phase velocity is found to be in complete agreement with the theory, and so is the variation of accelerated-particle current as a function of the input power level.

*The capture conditions were the same as in ordinary linear accelerators [9]. The calculated coefficient of capture was approximately 0.19.

The results of the above experimental investigation of a plasma waveguide confirm that there is effective capture of electrons by the wave field. In order to ensure acceleration of the electrons and an increase of the captured-particle current, we must ensure an adiabatic increase of the phase velocity of the waves along the waveguide and must increase the amplitude of the accelerating field [8]. To do this, we must increase the intensity of the external magnetic field and decrease the diameter of the plasma waveguide, while preserving the running density of the plasma. For a field intensity of the order of 30-50 kV/cm, the plasma waveguide under consideration is apparently most effective for accelerating ions in the (0.3-0.8)c phase-velocity range, owing to the existence of radial and phase stability at the same time [5, 6]. For a field intensity of the order of 10 kV/cm, the electrons acquire an energy of the order of the rest energy at a short distance. Therefore, in order to accelerate the electrons, we must develop plasma waveguides with a phase velocity close to the velocity of light. The prospects for achieving electron acceleration in a plasma waveguide have been improved by the recently discovered effect of focusing the wave field with $v_{ph} = c$ within a plasma waveguide [7].

LITERATURE CITED

1. Ja. Fainberg, Proc. Symp. CERN, 1, 84 (1956).
2. Ya. B. Fainberg, Reports at the All-Union Conference on High-Energy Particle Physics [in Russian], Izd-vo AN SSSR, Moscow (1956), p. 182.
3. O. G. Zagorodnov et al., Proc. Symp. CERN, 1, 685 (1959). O. G. Zagorodnov, A. F. Kivshik, and V. P. Prishchepov, Ukr. Fiz. Zh., 14, 641 (1969).
4. A. M. Egorov et al., At. Énerg., 25, 9 (1968).
5. Ya. B. Fainberg, At. Énerg., 6, 437 (1959).
6. Ya. B. Fainberg, At. Énerg., 6, 441 (1959).
7. A. K. Berezin et al., Zh. Éksperim. i Teor. Fiz., 13, 498 (1971).
8. Ya. B. Fainberg, in: Theory and Design of Linear Accelerators [in Russian], Gosatomizdat, Moscow (1962), p. 19.
9. O. A. Val'dner, O. D. Vlasov, and A. V. Shal'nov, Linear Accelerators [in Russian], Atomizdat, Moscow (1969).

DOSE FIELDS OF A CLINICAL PROTON BEAM STUDIED WITH A RADIATION TRACK-DELINEATING FLAW DETECTOR

M. F. Lomanov, G. G. Shimchuk, and R. M. Yakovlev

UDC 621.039.8:539.12.04

The dosimetry of a clinical proton beam raises problems, the solution of which, requires coverage of a vast range of doses. The proton beams make it possible to concentrate the dose within a specified, sharply delineated volume. Knowledge of the dose absorbed by the organs which are most involved in pathological injury is imperative. This dose, even if 0.1% of the absorbed dose at the seat of the injury, must be known in any case. Unfortunately, measurements in this range are hampered by the conversion from proton radiation to mixed radiation, on account of neutrons appearing, particularly at the edges of the beam.

Ionization chambers, semiconductor detectors, nuclear photographic emulsions, photographic films, etc., are employed in order to measure the proton dose distribution at dose rates on the order of 1000 rad/sec. Detectors with excellent spatial resolution are required when using a narrow beam of protons to perform local radiation operations replacing surgical operation on the brain. The dose rate in some cases is exceedingly high: 100 rad in pulses lasting 1.6 μsec and repeating every 4 sec in the pulsed beam of the ITÉF proton synchrotron. This prompted the need to develop special techniques of measurement.

Instruments designed to indicate the absorbed dose are commonly employed in measurements taken directly in the beam, since the biological effects of the high-energy protons and of the standard x-radiation (220 keV) are approximately the same. When mixed radiation is to be measured, differences in biological effects as a function of the quality of radiation must be measured. The criteria for equivalence between the physical dose and the biological dose must vary over a range of dose measurements governing six orders of magnitude. We therefore rely on Prêtre's suggestion [1] to deal with the quality factor K at two fundamentally different levels: 1) in the case of chronic exposure at low dose levels and low dose rate, when genetic disturbances and injuries to critical organs are of paramount importance; 2) in the case of acute exposure to large doses and at high dose rate (in radiation accidents and in radiation therapy).

In the first variant, the quality factor attains its highest possible values according to ICRU recommendations. The spread of experimental data on the basis of which K is determined supports the statement that these values are known with an uncertainty of two to four times, and probably they are on the high side of the true value [1]. In the second variant, the quality factor can be put equal to the RBE (relative biological effectiveness), which also varies over a rather broad range, depending on the conditions under which it is determined, and depending on the biological reaction under investigation.

For brevity, we term the quality factor in the first variant the "genetic" quality factor K_{gen}, and the quality factor in the second variant the "therapeutic" quality factor K_{ther} (Fig. 1). In view of the uncertainty referred to, Prêtre recommends adhering to permissible values falling within the zones indicated in Fig. 2 when calibrating any instrument taken as the rem-gage. We also plot (Fig. 2) values of the dose equivalent divided by unit neutron flux, in keeping with the remarks on the quality factor. Taking those data into account, we then consider the possibility of utilizing radiation flaw-detection, track-delineating detectors to measure the dose distribution in proton beams used in therapeutic irradiation, and also to measure the distribution of the equivalent dose of mixed radiation around the beam. The latter makes it possible to determine how great the total exposure of the body of the patient is when a program of radiation therapy is decided upon.

Translated from Atomnaya Énergiya, Vol. 34, No. 3, pp. 185-192, March, 1973. Original article submitted March 24, 1972.

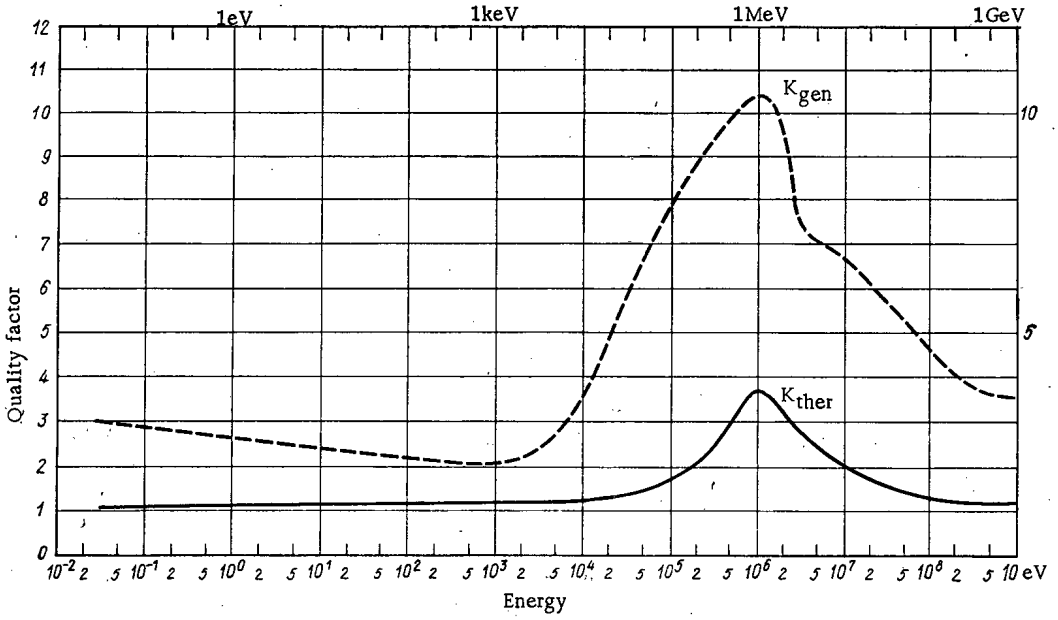

Fig. 1. Quality factors K_{gen} and K_{ther} for neutrons [1].

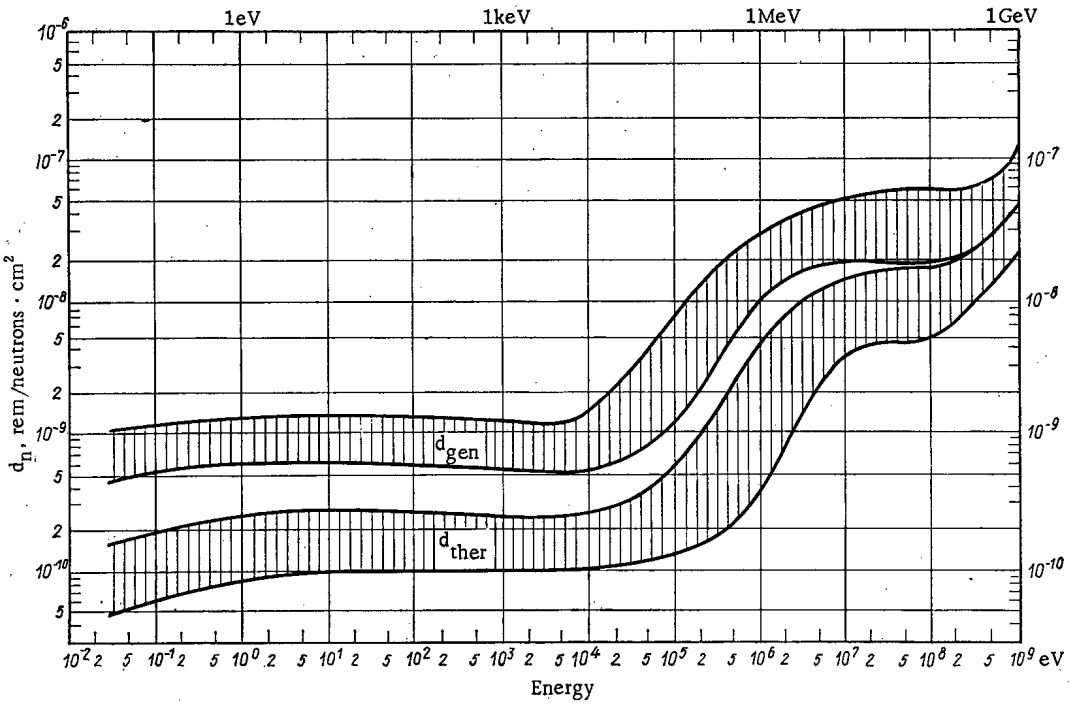

Fig. 2. Zones of dose equivalent values for neutrons.

Note that this method can also find application in ordinary professional dosimetry, in mixed radiation of fast neutrons and protons. We therefore take other possibilities, in addition to the clinical application of the method, into account. However, in view of the difficulties associated with the low sensitivity of the method, experimental validation of the use of the method for professional dosimetry is not discussed in this article.

Use of Radiation Flaw-Detection, Track-Delineating Detectors in Rem-metry of Protons and Accompanying Radiations

Radiation flaw-detection track detectors are employed to record the flux of particles on the basis of fission products of heavy nuclides (U, Th, Bi, Pu, Np, etc.). Fission products knocked out of the target

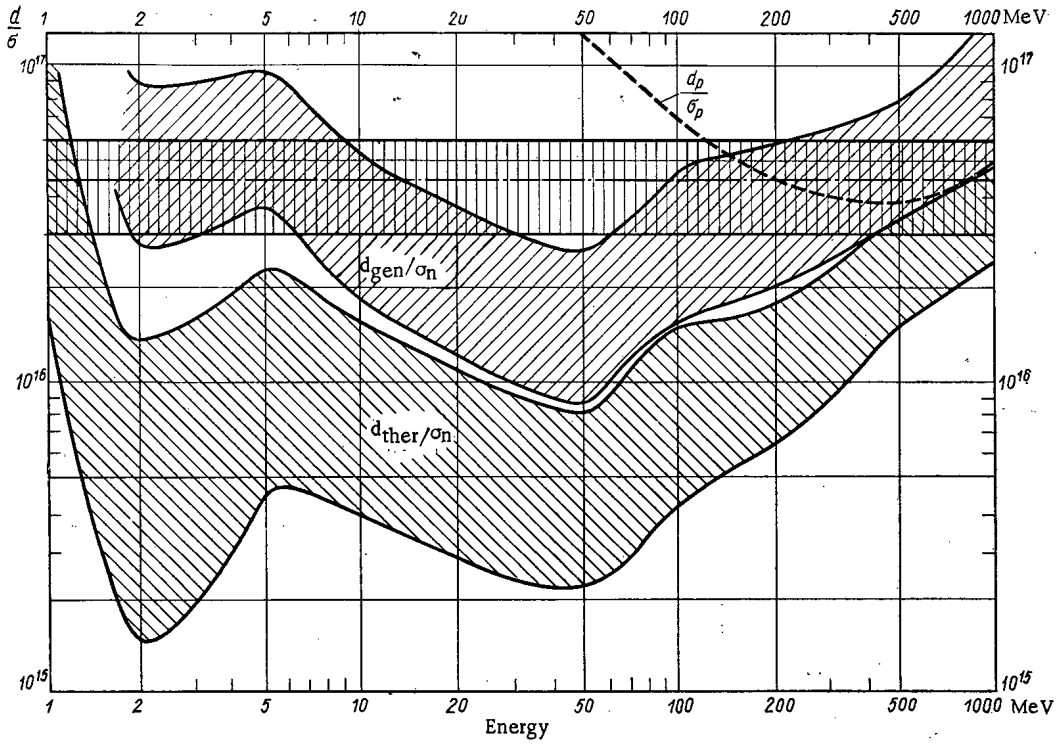

Fig. 3. Zones of d_n/σ_n and d_p/σ_p values for U^{238} detector.

leave traces of injuries in the substrate or glass, mica, or dacron. Following etching (e.g., etching glass in 3% hydrofluoric acid), these tracks can be seen with a microscope [2].

The flux density of protons and neutrons was determined from the number of tracks per unit area, respectively n_p and n_n (tracks per cm^2):

$$\Phi_p = \frac{n_p}{Nl\sigma_p\eta}, \quad \Phi_n = \frac{n_n}{Nl\sigma_n\eta} \tag{1}$$

where σ_n/σ_p are the effective cross sections of the reaction in which the nucleus is split by a bombarding neutron [3, 4] or proton; N is the number of nuclei per gram; η is the product of the recording efficiency for fragments recorded by the substrate and the scanning efficiency; l is the thickness of the layer of fissionable material. In assigning the thickness l, we must bear in mind the fact that the accuracy in the determination of the flux Φ improves as l is decreased, but that this means a lower yield of products. While the highest possible yield of products is needed for the experiment to succeed, thick layers of fissionable materials commensurate in thickness with the maximum path length of the products are actually used. The effective thickness l is arrived at by comparing the yield of products in the layer under investigation and thin layers of known thickness.

Let us consider the conditions under which a count of the number of products would furnish information useful in determining the equivalent dose of mixed radiation. In the case of fast protons, the equivalent dose is the same as the absorbed dose:

$$D_p = 1.608 \cdot 10^{-8} \frac{dE}{dx} \Phi_p = d_p \Phi_p \text{ rad}, \tag{2}$$

and in the case of neutrons it is

$$D_n = d_n \Phi_n \text{ rem}. \tag{3}$$

The equivalent dose of mixed proton and neutron radiation is arrived at by summing over the spectrum of radiation energies:

$$D = \sum_E D_p + \sum_E D_n = \sum_E \frac{d_p n_p}{Nl\sigma_p\eta} + \sum_E \frac{d_n n_n}{Nl\sigma_n\eta} \text{ rem}, \tag{4}$$

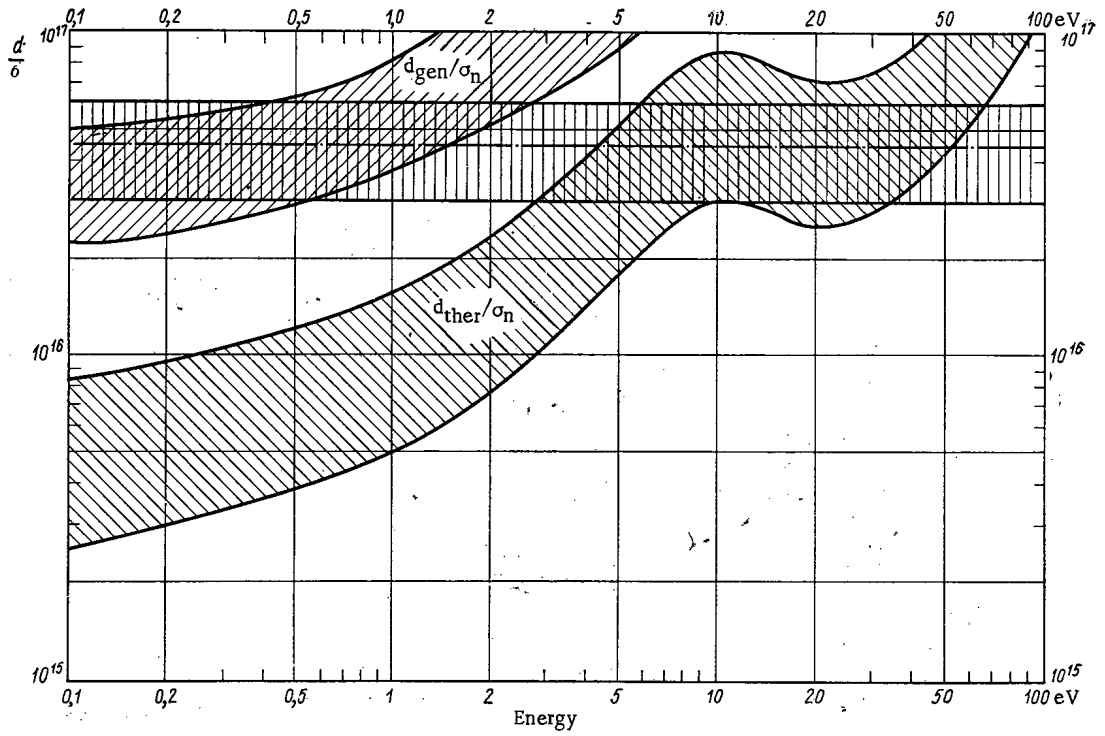

Fig. 4. Zones of d_n/σ_n ratios for U^{238} detector with admixture of U^{235} (0.4%)

where d_n is the equivalent dose per unit neutron flux, the energy dependence of which is plotted in Fig. 2 for different conditions observed in the determination of the quality factor. The value of D is proportional to the observed number of fission products $n = \Sigma n_p + \Sigma n_n$, for that portion of the spectrum in which all of
E E
the ratios d_p/σ_p and d_n/σ_n are equal. The values of those ratios for U^{238} are shown in Fig. 3. In the case of neutrons, two zones corresponding to different determinations of K_{gen} and K_{ther} are plotted. For example, let the beam of protons have energy 200 MeV. Corresponding* to this we have the ratio $d_p/\sigma_p = 4.5 \cdot 10^{16}$ rem. The same ratios d_n/σ_n are typical of neutrons with energies above 2 MeV, with ratio accuracy to within two. Hence, a product detector with a U^{238} target satisfies the rem-metry conditions with respect to the criterion K_{gen} for the indicated region of the spectrum. The range of permissible d/σ ratios corresponds to the hatched band in Fig. 3. Moreover, we can infer that the admixture of slower protons with energies in the range 100 MeV < E_p < 200 MeV will not distort the results of the measurements appreciably. Consequently, the U^{238} fission detector makes it possible to measure the proton dose and neutron dose with their quality factors K_{gen}, in the case of a beam of 200 MeV protons, precisely in that range of the spectrum of energies within which practically all of the primary and secondary radiation falls as a rule.

Determination of K_{ther} is a more difficult task. As is evident in Fig. 3 (bottom curve), in that case the neutron dose will turn out several times too high. But in the transition to higher proton energies, we draw gradually closer to the K_{ther} conditions. The method is unworkable for proton energies below 100 MeV, since the d_p/σ_p curve climbs steeply upward. But the contribution made by secondary neutrons also declines abruptly in that region, so that the need to conduct rem-metry is lifted.

The use of different isotopes greatly expands the possibilities of track-delineating detectors. We begin by considering how sensitivity can be increased over the broadest range of energies when the isotope U^{235}, which is present as a rule in a U^{238} sample, is added to U^{238}. Since the cross section of U^{235} fission by thermal neutrons is 100 or more times greater than the cross section of U^{238} fission by fast neutrons, and in addition the quality factor of the thermal neutrons is 1.3 to 1.5, even an insignificant addition (0.4%) of U^{236} makes it possible to record thermal neutrons with sufficient effectiveness. Figure 4 shows curves

*At that ratio d_p/σ_p, and detector thickness 1μ, the equivalent dose for 200 MeV protons at $n = 10^4$ products /cm^2 is found to be 200 rem ($\eta = 1$).

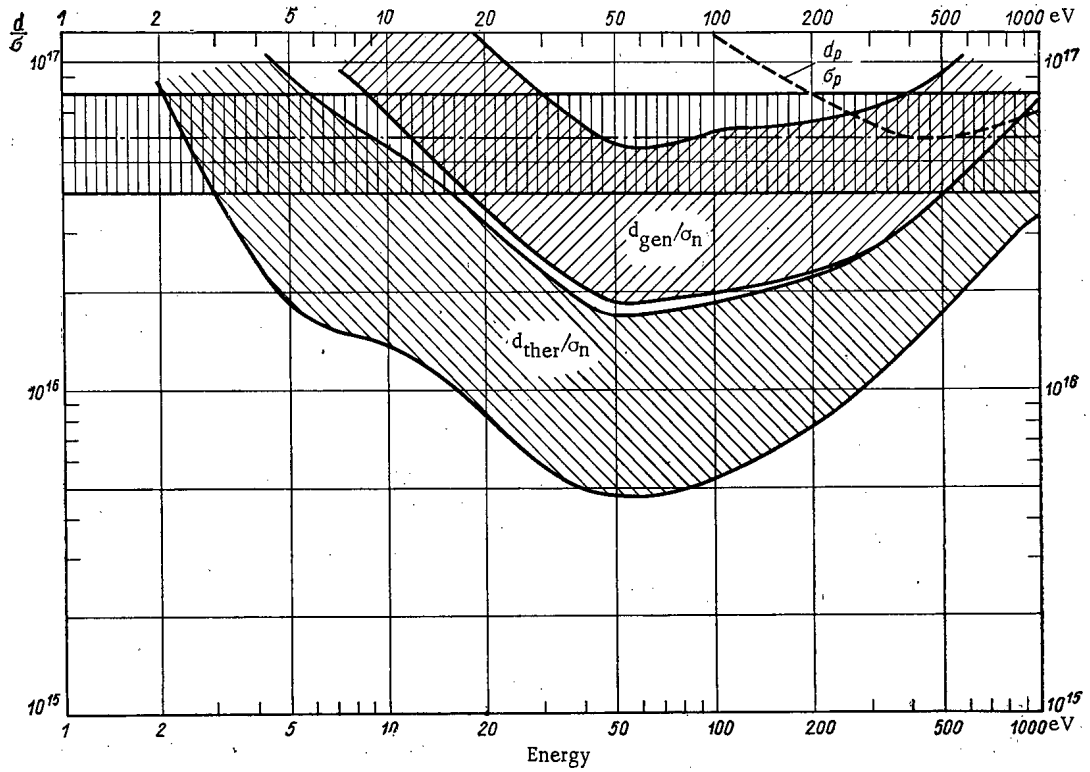

Fig. 5. Zones of d_n/σ_n and d_p/σ_p values for thorium detector.

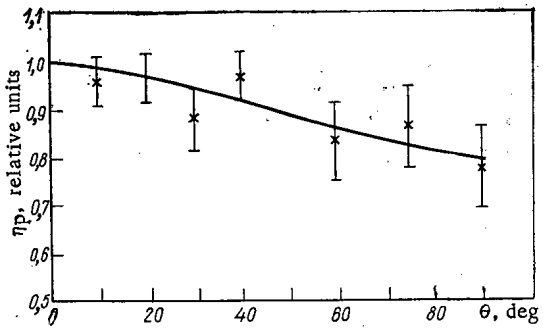

Fig. 6. Fission product yield as a function of the angle between bismuth detector and incident beam.

for this detector similar to the curves in Fig. 3. Detectors of that type show little sensitivity even in the range of intermediate neutrons. This shortcoming can be removed, obviously, if we make use of such isotopes as Pu^{240} and Np^{237}, for which the fission range is broader and includes intermediate neutrons. But the problem of using these isotopes in rem-metry of a clinical beam remains open, since the cross sections for fission of these isotopes by protons has not yet been measured. A study of the feasibility of using Th^{232}, which occurs in nature in rather pure form, is called for. The ratio d/σ for thorium is shown in Fig. 5.

The above arguments were advanced under the assumption that the detectors were placed at right angles to the incident beam. There is of course some anisotropy in the fission of heavy nuclei by protons [5]. The fission product yield was measured at different angles of beam incidence on the detector. Figure 6 shows the dependence of the fission products, as measured on bismuth, on the angle between the detector and the incident beam. The resulting angular dependence of fission product yields is insignificant, which makes it possible to employ detectors even when the angle of incidence of the proton beam on the detector is known only poorly.

Rem-metry of Clinical Proton Beam

From the above analysis, we can safely conclude that the rem-metry method using radiation-flaw track detectors is inferior in accuracy only to the method of nuclear photographic emulsions, which makes

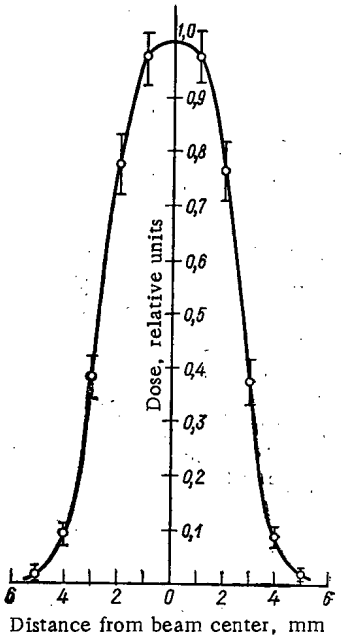

Fig. 7. Dose distribution in beam of 200 MeV protons produced with the aid of bismuth detector (beam diameter 6 mm).

it possible to measure the spectrum of particle energies and, on that basis, to compute the equivalent dose. But nuclear photographic emulsions are difficult to use when measurements are carried out in the immediate vicinity of the beam, since too large a dose is absorbed in the detectors at the beam intensities typical of clinical exposure conditions. In addition, data processing in this method is an exceedingly difficult job.

The method of track-delineating detectors is free from those shortcomings, and makes it possible to measure the dose distributions of narrow beams, resolution 0.2 mm, to within ±10%, and if necessary to attain even higher accuracy and resolution.

Both of these methods were utilized in the realization of a broad program of measurements carried out on the clinical beam of the ITÉF synchrotron [6]. The basis measurements were taken with the aid of track detectors capable of yielding fast results. Nuclear photoemulsions were employed in order to secure information on the spectral composition of the radiation (data obtained from measurements using nuclear photoemulsions will be published separately).

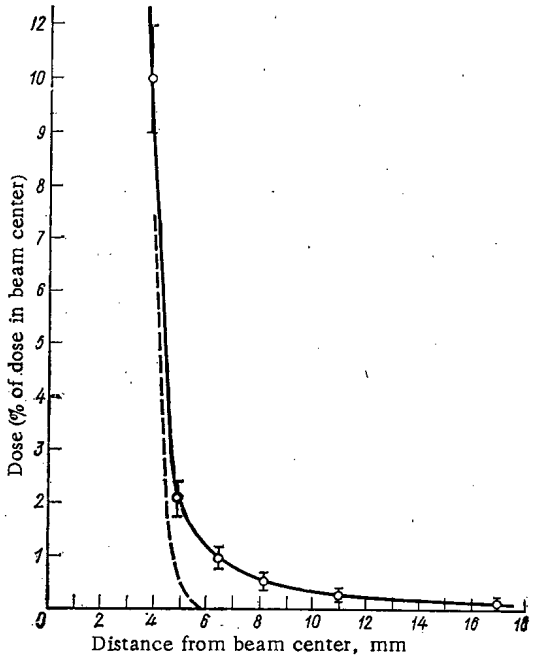

Fig. 8. Dose distribution at edge of beam of 200 MeV protons, measured with the aid of U^{238} detector (beam diameter 6 mm).

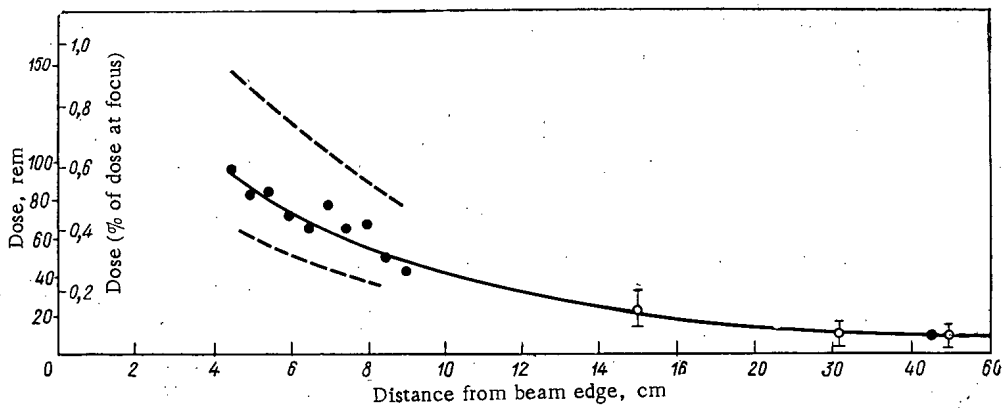

Fig. 9. Dose distribution near beam of 155 MeV protons (dose at focus 16 krad, collimator 7 × 9 cm): ●) track-delineating detector; ○) nuclear photographic emulsions.

Below, we discuss results of measurements performed on the narrow beam of 200 MeV protons. The collimator, with exit holes 6 mm in diameter, and a precollimator with holes 5 mm in diameter was placed 40 cm ahead of it. Figure 7 shows the dose distribution obtained in a homogeneous phantom with the aid of a bismuth detector embedded in transparent plastic at a depth of 6.3 cm.

When the exposure dose is increased tenfold, the central portion of the distribution becomes overexposed, while the peripheral portion is measured to a high accuracy (up to 1% isodose). Figure 8 shows the dose distribution on the edge of the beam, obtained by irradiating a phantom of the same geometry. The broken curve represents the dose distribution due to protons alone. The discrepancy between the predicted curve and the experimental curve can be explained by the contribution made by neutrons, and also by that made by protons, scattered by the edges of the collimator.

Irradiation at a still higher dose level is required in order to obtain lower levels of dose distribution. Figure 9 shows the dose distribution at points remote from the broad beam of 155 MeV protons. The diagram also shows results obtained with the aid of nuclear photographic emulsions. The dashed curves indicate the range of possible errors in the method.

* * *

The method described above can be used in the dosimetry of mixed radiation in zones of enhanced radiation hazard: for clinical dosimetry on narrow and broad proton beams used in radiotherapy, for measurements of exposure doses experienced by astronauts, for dosimetry of "hot" spots on an accelerator of heavy charged particles. In those instances, the exposure pattern differs from "traditional" professional exposure regulated by familiar recommendations and instruments in that the radiation hazard criteria are not given such a generous margin on the high side. Prêtre [1] has proposed introducing two distinct types of criteria for radiation hazard, to which he assigns the terms "genetic" and "therapeutic." Prêtre's suggestion is deemed convenient for our purposes in that it makes it possible to utilize the equivalent dose concept in a broader sense – it covers not only ordinary professional exposure, but also emergency exposure situations and even therapeutic irradiation of patients. Consequently, an equivalent dose of mixed radiation of protons and neutrons can be determined in different ways. By selecting specific isotopes as targets for the radiation-flaw track detector, in the choice of diverse criteria over a broad range of proton energies and neutron energies, we can determine readings proportional to the equivalent dose. This method makes it possible to measure the dose distribution with a high resolution, as well as the equivalent dose picked up by the critical organs. Compared to the nuclear photoemulsion method, this method does not require laborious measurements and does cover a broad range of doses. The radiation-flaw track detectors do not record γ-radiation in practice, nor protons and neutrons with energies below fission threshold, and these can be considered shortcomings of the method.

The basic difficulty in rem-metry of mixed radiation consists in the uncertainty of the experimental data on the basis of which the neutron energy dependence of the equivalent dose was obtained. The method

proposed makes it possible to measure the dose directly in rem units at the level of accuracy with which the generally accepted equivalent dose values can be validated.

LITERATURE CITED

1. S. Prêtre, "Neutron depth doses in man and corresponding quality factors," FMB, 70-16, Zürich (1971).
2. R. Brandt et al., CERN, 71-2 (1971).
3. Fast Neutron Physics [in Russian], Vol. 2, Atomizdat Moscow (1966), p. 704.
4. Neutron Cross Sections, BNL-325, Supplement No. 2, Vol. 2 (1965).
5. A. I. Obukhov and N. A. Perfilov, Usp. Fiz. Nauk, 92, No. 4, 621 (1967).
6. S. I. Blokhin et al., "Clinical dosimetry of high-pulsed power proton beams," IV All-Union Conference on the Dosimetry of High-Intensity Beams of Ionizing Radiations [in Russian], Moscow (1971).

ABSTRACTS

OPTIMIZATION OF REACTOR REACTIVITY BEHAVIOR BY BURNABLE POISONS

A. V. Voronkov and V. A. Chuyanov

UDC 621.039.515

Attainment of a high fuel burnup level in reactors involves substantial difficulties, and complexities in burnup control is one of the reasons for those difficulties. To simplify the system of moving control devices, use is frequently made of burnable poisons [1, 2]. In some cases, a specified law of reactivity variation during the reactor campaign [3] is arrived at successfully through the use of several burnable isotopes in layered blocks. The annotated paper discusses the following problem: how to devise a burnable poison suitable for fashioning some prespecified reactivity behavior throughout the reactor campaign for a specified reactor geometry (or reactor cell geometry) and in the presence of a definite set of absorbing materials.

The mathematical formulation of the problem is presented and application of different types of optimizing functionals is discussed. The principal mathematical features of the problem formulated are pointed out.

1. Campaign optimization, i.e., optimization of reactor behavior with time, with the aid of control over some initial condition (over the initial distribution of burnable poisons), bears relation to incorrectly formulated problems. Large fluctuations in the density of burnable poisons concentrated in small volumes can affect the final result.

2. The requirement that the control variables (concentrations of burnable poisons) be positive is an essential one. This restriction stands in the way of the accuracy of the approximation to the time variation of the reactivity increasing without bound. The extreme-value problem is not the classical problem.

3. Essential difficulties are brought about by the local form of the optimizing functional, which leads to a search for a minimum in the case of surfaces on which discontinuities of the derivative exist. This restricts the range of validity of local methods of searching for a minimum (e.g., the method of steepest descent). The incorrectness of the problem is not discussed in detail in the article, since regularization of the problem takes place automatically, in practical calculations, in the transition to the zone arrangement of burnable poisons. The second and third features occur everywhere, so that they must be taken into account directly or indirectly in the solution of that type of problem.

The effect of the nonclassical nature of the variational problem on the solution of the problem is discussed in the article in the light of simple examples: homogeneous arrangement of the poison in the reactor. It is proved that what is required for the optimal solution as a dependence of the reactor campaign is one or two burnable poisons with microscopic absorption cross sections closest to the absorption cross section of the fuel. The use of a large number of burnable poisons (in classical variational calculus, an approximation of the optimizing functional as close as we wish to zero would be possible [4]). It is evident from the examples cited that the theory of optimal process, in which restrictions on control come under consideration, must be employed in the solution of the extreme-value problem formulated.

LITERATURE CITED

1. V. V. Orlov et al., Paper No. 354, III Geneva Conference (1964) on the Peaceful Uses of Atomic Energy, USSR.
2. A. Radkovskii, in: Nuclear Reactor Physics [in Russian], Atomizdat, Moscow (1959).

Translated from Atomnaya Énergiya, Vol. 34, No. 3, p. 193, March, 1973. Original article submitted March 21, 1972.

3. V. N. Artamkin and A. V. Voronkov, At. Énerg., 22, No. 3, 215 (1967).
4. N. I. Akhiezer, Lectures on Approximation Theory [in Russian], Nauka, Moscow (1965).

SOLUTION OF NEUTRON-DIFFUSION PROBLEMS IN HETEROGENEOUS FLAT REACTORS BY THE DIRECT VARIATIONAL METHOD

N. V. Isaev and I. S. Slesarev

UDC 621.039.51.13

We consider a method of solution of the equation of neutron diffusion in a reactor [1] that consists of arbitrarily positioned multiregion cylindrical modules. By such modules, we mean control rods, separate coaxial zones of the reactor, etc. The calculation of the neutron field in such reactors using finite-difference methods is hindered by the fact that it is necessary to introduce a large number of mesh points. Therefore direct variational methods [2] can prove to be preferable for solving such problems. However, if we do not take into account the reactor geometry, then in order to select coordinate functions we must require too large a number of such functions.

In the paper we propose a method of constructing a two-dimensional neutron field, described by a diffusion equation in the (r, φ) geometry, from solutions of the corresponding one-dimensional problems. It is shown that an arbitrary function $\Phi(r, \varphi)$ from the class of solutions of the diffusion equation can be represented by the superposition of at least two functions $f_1(r, \varphi)$ and $f_2(r, \varphi)$, periodic in φ with period 2π, symmetric with respect to some lines $\varphi = \varphi_1$ and $\varphi = \varphi_2$, respectively $(\varphi - \varphi_2 \neq m\pi;\ m = 0, 1, \ldots)$, i.e., $\Phi(r, \varphi) = f_1(r, \varphi) + f_2(r, \varphi)$. If the reactor has two multiregion modules, positioned on the lines φ_1 and φ_2 and producing an azimuthal dependence of the neutron field, then each of the functions f_i $(i = 1, 2)$ can be represented in the form of a series in one-dimensional functions:

$$f_i(r, \varphi) = \sum_{n, m} a^i_{nm} R_n(r)\, W^i_m(r_i), \tag{1}$$

where r_i is the distance from the center of the i-th module to the point with coordinates (r, φ). The one-dimensional functions $W^i_m(r_i)$ have coordinate origin at the center of the module with number i, and the functions $R_n(r)$ have their origin at the center of the reactor.

The neutron field in a reactor in which there are several modulus can be conveniently represented in the form

$$f_i(r, \varphi) = \sum_{inm} a^i_{nm} R(r)\, W^i_m(r_i). \tag{2}$$

For solution of the initial problem, the functions $R_n(r)$ and $W^i_m(r_i)$ are assumed known, and the unknown coefficients a^i_{nm} are determined from the conditions of the extremal properties of the corresponding functional [2] (e.g., the functional corresponding to the neutron-multiplication constant in the reactor), as for the case of the one-velocity problem, or from the condition of its stationarity [3].

Recommendations are given for the selection of coordinate functions $R_n(r)$ and $W^i_m(r_i)$, obtained from solutions of the "similar" one-dimensional problems. When functionals with "natural" boundary conditions are used [2], the requirements on the satisfaction of the corresponding boundary conditions for one-dimensional functions can be relaxed. Carrying out the actual calculations showed that when series (2) is used we succeed in reducing the number of coordinate functions necessary for a satisfactory description of the neutron field, and we decrease the laboriousness of the direct method in comparison with the "traditional" representation of the solution.

Translated from Atomnaya Énergiya, Vol. 34, No. 3, p. 194, March, 1973. Original article submitted May 18, 1972; abstract submitted November 24, 1972.

We give an example of a calculation of a two-region reactor with isometrically positioned rod in the one-velocity approximation. The method proposed is especially convenient for calculations of reactors with a small number of different multiregion rods, or with a large number of uniform rods.

LITERATURE CITED

1. G. I. Marchuk and V. I. Lebedev, Numerical Methods in Neutron-Transport Theory [in Russian], Atomizdat, Moscow (1971).
2. S. G. Mikhlin, Variational Methods in Mathematical Physics [in Russian], Nauka, Moscow (1970).
3. V. V. Khromov and I. S. Slesarev, At. Énerg., 30, 296 (1971).

EFFECT OF SPACE CHARGES IN INSULATOR ON ACCURACY OF EMISSION DETECTOR READINGS

N. A. Aseev and B. V. Samsonov

UDC 621.039.519

Emission sensors, such as the direct-charging transducer, are widely used in reactor practice for neutron flux measurements. The use of direct-charging transducers calls for a thoroughly rounded discussion of the special features affecting their performance (e.g., the study of the effect of the dielectric surrounding the detector and the emitter circuit).

In-pile tests of a direct-charging transducer in the SM-2 reactor expedited a study of the effect of temperatue (at constant neutron flux intensity) and exposure dose on current measured.

The diagram (Fig. 1) shows experimental dependences of the direct-charging transducer current on temperature and on exposure dose, at constant temperature. The direct-charging transducer emitter was made of silver, the insulator of porcelain tubing (wall thickness 2 mm). The resistance presented by the measuring device was $3 \cdot 10^3\ \Omega$, and the resistance presented by the circuit insulation at maximum temperature was $10^7\ \Omega$. It is clear from the diagram (see curve 1) that the current recorded by the instrument declined appreciably in response to an increase in the temperature of the direct-charging transducer, which was measured by a type gr. KhA thermocouple, while the neutron flux was kept constant. A drop in the

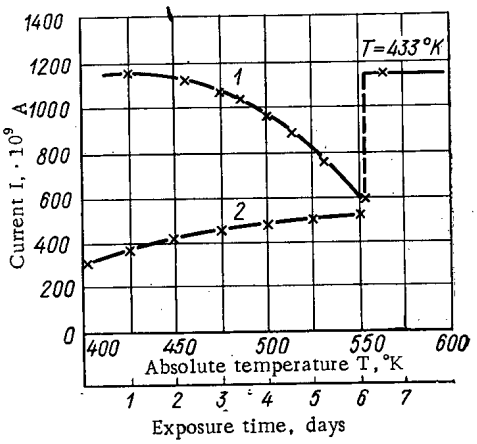

Fig. 1. Dependence of the measured current flowing through the direct-charging transducer on the temperature (1) and on the exposure dose (2).

Translated from Atomnaya Énergiya, Vol. 34, No. 3, pp. 194-196, March, 1973. Original article submitted May 15, 1972; abstract submitted November 10, 1972,

temperature leads to restoration of the initial values. It is clear from curve 2 (see Fig. 1) that the measured current increases monotonically as the dose is increased, and this effect is due only partially to the variation in neutron flux (as a result of displacement of control rods) and to activation of the emitter circuit conductor.

The article demonstrates that the variation in current is affected primarily by the space charges in the dielectric. The reduction in the current flowing through the direct-charging transducer in response to a temperature rise is explained by thermal excitation of electrons leaving the emitter and striking the insulator, and piling up in traps. The electrons released partially compensate the emitter charge. When the emitter charge relaxation on the collector circiut is taken into account, the expression for the current measured by the instrument becomes

$$I_{\text{ins}} = I_{\beta}\left(1 - \frac{l_{\text{em}}}{L} \cdot \frac{\tau_{\text{eff}}}{\tau_{\text{c}}}\right),$$

where l_{em} is the emitter length; L is the total length of the emitter circuit; τ_{c} is the collector circuit relaxation time, a function of the temperature, in sec; τ_{eff} is the effective relaxation time, in sec.

The increase in the current flowing through the direct-charging transducer with increasing exposure dose is also due to the increase in the positive space charge in the insulator.

The article yields an expression useful in determining the loss of emitter effectiveness because of β-decay electrons of the insulator isotopes.

THEORY OF THE TRANSPORT OF NONSTATIONARY GAMMA RADIATION

N. A. Seleznev

UDC 539.166.2

Transition processes associated with the transport of gamma radiation which is nonstationary in time is considered. It is shown that scattered and regenerated quanta come to a point of a medium with a delay relative to the source quanta, the delay being distributed over time.

In the general case the phenomenon of the transport of nonstationary gamma radiation is described by a system of inhomogeneous linear integro-differential equations, each of which corresponds to a definite form of radiation: gamma quanta, secondary particles (neutrons, electrons), etc. Some of the equations of the system contain a time argument with delay, caused by this or that process of interaction of secondary particles with matter (e.g., the finite lifetime of positrons, metastable isomers, etc.)

The paper considers the conditions of existence and uniqueness of the solution of the above-mentioned system: these conditions are the conditions for a sufficiently complete set of boundary conditions in relationship to the space-angle variables and initial conditions on the time argument.

An exact solution of the transport problem has as yet not been found (even for the most studied cases of stationary sources and media). Consequently there is special interest in the development of approximate methods of solution (numerical or analytical); each of these is satisfactory for a comparatively narrow range of problems.

Translated from Atomnaya Énergiya, Vol. 34, No. 3, p. 196, March, 1973. Original article submitted October 17, 1972.

As an example, the paper presents the results for two cases:

1) when only gamma quanta from the source are taken into account, i.e., the geometry of a narrow (collimated) beam;

2) when the influence of quanta scattered by the Compton interaction is significant; i.e., the geometry of a wide beam in the range of energies of the source of gamma radiation from ten kiloelectronvolts to tens of megaelectronvolts.

LETTERS TO THE EDITOR

POWER DISTRIBUTION IN FUEL ELEMENT MEAT

N. N. Ponomaev-Stepnoi, A. M. Krutov, V. A. Lobyntsev, and V. I. Nosov

UDC 621.039.512.45

Flattening of the power release field over the cross section of the core of a heterogeneous reactor has been discussed in earlier articles [1, 2]. The present article cites some results of experimental and theoretical investigations of the power release distribution over the meat portion of fuel elements.

The bulk of the power released in the core of the fuel element $q_V(\rho, \varphi)$, is due to fission of fuel nuclei. Hence,

$$q_v(\rho, \varphi) \approx \text{const}\, I(\rho, \varphi),$$

where $I(\rho, \varphi) = \int \Sigma_f(\rho, E)\Phi(\rho, \varphi, E)dE$ is the fission integral; ρ is the radius; φ is the azimuthal angle (system of coordinates fixed in the center of the fuel element); the remaining notation is that usually accepted.

The scalar flux distribution $\Phi(\rho, \varphi, E)$ can be determined for the fuel element meat on the basis of calculations of a heterogeneous reactor in a high-order approximation to the transport equation. In engineering work, however, such calculations are exorbitantly laborious, so that there is justification for simplifying the problem in multivariate calculations. Heterogeneous techniques [3-5], in which the diffusion approximation is employed with the effective or albedo boundary conditions on the surface of the (absorbing, scattering, and multiplying) blocks, should be resorted to in order to ascertain the scalar neutron flux in the moderator region. The neutron distribution in regions occupied by the fuel, coolant, and structural materials can be determined by solving the transport equation in integral form. Certain simplifications are dictated in this approach, however. In what follows, we shall neglect scattering and moderation of neutrons in the block as much smaller than absorption, and we shall utilize the P_1-distribution:

$$\varphi(\rho\Omega) = \frac{1}{4\pi}\{\Phi(\rho) - 3D\varepsilon[\Omega, \nabla\Phi(\rho)]\} \quad \text{for} \quad (\Omega, n) < 0$$

for the angular distribution of neutrons emerging from the moderator. Here D is the diffusion coefficient in the moderator; Ω is the vector of the direction of neutron flight; n is the external normal to the surface of the block; ε is the correction to the P_1-approximation which takes the curvature of the block into account. The values of the scalar flux $\Phi(\rho)$ are taken from the heterogeneous reactor about which more will be said later on.

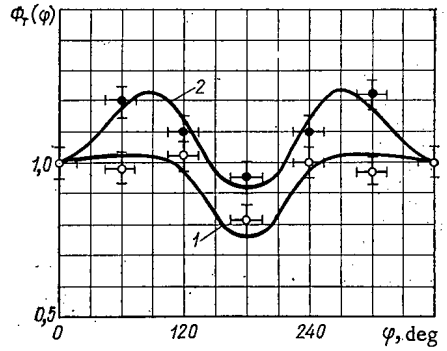

Fig. 1. Relative distribution of scalar thermal flux $\Phi_T(\varphi)$ as a function of azimuthal angle φ on boundary separating moderator and fuel element: 1 (○)) R = 0.308 R_{core}; 2 (●)) R = 0.838 R_{core} (R is distance from center of reactor to center of fuel element); ——) calculations.

Translated from Atomnaya Énergiya, Vol. 34, No. 3, pp. 197-198, March 1973. Original article submitted June 7, 1972; final revision submitted September 18, 1972.

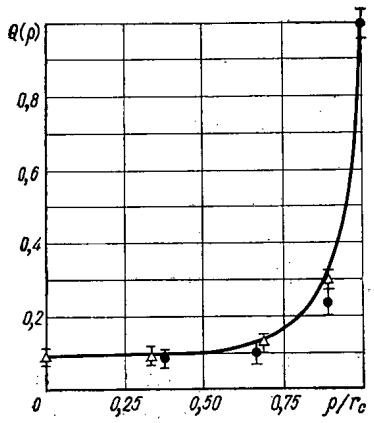

Fig. 2

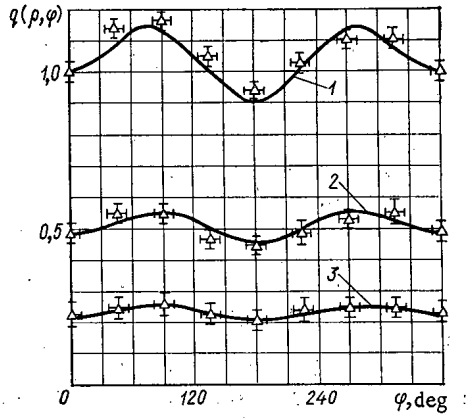

Fig. 3

Fig. 2. Relative power release distribution $Q(\rho)$ over radius of fuel element meat: ———) calculations; ●) uranium detector; Δ) Dacron film (r_c is radius of fuel element meat).

Fig. 3. Relative power distribution $q(\rho, \varphi)$ over meat of fuel element as a function of azimuthal angle φ and of distance from center of fuel element ($R = 0.838\ R_{core}$): ———) calculations; Δ) Dacron film; 1) $\rho = r_c$; 2) $\rho = 0.945\ r_c$; 3) $\rho = 0.822\ r_c$.

When these assumptions are entertained, we can go over to a set of single-velocity problems on the neutron distribution in a multilayered absorbing block with no sources, with a specified angular distribution of neutrons on the boundary, in a manner similar to that observed in [6].

The FIBL-2 program was written in ALGOL-60 language, and then translated for input to an M-220 computer, in order to obtain concrete results. Results of computations using that program are cited below.

Since certain assumptions were entertained in the theoretical discussion, exact experimental results of the investigation of uneven power release over the fuel element cross section must be used, to make it possible to estimate the range of validity of the computational techniques relied upon.

The experimental investigations were conducted on a heterogeneous critical assembly (moderator –water) with cylindrical enriched-uranium fuel elements [2]. The neutron flux distribution over the cross section of the cylindrical fuel assembly was measured on the basis of the activity of indium foils irradiated with and without a cadmium cover in place. The neutron flux distribution in the moderator was also determined both radially over the core and with respect to azimuth in the vicinity of the fuel elements. In the azimuthal measurements, the detectors were arranged on a concentric circle around the fuel element, with the detectors spaced such that their mutual effect on each other would be minimized [7]. The predicted and empirical scalar thermal flux distributions $\Phi_T(\varphi)$ are plotted in Fig. 1 with respect to azimuth on the boundary between the moderator and the fuel elements. The rms error in the measurements was roughly 5%.

Solid-state track detectors were also employed, in order to study the radial-azimuthal distribution of power released over the meat portion of the fuel element, in addition to uranium detectors. The uranium detectors, fashioned in the form of concentric rings and a central disk, were used in a study of the power release distribution over the fuel element radius. Figure 2 displays experimental and predicted values of the power released $Q(\rho)$ over the radius of the fuel element meat (with experimental corrections for detector radiation leakage). The rms error in measurements performed with the uranium detectors was ~7%.

A detailed power distribution in the fuel element meat was measured with the aid of a solid-state track detector, namely Dacron [lavsan] polymer film 30μ thick. The procedure followed in fabricating this detector has been described elsewhere [8, 9]. The power distribution over the radius of the fuel element, as obtained from these measurements, is shown in Fig. 2; the rms error in the results of the measurements ~5%. The close agreement between results of power release measurements obtained with the uranium detectors and with the Dacron film is conspicuous.

We find the azimuthal distribution of the power $q(\rho, \varphi)$ released in the fuel element meat at different distances ρ from the center of the fuel element in Fig. 3. It is clear from the graphs plotted that the results of calculations are in satisfactory agreement with experimental data.

It is clear from this comparison that the radial-azimuthal power distribution over the meat of the fuel element, obtained in calculations based on this procedure, is in satisfactory agreement with the results of measurements, within the limits of experimental error (approximately 5-7%), which is entirely acceptable in variant calculations.

The procedure developed for the calculations is useful, consequently, in engineering design of reactors with a small number of fuel elements.

In conclusion, the authors welcome this opportunity to thank E. S. Glushkov and V. G. Kosovskii for their kind assistance in carrying out the investigations.

LITERATURE CITED

1. N. N. Ponomarev-Stepnoi, et al., At. Énerg., 28, 58 (1970).
2. N. N. Ponomarev-Stepnoi, A. M. Krutov, and V. I. Nosov, At. Énerg., 30, 303 (1971).
3. V. I. Nosov, At. Énerg., 23, 25 (1967).
4. S. N. Barkov, At. Énerg., 24, 335 (1968).
5. V. I. Nosov, Vestni Akad. Navuk BSSR, Seriya Fiz. -Energ. Navuk, 3, 5 (1970).
6. V. A. Lobyntsev, At. Énerg., 25, 138 (1968).
7. N. Khan et al., Nucl. Instrum. Methods, 65, 137 (1968).
8. C. Besant and S. Ipson, J. Nucl. Energy, 24, 59 (1970).
9. D. Jowitt, Nucl. Instrum. Methods, 92, 38 (1971).

ON THE USE OF AN ELECTRON CYCLOTRON FOR THE RAPID PHOTON ACTIVATION ANALYSIS OF ORE SAMPLES FOR GOLD

S. P. Kapitsa, Yu. T. Martynov
V. V. Sulin, and Yu. M. Tsipenyuk

UDC 543.53

The abundance of gold in nature is very small. Its average content in the earth's core is $5 \cdot 10^{-7}$ wt.%, reaching 10^{-5}-10^{-2} wt.% in gold ores. Therefore for the determination of the gold content in samples of minerals, rocks, and ores during prospecting and for surveying strata it is necessary to use extremely sensitive highly efficient analytical methods. For example, just in prospecting alone each year many samples from newly discovered large scale gold ore deposits must be analyzed for gold, sometimes amounting to at least ten thousand per year. In order to obtain results for the analysis of samples for gold, which is very irregularly distributed in ore bodies, it is necessary to take large samples (ten or even one hundred grams). Therefore the problem of finding new rapid methods of mass analysis for gold in representative ore samples becomes timely.

In this method a modification of photon activation analysis for gold is used, based on the use of a short-lived indicator for gold, Au^{197m}, which is formed as the result of a γ, γ' activation reaction. The half life of this isomer is 7.3 sec, and the gamma ray of highest intensity is at 277 keV.

By stopping a beam of electrons accelerated to an energy of 3-6 MeV [1-3], gamma photons are provided for the inelastic scattering reaction with the gold nucleus used in the determination. It is obvious that with the increased energy of the accelerated electrons one must increase the sample weight to have a sensitive method. The radioactive isomer Au^{197m} is formed approximately four times as fast with electron energies of 3-6 MeV and approximately eight times as fast with 3-8 or 9 MeV [4, 5]. In addition the increased energy permits the formation of a mixture of activities caused by γ, γ' activation reactions on the nuclei of elements which can be used to study the rock or ore samples.

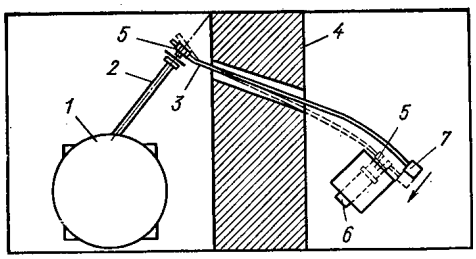

Fig. 1. Experimental layout: (1) cyclotron; (2) extraction tube with tungsten stop target at the end (the dash-dotted line indicates the electron path); (3) monorail transport; (4) concrete shielding wall; (5) carriage with cell; (6) scintillation counter in lead housing; (7) mechanism for transferring cell and monorail (the dashed line shows the position of the monorail and carriage with the cell in place for detecting gamma rays from the induced activity in the sample being studied).

Calculation of the sensitivity of the photon activation analysis of samples from a quartzite vein for gold using the γ, γ' reaction gave an optimum energy of 8.5 MeV [6].

Therefore the possibility of the practical application of the cyclotron for analysis of gold ore samples at an electron energy of 9 MeV was considered. The experimental layout is shown in Figure 1. The samples studied were powdered gold ores between 100 and 200 g packed in a mushroom shaped Plexiglas cell and placed in a transport carriage aligned with the back stop of the 17 orbit cyclotron of the Institute of Physical Problems, Academy of Sciences of the USSR [7]. The distance between the cell and the tungsten target of the cyclotron is determined by the end of the extraction tube and is 10 cm. Each cell with sample is irradiated for 18 sec in an average electron beam of 30 μA. The irradiated cell

Translated from Atomnaya Énergiya, Vol. 34, No. 3, pp. 199-200, March, 1973. Original article submitted May 18, 1972.

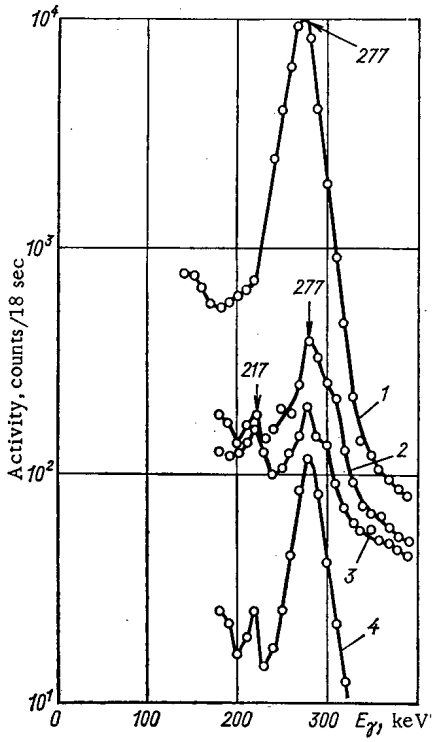

Fig. 2. Instrumental gamma ray spectrum of the induced activity in the sample: (1) metallic gold; (2) ore with large amounts of sulfide minerals; (3) ore with high content of naturally radioactive minerals; (4) quartz carbonate ore. Gold content, g/ton: (2) 50; (3) 17.5; (4) 30. The numbers with arrows point out the gamma quanta in keV.

with sample is signaled by a pulse and transported to the well scintillation counter (NaI(Tl) crystal, 70 × 70 mm with an FEU-52 photomultiplier and shield) initially on the monorail, and later together with the monorail, so that the cell enters the scintillation detector shield. To protect the detector from the external background it was put in a small lead chamber of 100 mm wall thickness. In one wall of the chamber a window was made for the entrance of the transport with carrier. Probes from the counter were measured by a single channel analyzer. The "cooling off" time (for transport) of the irradiated holder with sample was 3 sec, the measuring time for the induced gamma rays was 18 sec.

Studies of the gold content of the samples showed three types of ores differing in the following particulars: quartz carbonate ores; ores with large amounts of sulfide minerals; ores with high contents of naturally radioactive minerals.

Figure 2 gives the instrumental gamma ray spectra of the activity induced in samples of these ores containing 30, 50, and 17.5 g/ton of gold. In this figure also is shown the instrumental gamma ray spectrum of the activity induced in a chemically purified gold sample. The sample weight is 40 mg. The gold sample was irradiated and determined in the same manner as the gold ore samples. As is evident in Fig. 2, the gold activity (277 keV photopeak) is sharply separated in the spectra of all three samples. The 217 keV photopeak is apparently due to hafnium (Hf^{179m}, $E_\gamma = 217$ keV, $t_{1/2} = \sim 18.6$ sec).

The most common shape characterizing the gamma spectrum of the induced activity in the gold containing samples is for the quartz carbonate compounds. There is a smaller increase in the baseline near the gold photopeak and in the activity in the higher energy region of the spectrum, as compared to the gamma spectrum of the induced activity than in the ore samples with large amounts of sulfide minerals.

By using the available information about the gold content of the sample, that is, taking the sum of the counts in five channels corresponding to the 277 keV photopeak maximum, and taking the number of counts in the background for the photopeak, it is possible to obtain the limiting sensitivity for determining the gold content in the samples. If the root mean square error is determined for three background determinations, and twice that value is called the threshold sensitivity for determining the gold content in quartz carbonate ore samples, ores with high content of radioactive elements and ores with large amounts of sulfide minerals, the values are correspondingly $3 \cdot 10^{-4}$, $5 \cdot 10^{-4}$, and $7 \cdot 10^{-4}$%. Note that even if a ten cycle analysis is used which will lower the detection limit by a factor of three, the production for gamma activation analysis will be ten times larger than the production of existing analytical methods.

Using a high resolution, large volume Ge(Li) semiconductor detector or a multiple-crystal scintillation spectrometer (as used in [3]) will give sharply differentiated and useful information about interfering background activities as well as a large improvement in the sensitivity of the analysis.

The authors express deep gratitude to P. L. Kapits and G. N. Flerov for supporting this investigation and also to V. S. Anikin, V. V. Zhuchkov, and A. A. Kolosov for technical assistance.

LITERATURE CITED

1. J. Otwos et al., Nucl. Inst. and Meth., 11, No. 1, 187 (1961).
2. O. Abbosov, S. Kodiri, and L. P. Starchik, Symposium, "Nuclear Physical Methods for the Analysis of Substances" [in Russian], Atomizdat, Moscow (1971), p. 244.
3. A. K. Borzin, Yu. V. Gruzdev, and V. V. Sulin, ibid., p. 236.
4. H. Lukens, "Modern Trends in Activation Analysis," NBS, Washington, DC, 20234 (1958), p. 853.
5. H. Lukens, Trans. Amer. Nucl. Soc., 10, 89 (1967).
6. M. G. Davidov and V. A. Shcherbachenko, Atomnaya Énergiya, 27, 205 (1969).
7. S. P. Kapitsa et al., Pribori, Tekhnika Éksperimenta, 1, 15 (1969).

FEATURES OF ACTIVATION ANALYSIS OF MOVING MATTER USING A FAST NEUTRON SOURCE

V. V. Strel'chenko and K. I. Yakubson

UDC 539.1.06

The basic concepts of the activation analysis theory of moving matter relative to the study of wells were first published in the work cited in reference [1], in which the exponential character of changes in the intensity of activated radiation with a growth in distance between the γ-quanta detector and the neutron source (probe diameter d) was described. Later experiments, detailed in reference [2], indicated that the intensity of the radiation activated by thermal neutrons is dependent on probe diameter and can be best approximated by a function of the type $I_0 e^{-d^2/\Delta^2}$. For a similar type function, I(d, Δ), I. I. Brednev derived the following expression for the intensity of the activated radiation of moving matter (I_N):

$$I_N = I_0 G = \frac{\sqrt{\pi}}{2v} I_0 \lambda\Delta \left[1 - \Phi\left(\frac{\lambda\Delta}{2v} - \frac{d}{\Delta}\right)\right] \exp\left[-\frac{\lambda d}{v} + \left(\frac{\lambda\Delta}{2v}\right)^2\right], \quad (1)$$

where I_0 is the intensity of activated radiation when v = 0, d = 0; v is the velocity of matter moving in a particular detector; λ is the continuous decomposition of the isotopic indicator; $\Phi(x)$ is the probability integral. Analysis of expression (1) indicates that the intensity of the activated radiation, I_N, moving the matter at fixed values of λ, d, and v, depends on the two parameters I_0 and Δ. In turn, parameters I_0 and Δ are functions of a number of variables, including the density and the composition of the matter being analyzed, and the measurement geometry.

In the current work, research results are presented regarding the dependence of the I_0 and Δ parameters on the change in media density and measurement geometry during activation analysis using 14-MeV neutrons. On the basis of such results, the problems of optimizing the conditions for determining the composition of moving matter are examined.

Experimental study of the dependence of I_0 and Δ on the density of the media being analyzed and on the measurement geometry was carried out in keeping with similarity theory principles applied to a sand bed model intersected by a wall. A 14-MeV neutron generator with an NT-16 tube was used to create a

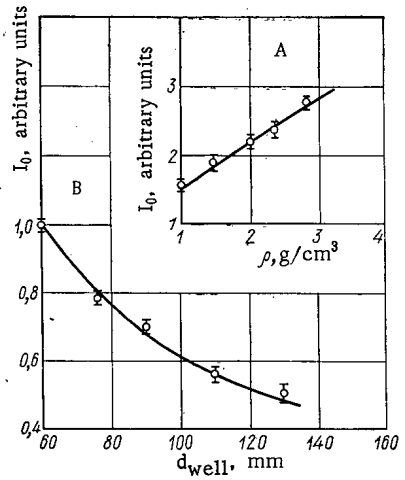

Fig. 1. Intensity of activated γ-radiation, resulting from 14-MeV neutron activity, as a function of media density (A) and diameter of wells not filled with water (B).

Translated from Atomnaya Énergiya, Vol. 34, No. 3, pp. 201-202, March, 1973. Original article submitted December 30, 1971.

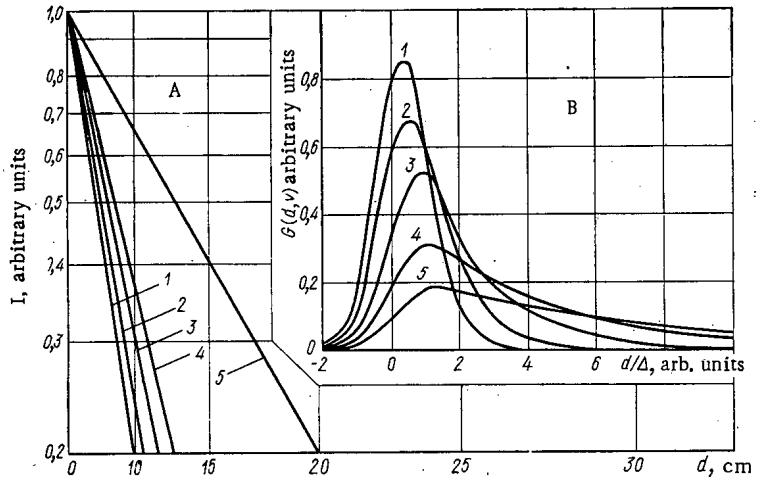

Fig. 2. Intensity of activated γ-radiation, resulting from 14-MeV neutron activity, as a function of the probe diameter (A) and the value of parameter Δ (B). A: 1) ϕ = 76 mm, ρ = 3.0 g/cm^3; 2) ϕ = 142 mm, ρ = 3.6 g/cm^3; 3) ϕ = 170 mm, ρ = 3.0 g/cm^3; 4) ϕ = 170 mm, ρ = 3.0 g/cm^3; 5) ϕ = 142 mm, ρ = 1.6 g/cm^3; 1, 2, 4, and 5 are dry wells and 3 is a water-filled well. B: 1) v = 0.5$\lambda\Delta$; 2) $\lambda\Delta$; 3) 2$\lambda\Delta$; 4) 4$\lambda\Delta$; 5) 8$\lambda\Delta$.

fast neutron field. Detection of γ-quanta in the E_γ = 1.78 ± 0.2 MeV energy range was accomplished with the aid of a 30 × 70 mm NaI(Tl) crystal. There were 6 periods of bombardment, cooling, and measurement, of 1 (for suppressing isotope N^{16} activity) and 6 min, respectively. The principal results of the experiments are shown in Figs. 1 and 2. In Fig. 1, the A section of the graph illustrates the dependence of the intensity values of γ-radiation I_0, which results from the $Si^{28}(n, p)Al^{28}$ reaction, on the density variation ρ of the media being analyzed. In the range of density changes studied, the dependence of $I_0 = f(\rho)$ is near to linear. The curve shown in Fig. 1, the B section of the graph, illustrates the changing values of I_0 according to various diameters of wells not filled with water. The intensity of I_0 decreases quite rapidly with increases in well diameter. In Fig. 2, the A section of the graph shows the dependence of the intensity of activated radiation I_0 on probe diameter d. Measurements were made in wells with diameters of 76, 142, and 170 mm, which intersected sand beds with densities of 1.6, 3.0, and 3.6 g/cm^3 (for which intensity values were obtained by calculating according to the similarity theory). In all cases where d ≤ 15-20 cm, the relationship $I_0 = f(d)$ exhibited a type of Gaussian curve. The value of parameter Δ of these curves depends on the media properties and measurement geometry, as follows:

a) by increasing the density of the media being activated from 1.60 to 3.6 g/cm^3, the value of parameter Δ changes from 16.3 to 8.9 cm;

b) by changing the diameter of a well not filled with water from 76 to 170 mm, the value of parameter Δ increases from 8.1 to 10.5 cm;

c) filling a well with water is not significant (by 5-6%) and decreases the value of Δ.

The quoted values of parameter Δ were obtained by measurements involving the 30 × 70 mm NaI(Tl) crystal; the values of parameter Δ, corresponding to measurements with the point detector, are 11% lower. Comparison of the Δ values with data in reference [3] indicates that activation analysis using fast neutrons results in the distribution width of $I(d) = I_0 e^{-d^2/\Delta^2}$ being two times less than the width obtained during activation with thermal neutrons of identical measurement geometry.

By viewing together the curves in Figs. 1 and 2 (the A sections of the graphs), a change in the density of the media under study and also the well diameter leads to a reversal of the sign of the I_0 and Δ parameters. This circumstance perhaps can be used in selecting the optimal conditions for activation analysis of moving matter from the standpoint of lessening the dependence of measurement results on the variations in media properties and measurement geometry. From equation (1), curves may be derived (Fig. 2, B section of the graph) which characterize the dependence of the relationship $I_N/I_0 = G(d, v)$ on the value of

the probe diameter d, expressed in units of Δ (the numbers of the curves are the values of the velocity of moving matter expressed in units of $\lambda\Delta$). The configuration of these curves is very similar to the curves presented in reference [1]. For each velocity value it is possible to indicate the optimal value of the d/Δ ratio, at which the I_N/I_0 ratio reaches a maximum.

Analysis of the curve forms in Fig. 2 (the B section of the graph), from the standpoint of optimizing the measurement conditions in the context indicated above, allows identification of two areas of measurement of the d/Δ relationship. In the area of the d/Δ values, including values between zero and the d/Δ values, corresponding to the peaks of the curves $G(d, v) = f(d, \Delta)$, the intensity of the activated radiation of moving matter is strongest depending on its density and measurement geometry. This is confirmed by the agreement of the directions (signs) of the I_0 and $G(d, v)$ changes at various media density and measurement geometry. Outside the indicated area of values of the d/Δ relationship, the influence of the variable physical properties and the measurement geometry on the I_N value is considerably less, because the changes in the I_0 and $G(d, v)$ parameters in this case compensate each other to a large degree.

Using the curves shown in Figs. 1 and 2, one can select a regime of measurements (values of d and v) at which the influence of one of the variables (whether media density or measurement geometry) is practically nil. Thus, for example, to exclude the influence of density variations in the 1.6-3.6 g/cm^3 range on the I_N intensity, a probe diameter of $2d/\Delta$ (about 30 cm) can be selected and a velocity of moving matter approximating $3\lambda\Delta$. A probe of such diameter can be used when an impulse regime of measurements is employed.

LITERATURE CITED

1. Yu. P. Bulashevich and S. A. Shulyat'ev, Izv. AN SSSR, Ser. Geofiz., No. 2, 253 (1960).
2. G. S. Vozzhenikov, Activational Analysis [in Russian], Nedra, Moscow (1965), p. 37.
3. G. S. Vozzhenikov and I. I. Brednev, Radioisotopic Automation Systems in Mining [in Russian], Transactions of the A. A. Skochinskii Mining Institute, Izd. IGD im A. A. Skochinskii, Moscow (1969), p. 37.

SOME CHARACTERISTICS OF ELECTRON-EMISSION NEUTRON DETECTORS WITH Ag, Ag^{109}, Rh, AND Gd EMITTERS

I. Ya. Emel'yanov, Yu. I. Volod'ko, O. K. Egorov, L. V. Konstantinov, and V. V. Postnikov

UDC 539.7.074.8

Two types of Electron-Emission Neutron Detectors (EDN), described in references [1-3], are used extensively in controlling neutron flux distribution in reactor cores. In the first type of detector, the output signal of the EDN is the current between the emitter and collector electrodes, resulting chiefly from neutron activation of the emitter material. In the second type of detector, the output signal results from radioactive capture processes. The currents are easily distinguishable in the neutron flux of the EDN reaction, which changes over time [2].

Designing a control system for energy release in the reactors, with use of an EDN, requires data on the absolute sensitivity capabilities of various detectors and the characteristics necessary for developing electron correctors of the inertness of the EDN [2].

In this connection, in the core of the experimental water–water reactor, type IRT-1000, the performance characteristics of EDN with Ag, Ag^{109}, and Rh emitters, and emitters containing Cd were examined (Table 1). The average current flux of thermal neutrons along the length of the sensitive part of the EDN did not exceed $(1.0\text{-}1.3) \cdot 10^{12}$ neutrons/$cm^2 \cdot$ sec in the experimental data; the average current flux of fast

TABLE 1. Results of Determining the Absolute Sensitivity of an EDN

Outside shell diameter, mm	Emitter		Insulator		Shell (collector)		Absolute sensitivity, $\cdot 10^{20}$ (A/m)/(neutrons/$cm^2 \cdot$ sec)	Absolute sensitivity to neutrons according to Westcott, $\cdot 10^{20}$ (A/m)/(neutrons/$cm^2 \cdot$ sec)	Remarks
	material	diameter, mm	material	thickness, mm	material	thickness, mm			
4,37	Ag	0,75	Magnesium oxide	1,0	Stainless steel	0,81	6,6	8,7	The EDN were prepared by the same technology used in making the cable with magnesium insulation ([4])
3,05	"	0,67	The same	0,65	The same	0,54	6,0	8,0	
2,34	"	0,44	" "	0,54	" "	0,41	3,6	4,8	
1,77	"	0,25	" "	0,40	" "	0,36	2,1	2,8	
1,07	"	0,27	" "	0,31	" "	0,094	1,9	2,5	
1,07	"	0,21	" "	0,35	" "	0,081	1,6	2,1	
1,50	Ag^{109}	0,38	Quartz	0,41	" "	0,15	4,8	6,4	
1,80	Rh	0,50	Quartz	0,40	" "	0,15	8,7	11,5	
1,80	Ag	0,50	Quartz	0,40	" "	0,15	3,9	5,1	
5,00	Al – Gd alloy (10% Gd)	1,00	Polychlorvinyl	0,75	" "	0,75	4,5	5,3	
3,50		1,00		0,50	" "	0,50	3,4	4,0	
3,00	Stainless steel with 0.5% Gd addition	1,50	Quartz	0,20	" "	0,30	1,5	1,9	

Translated from Atomnaya Énergiya, Vol. 34, No. 3, pp. 203-205, March, 1973. Original article submitted February 1, 1972.

TABLE 2. Values Characterizing the Inertness of an EDN of the Activated Type

Emitter material	Emitter diameter	Insulation material	Short-life component		Long-life component		"Prompt" component
			period $\tau_{1/2}$, sec	full current fraction	period $\tau_{1/2}$, min	full current fraction	full current fraction
Ag	0,75	Magnesium oxide	24,6±1,2	0,806±0,040	2,40±0,08	0,102±0,030	0,092±0,040
	0,67		22,1±1,2	0,761±0,040	2,33±0,08	0,127±0,030	0,112±0,040
	0,44		21,0±1,2	0,760±0,040	1,98±0,08	0,136±0,030	0,104±0,040
	0,25		22,5±1,2	0,770±0,040	2,19±0,08	0,153±0,030	0,077±0,040
	0,27		22,4±1,2	0,763±0,040	2,27±0,08	0,155±0,030	0,082±0,040
Ag^{109}	0,38	Magnesium oxide	22,7±1,2	0,950±0,040	No data		0,050±0,040
Rh	0,50	Quartz	41,2±1,2	0,900±0,040	4,67±0,08	0,050±0,030	0,050±0,030
Ag	0,50	Quartz	23,8±1,2	0,784±0,040	2,41±0,08	0,134±0,030	0,082±0,030
Generally accepted periods of isotopic decay, which occur as the result of activation of silver and rhodium [6]							
Ag			24,0±0,5		2,44±0,06		
Rh			41,8±0,7		4,37±0,5		

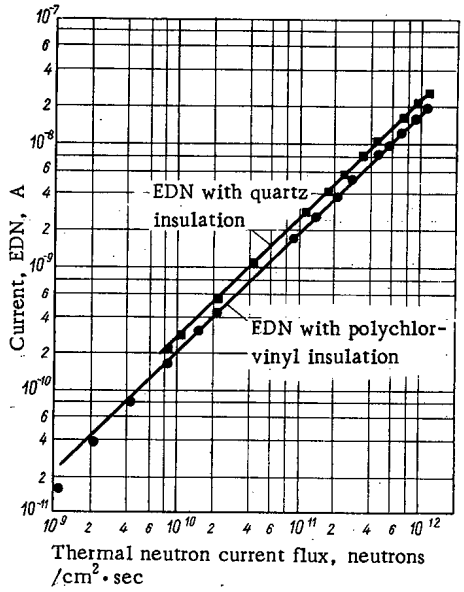

Fig. 1. Current of an EDN having Al–Gd alloy emitters, as a function of thermal neutron current flux.

neutrons with energies greater than 0.5 MeV was $7.6 \cdot 10^{11}$ neutrons/cm^2 · sec; and, the average γ-radiation dose was $1.7 \cdot 10^3$ rad/sec.

Measuring the Absolute EDN Sensitivity. The absolute EDN sensitivity was determined by the ratio of EDN current along a one meter detector length to the average value of thermal neutron current flux measured directly at the surface of the detector. The error in determining the absolute EDN sensitivity to thermal neutrons was ±10-12%.

The measurements indicated that the EDN current with Ag, Ag^{109}, and Rh emitters was proportional to the thermal neutron current flux with an accuracy of 2.5% in the 10^{11}-10^{12} neutrons/cm^2 · sec range. In Fig. 1, the relationship of the current of an EDN with Al–Gd emitters to thermal neutron current flux is shown. From Fig. 1 it follows that the current of the Gd EDN, with quartz as well as polyvinyl chloride insulation, is proportional to the thermal neutron current flux with an accuracy of 2.5% in the 10^{10}-10^{12} neutrons/cm^2 · sec range.

The results of determining the absolute sensitivity of an EDN are presented in Table 1. It is not difficult to ascertain that there is a linear relationship of the sensitivity of the EDN with an Al emitter to the diameter of the emitter (d_e = 0.2-0.8 mm), which can be determined with an accuracy of ±10% using the following empirical formula:

$$K = (9.6 d_e - 0.57)\, 10^{-20}, \quad (1)$$

where K is the EDN sensitivity relative to a meter of detector length, (A/m)/(neutrons/cm^2 · sec); d_e is the emitter diameter in mm.

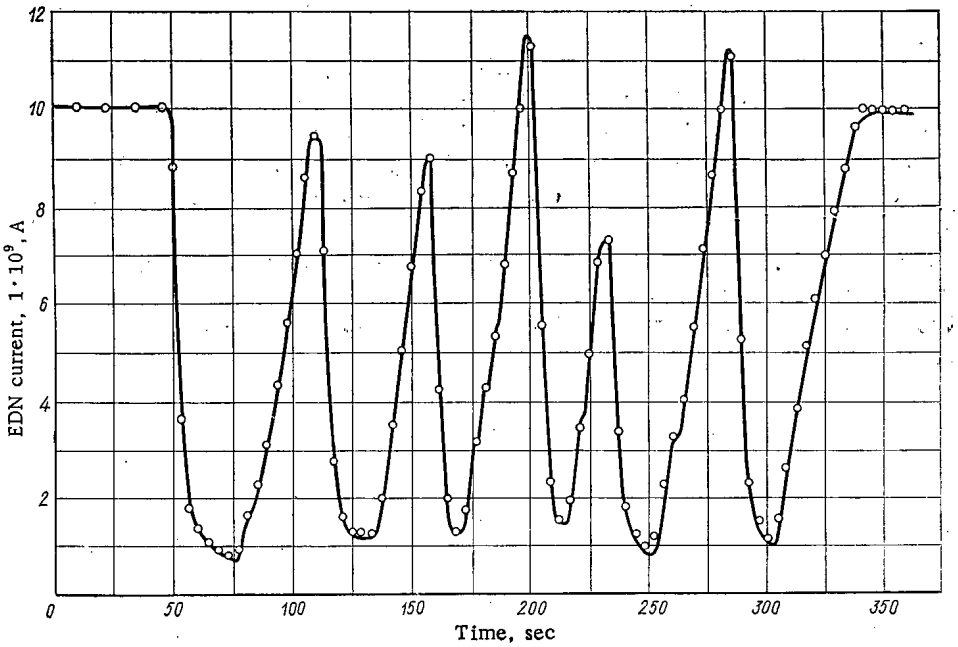

Fig. 2. Changes in the current of a Gd EDN with quartz insulators during changes in reactor capacity: ———) EDN current; and ○) ionization chamber current, relative units.

It should be noted that formula (1) was derived for detectors which were prepared by successive operations of drawing a silver-core cable through them. After each such operation, the thickness of the insulation became somewhat smaller (Table 1).

Using formula (1) and data from Table 1, it can be shown that with the same diameter emitter (for d_e = 0.35-0.50 mm), the sensitivity of a detector with an Rh emitter is 1.3-1.4 times greater than the sensitivity of an EDN with an Ag^{109} emitter, which in turn, is approximately 1.6 times greater than the sensitivity of an EDN with a common silver emitter. The sensitivity of a Gd EDN is about 2 times less than an EDN with a silver emitter.

Determination of the values characteristic of the inertness of an EDN was carried out by analyzing in a computer the curvilinear fall of current in an EDN for 30 min, after holding the detector in a continuous current for 20 minutes and then rapidly withdrawing the recorder from the reactor core. By this technique the full current fractions of an EDN were obtained for a stationary level of neutron flux, which resulted from the decay of radioactive isotopes having periods of $\tau_{1/2}$ that correspond to a twofold lowering of the component current of the EDN from these isotopes and also the "prompt" current component, which resulted from the processes of radioactive capture of neutrons in the emitter (references [2] and [5]). As shown in Table 2, the differences between $\tau_{1/2}$ and the standard half-life periods are caused apparently by the effects of spatial charges in the insulation. The primary expenditure of current in the EDN for all detectors studied is determined from the short-lived component ($\tau_{1/2} \simeq 22$ sec for Ag and $\tau_{1/2} \simeq 41$ sec for Rh). However, the expenditure of the long-lived component ($\tau_{1/2} \simeq 2.4$ min for Ag and $\tau_{1/2} \simeq 4.4$ min for Rh) is sufficiently large for detectors with Ag and Rh emitters. The "prompt" current component for the EDN was recorded in all cases. With the growth of emitter diameter in an EDN having a silver emitter, the relative expenditure of the "prompt" component increases, reaching approximately 10% at an emitter diameter of 0.7 mm. With increases in emitter diameter, the ratio of the short-lived component to the long-lived component increases. This phenomenon, apparently, is connected with the fact that β-particle energies, released by radioacitve Ag^{110} (2.24 and 2.82 MeV as reported in reference [6]), are higher than those for Ag^{108} (1.15 MeV).

The changes in the current of the Gd EDN at various reactor capacities are shown in Fig. 2. The changes indicate that the Gd EDN is practically inertialess.

LITERATURE CITED

1. I. Ya. Emel'yanov et al., Atomnaya Énergiya, 30, 275 (1971).
2. I. Ya. Emel'yanov et al., Atomnaya Énergiya, 27, 230 (1969).
3. V. F. Suchkov et al., Kabel'naya Tekhnika, Branch of VNIIEM on Scientific-Research Data, Standardization, and Normalization in Electrical Engineering, No. 72 (1971).
4. V. F. Suchkov et al., Heat Resistant Cable with Magnesium Insulation [in Russian], Énergiya, Moscow (1969).
5. W. Loosemore and G. Knill, "Radiation measurements in nuclear power," Proc. of the Internat. Conf. (September, 1966), p. 430.
6. A. N. Nesmeyanov et al., Obtaining Radioactive Isotopes [in Russian], GIKhL, Moscow (1954), pp. 92 and 94.

RADIATION CHEMICAL CONVERSIONS OF IODINE IN THE SYSTEM TRIBUTYL PHOSPHATE – HEXANE – H_2O–HNO_3

P. A. Zagorets, Z. I. Raskina,
G. P. Bulgakova, V. M. Makarov,
T. G. Sazhina, and T. N. Agafonova

UDC 541.15:(547.264,118, 5 + 546.15)

The problem of iodine, arising in the extraction technology of highly irradiated nuclear fuel, was characterized in our previous communication [1]. In this work investigations of the radiation chemical behavior of iodine in tributyl phosphate (TBP) and in solutions of tributyl phosphate in hexane were continued. The role of additives (H_2O, HNO_3) in the processes of radiolysis of such systems was studied.

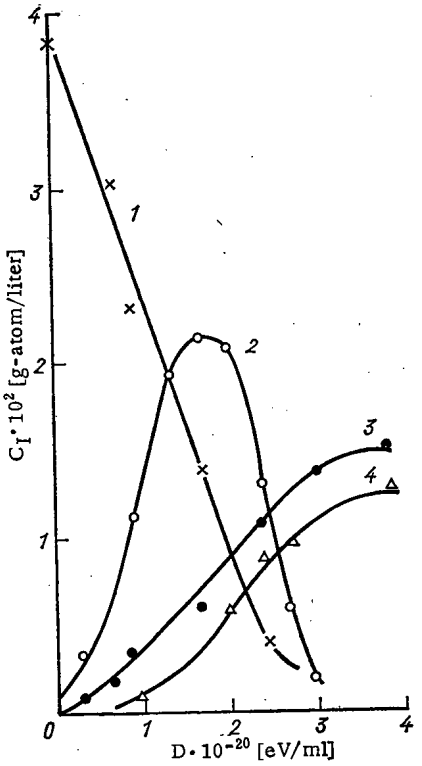

Fig. 1

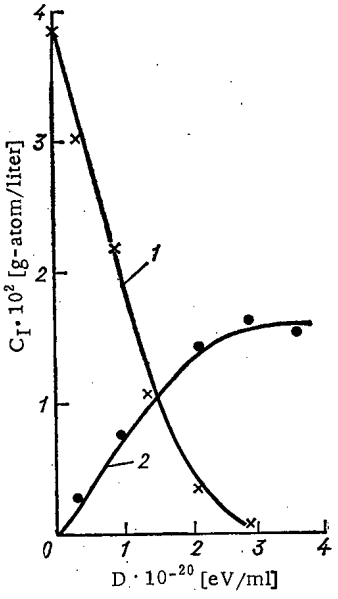

Fig. 2

Fig. 1. Radiation chemical conversions of iodine ($C_{I_2} = 1.97 \cdot 10^{-2}$ M) in the system TBP (20 vol. %) + hexane in the absence of O_2: 1) TBP · I_2; 2) I_3^-; 3) $C_6H_{13}I$; 4) C_4H_9I.

Fig. 2. Radiation chemical conversions of iodine ($C_{I_2} = 1.97 \cdot 10^{-2}$ M) in the system TBP (20 vol. %) + hexane + HNO_3: 1) TBP · I_2; 2) $C_6H_{13}I$.

Translated from Atomnaya Énergiya, Vol. 34, No. 3, pp. 205-207, March, 1973. Original article submitted July 10, 1972.

TABLE 1. Radiation Chemical Yields of Processes of Conversion of Iodine (C_{I_2} = $1.97 \cdot 10^{-2}$) in TBP and TBP + Hexane in the Absence of O_2

Additive process	TBP concentration, vol.%	without additive	H_2O	HNO_3
		radiation chemical yield, G, 1/100 eV		
Decomposition of TBP·I_2	20	4,6	5,5	5,5
	100	6,8	6,1	3,9
Formation of I_3^-	20	3,8	4,5	—
	100	4,4	4,5	—
Decomposition of I_3^-	20	4,0	3,0	—
	100	4,3	4,5	—
Formation of C_4H_9I	20	3,5	3,0	—
	100	7,7	1,2	—
Formation of $C_6H_{13}I$	20	3,5	3,0	4,8
	100	—	—	—

The preparation of the samples, method of irradiation, and dosimetry were presented in [1]. An analysis of the radiolysis products of iodine solutions was carried out spectrophotometrically (I_3^-) by the method of potentiometric titration of aqueous extracts from irradiated solutions (HI) with a solution of $AgNO_3$ and by the method of gas–liquid chromatography (alkyl iodides). The following were used: a Pye-104 chromatograph with flame-ionization detector; a column 1.5 m long with inner diameter 4 mm; consumption of the carrier gas (N_2) 60 ml /min; column temperature 120°C. Apiezon-L in an amount of 15% by weight on celite C-545, preliminarily treated with hydrochloric acid, was used as the liquid phase.

In the γ-irradiation of solutions of iodine ($C_{I_2} \sim 2 \cdot 10^{-2}$ M) with dry pure 100% TBP, a process of conversion of the complex TBP·I_2 through the intermediate form I_3^- to alkyl iodides, chiefly to C_4HI, is observed. Small quantities of HI are also formed. As C_4H_9I is accumulated, the process of its radiation chemical decomposition according to the mechanism [2, 3]:

$$RI + \bar{e} \rightarrow R^{\cdot} + I^- \qquad (1)$$

becomes appreciable. In this case ethylpropyl and certain other alkyl iodides are formed. The values of the radiation chemical yields of the indicated processes of conversions of iodine in TBP are cited in Table 1.

In the case of saturation of solutions of iodine in TBP with water (~5% by weight), the radiation chemical yield of butyl iodide is significantly reduced (see Table 1), but the yield of HI is strongly increased. The influence of H_2O on the radiolysis of TBP (and, consequently, on the yield of C_4H_9I) is associated [4] with the protective action of hydrogen bonds on the decomposition of excited TBP molecules.

The radiolysis of the investigated system, brought into equilibrium with an aqueous solution of 2 N HNO_3, did not reveal the formation of I_3^- ions; butyl iodide is formed in negligible amounts. The composition of the radiolysis products of iodine arising in the presence of HNO_3 has not been definitively established. It is suggested that redox reactions of iodine with the radiolysis products of nitric acid occur, with the formation of hydroiodic, hypoiodic, and iodic acids or their organic derivatives.

In the γ-radiation of solutions of iodine in TBP + hexane (without additives), the general picture of the radiation chemical conversions of iodine is close to that for pure TBP (Fig. 1). In both cases the complex TBP·I_2 is broken down and is converted through the intermediate form I_3^- chiefly to C_4H_9I. In the presence of hexane a parallel formation of $C_6H_{13}I$ is observed (without inductive period):

$$TBP \cdot I_2 + C_6H_{13}^{\cdot} \rightarrow C_6H_{13}I + I^{\cdot} + TBP. \qquad (2)$$

The values of the radiation yields of the processes of radiolysis of iodine that occur in TBP + hexane and in solutions with additives are cited in Table 1. The influence of H_2O in solutions diluted with hexane is not manifested, which is apparently associated with the negligible solubility of water in the investigated system (1% by weight according to the data of [4]).

The radiation chemical conversions of iodine in a solution of TBP + hexane, brought into equilibrium with an aqueous solution of 2 N HNO_3, are shown in Fig. 2. In such a system, just as in pure TBP containing HNO_3, no I_3^- ions are formed, and C_4H_9I is formed in negligible amounts. And yet, the presence of HNO_3 does not influence the iodination of the diluent (hexane).

The role of iodine in certain processes of radiation chemical nitration of a hydrocarbon diluent was followed. It is known [5] that in the radiolysis of the system TBP + octane + HNO_3 in the absence of O_2, chiefly nitrooctane ($G = 8 \cdot 10^{-3}$ eV) and octyl nitrite ($G = 8 \cdot 10^{-3}$ eV) are formed. In experiments with an analogous system (in the absence of iodine), nitrooctane was identified spectrophotometrically according to the absorption with λ_{max} = 290 nm [6].

In the irradiation of solutions containing iodine ($C_{I_2} = 3.92 \cdot 10^{-2}$ M), there is no absorption with λ_{max} = 290 nm. Evidently the basic nitrating agent (NO_2) is consumed to a substantial degree in oxidative reactions with iodine and with its derivatives.

LITERATURE CITED

1. P. A. Zagorets et al., At. Énerg., 32, No. 5, 422 (1972).
2. L. S. Polak, P. Ya. Chernyak, and A. S. Shcherbakova, Khim. Vys. Énerg., 2, No. 4, 317 (1968).
3. J. Thomas, Journ. Phys. Chem., 71, No. 6, 1919 (1967).
4. L. Burger and E. McClanahan, Ind. Eng. Chem., 50, No. 2, 153 (1958).
5. G. F. Egorov and V. I. Medvedovskii, Khim. Vys. Énerg., 5, No. 1, 78 (1971).
6. A. Gillem and E. Stern, Electronic Absorption Spectra of Organic Compounds [Russian translation], Izd-vo Inostr. Lit., Moscow (1957).

SPIRAL INSTABILITY OF A PLASMA FILAMENT OF ELLIPTICAL CROSS SECTION

L. S. Solov'ev

UDC 533.9.01

The present paper derives the hydromagnetic stability conditions for a plasma filament of elliptical cross section relative to spiral perturbations for the cases of homogeneous and surface longitudinal currents.

For hydromagnetic stability of a plasma configuration held in equilibrium by a magnetic field,

$$\nabla p=[\mathbf{jB}],\ \mathbf{j}=\operatorname{rot}\mathbf{B},\ \operatorname{div}\mathbf{B}=0, \tag{1}$$

a potential energy $\delta W = \delta W_i + \delta W_\Sigma + \delta W_e$ is necessary and sufficient, with the following arbitrary translations of the plasma ξ [1-3]:

$$\delta W_i=\frac{1}{2}\int_{V_i}\{(\mathbf{Q}+[\mathbf{je}]\xi)^2+\gamma p(\operatorname{div}\xi)^2-(\Omega+[\mathbf{je}]^2)\xi^2\}\,d\tau; \tag{2}$$

$$\delta W_\Sigma=\frac{1}{2}\int_{\Sigma}\{\mathbf{B}(\mathbf{B}\nabla)\,n-\mathbf{B}_e(\mathbf{B}_e\nabla)\,\mathbf{n}\}\,\xi_n^2\,d\sigma; \tag{3}$$

$$\delta W_e=\frac{1}{2}\int_{V_e}(\operatorname{rot}\delta\mathbf{A}_e)^2\,d\tau,\ \mathbf{Q}=\delta\mathbf{B}=\operatorname{rot}[\xi\mathbf{B}], \tag{4}$$

where p is the plasma pressure; $\mathbf{B}$ and $\mathbf{B}_e$ are unperturbed and $\delta\mathbf{B}$ and $\delta\mathbf{B}_e = \operatorname{rot}\delta\mathbf{A}_e$ are perturbed magnetic fields inside and outside the plasma; Σ is the boundary of the plasma with the external magnetic field; n is the external normal to the surface Σ; $\xi \equiv \xi^3 = \boldsymbol{\xi}\nabla V$, $\mathbf{e} = \mathbf{e}_3$ is the translation component, and the coordinate vector in the natural coordinate system [4] is

$$d\mathbf{r}=\mathbf{e}_i\,dx^i=\mathbf{e}_1\,d\theta+\mathbf{e}_2\,d\xi+\mathbf{e}_3\,dV,\ \Omega=I'\Phi''-J'\chi'',$$

where $\Phi(V)$ and $J(V)$ are longitudinal and $\chi(V)$ and $I(V)$ are transverse fluxes of vectors $\mathbf{B}$ and $\mathbf{j}$.

If we introduce the combinations of translation components $\mu = \Phi'\xi^1-\chi'\xi^2$, $\lambda = J'\xi^1-I'\xi^2$, then

$$\operatorname{div}\xi=\xi'+(\mathbf{j}\nabla\mu-\mathbf{B}\nabla\lambda)/p'; \tag{5}$$

$$\mathbf{Q}=[\nabla\mu\nabla V]+(\mathbf{B}\nabla\xi)\,\mathbf{e}-(\mathbf{B}\xi)', \tag{6}$$

where primes denote differentiation with respect to v, and the vector $\mathbf{B}'$ is accordingly defined by the equation $\mathbf{B}' = \chi''\mathbf{e}_1 + \Phi\mathbf{e}_2$.

To obtain the potential energy δW_i of a single spiral harmonic of perturbation, we take $\xi = \xi(V)\cos 2\pi(n\xi-m\theta)$, and $\mu = \mu_1(V)\sin 2\pi(n\xi-m\theta) + \mu_2(V)\cos 2\pi(n\xi-m\theta)$. If we limit ourselves to the case of axially symmetric toroidal configurations, then minimization of δW_i over μ_1, μ_2 and integration over ξ yields the expression [5]

$$\delta W_i=\frac{1}{4}\int\left\{\frac{1}{c^2}(\nabla V(u\xi)'-[\mathbf{c}[\mathbf{je}]]\,\xi)^2+\left(\frac{4\pi^2u^2}{c^2}[\mathbf{ce}]^2-\Omega-[\mathbf{je}]^2\right)\xi^2\right\}d\tau. \tag{7}$$

Here and later, $\mathbf{c} = n\mathbf{e}_1 + m\mathbf{e}_2$, $u = n\Phi'-m\chi'$, and $v = nJ'-mI'$. Averaging over the volume of a layer between neighboring magnetic surfaces $\langle f\rangle = (d/dV)\int f\,d\tau$ and integrating by parts gives $\delta W_i = \delta W_v + \delta W_\sigma$, where

Translated from Atomnaya Énergiya, Vol. 34, No. 3, pp. 207-209, March, 1973. Original article submitted April 10, 1972.

$$\delta W_V=\frac{1}{4}\int\left\{\left\langle\frac{|\nabla V|^2}{c^2}\right\rangle(u\xi)'^2+\left\langle\frac{4\pi^2u^2}{c^2}[ce]^2+u\left[\frac{v}{\chi'}\frac{I'+\mathbf{B}'\mathbf{e}_2}{c^2}-\frac{nI'p'}{\chi'^2c^2}-\left\langle\frac{\mathbf{jc}}{c^2}\right\rangle'\right]-\frac{n^2p'p'}{c^2}\right\rangle\xi^2\right\}d\tau; \tag{8}$$

$$\delta W_\sigma=\frac{1}{4}\left\langle\frac{\mathbf{jc}}{c^2}u\xi^2\right\rangle_\Sigma,\quad P'\equiv p'+\mathbf{BB}'=\left(p+\frac{\mathbf{B}^2}{2}\right)'. \tag{9}$$

If we choose the perturbation of the external magnetic field in the form $\delta\mathbf{B}_e = \mathrm{rot}\,[\xi\mathbf{B}_e]$, then the quantity δW_e, and also δW_i, will be defined by Eq. (8) when $j = 0$.

For a homogeneous longitudinal current, we have approximately

$$\delta W_V=\frac{1}{4}\int\left\{\left\langle\frac{|\nabla V|^2}{c^2}\right\rangle F^{12}+4\pi^2\left\langle\frac{[ce]^2}{c^2}\right\rangle F^2\right\}d\tau,\quad F=u\xi, \tag{10}$$

and δW_e is defined by a similar expression. If we disregard the positive terms in δW_V and δW_e, then in the absence of surface currents (when $\delta W_\Sigma = 0$), the stability condition will be $\delta W_\sigma > 0$ or

$$(nj_1+mj_2)(n\Phi'-m\chi')_\Sigma>0. \tag{11}$$

Hence, the stabilization criterion for the spiral instability ($m = 1$ and $n = 1$) can be written in the form

$$|\chi'/\Phi'|_\Sigma<1 \tag{12}$$

for an arbitrary shape of the cross section of the plasma torus.

With surface current, the destabilization related to the surface integral is $\delta W_\Sigma < 0$ and (disregarding the quantity $\delta W_e > 0$) the stability condition will be $\delta W_i + \delta W_\Sigma > 0$. The instantaneous volume enclosed within the magnetic surfaces of elliptical cross section, disregarding the slope of the magnetic axis, is

$$V=\pi L(1-\varepsilon^2)^{-1/2}(1-\varepsilon\cos 2\omega)\rho^2,$$

where ρ, ω, and φ are polar coordinates with the axis $r = R$, $L = 2\pi R$; ε is the ellipticity parameter;

$$\varepsilon\equiv\mathrm{th}\,\eta=(\nu^2-1)/(\nu^2+1),\quad \nu=l_z/l_r \tag{13}$$

is the ratio of the half-axes of the elliptical cross section of the magnetic surfaces.

If within the plasma there is a homogeneous longitudinal field $\mathbf{B}$, then from the pressure-balance condition at the boundary $p + B^2/2 = B_e^2/2$ it follows that the external field B_e is constant in absolute value at the plasma boundary Σ. Here, $\mathbf{n} = \nabla V/|\nabla V|$, and $\mathbf{B}_\perp = |B_\perp|[\mathbf{ne}_\varphi]$. Consequently, for the spiral harmonic $\xi = \xi(V)\cos 2\pi(\zeta-\theta)$, $\zeta = \varphi/2\pi$, $\theta = \omega/2\pi$ we obtain

$$\delta W_\Sigma=-\frac{|B_\perp|^2\xi^2}{8V\sqrt{1-\varepsilon^2}}. \tag{14}$$

The quantity δW_i is determined by Eq. (10) (with $u = \Phi'$), and in the approximation $\mathbf{c} \simeq L\mathbf{e}_\varphi$ after integration by parts can be represented in the form

$$\delta W_i=\frac{1}{4}\left\langle\frac{|\nabla V|^2}{L^2}FF'\right\rangle_\Sigma-\frac{1}{4L^2}\int\{(\langle|\nabla V|^2\rangle F')'-4\pi^2\langle|\mathbf{e}^1|^2\rangle F\}F\,d\tau. \tag{15}$$

The coordinate vectors $\mathbf{e}^1$, $\mathbf{e}^2$, $\mathbf{e}^3 = \Delta V$ of the natural coordinate system in "circularizing" coordinates ρ, ϑ, s [6] in the case of quasihomogeneous configurations are approximately

$$\begin{aligned}\mathbf{e}^1&=(e^{-\eta/2}\cos\vartheta\boldsymbol{\beta}-e^{\eta/2}\sin\vartheta\boldsymbol{\nu})/2\pi\rho;\\ \mathbf{e}^2&=\mathbf{e}_\varphi/L;\\ \mathbf{e}_3&=(e^{\eta/2}\cos\vartheta\boldsymbol{\nu}+e^{-\eta/2}\sin\vartheta\boldsymbol{\beta})\,2\pi\rho L,\end{aligned} \tag{16}$$

where $\boldsymbol{\nu}$, $\boldsymbol{\beta}$ are the unit vectors of the normal and binormal to the magnetic axis and ρ is the characteristic of the instantaneous volume $V = \pi\rho^2 L$. The mean values are $\langle|\nabla V|^2\rangle = 4\pi L/\sqrt{1-\varepsilon^2}$, $\langle|\mathbf{e}^1|^2\rangle = L/4\pi V\sqrt{1-\varepsilon^2}$ and, consequently, the Euler equation for the functional δW_i has the form

$$4V(VF')'-F=0 \tag{17}$$

with its solution $F = \sqrt{V}$.

Thus

$$\delta W_i=\pi B_\parallel^2\xi^2/2L^3. \tag{18}$$

The stabilization criterion of the instability is

$$B_{\perp}^2/B_{\parallel}^2 < 4\pi V/L^3. \tag{19}$$

This condition (as with Eq. (12) for the case of homogeneous, longitudinal current) does not contain the ellipticity parameter ε. In the case of a circular cross section of the boundary magnetic surface, the criteria in Eqs. (12) and (19) coincide and give the necessary condition for spiral stability of a plasma cylinder with an arbitrary current distribution [7-9]. Obviously, the higher modes of the surface instability which we are considering are stabilized when the current density falls off the sufficient rapidity [9]. The conditions for the absence of the spiral instability (m = 1, n = 1) of a plasma filament of elliptical cross section, lead, according to Eqs. (12), (19), to the following limitations on the longitudinal current:

$$|JL/\Phi|_{\Sigma} < 4\pi/\sqrt{1-\varepsilon^2} = 2\pi(\nu + 1/\nu); \tag{20}$$

$$|JL/\Phi|_{\Sigma} < 2L_{\Sigma}\sqrt{\pi/\sigma}, \tag{21}$$

where l_{Σ} is the length of the contour; σ is the area of the cross section Σ of the plasma torus. Stabilization of the spiral instability, as we see from the derivation of Eqs. (12) and (19), is realized because of the internal longitudinal magnetic field and the finite length of the configuration L.

Thus, the stability conditions we have obtained are a generalization of the well-known Shafranov–Kruskal criterion for the case of a plasma filament of elliptical cross section, and in electromagnetic units they take the form for the cases of homogeneous current and surface current:

$$|JR/B| < (l_r^2 + l_z^2)/4; \tag{22}$$

$$|JR/B| < \sqrt{l_r l_z}\, l_{\Sigma}/4\pi, \tag{23}$$

where J is the total longitudinal current in the plasma and $R = L/2\pi$ is the radius of the magnetic axis of the plasma torus.

LITERATURE CITED

1. K. Hain et al., Z. Naturforsch., 12a, 833 (1957).
2. I. Bernstein et al., Proc. Roy. Soc. (London), A244, 17 (1958).
3. L. S. Solv'ev, Zh. Éksp. Teor. Fiz., 53, 2063 (1967).
4. S. Hamada, Nucl. Fusion, 1-2, 23 (1962).
5. L. S. Solov'ev, At. Énerg., 30, 14 (1971).
6. L. S. Solov'ev and V. D. Shafranov, Questions in Plasma Theory [in Russian], No. 5, Atomizdat, Moscow (1967).
7. V. D. Shafranov, At. Énerg., 5, 38 (1956).
8. V. D. Shafranov, Plasma Physics and Problems of Controlled Thermonuclear Reactions [in Russian], Vol. 4, Izd. AN SSSR, Moscow (1958).
9. V. D. Shafranov, Zh. Teor. Fiz., 40, 241 (1970).

SYNCHRONOUS MOTION OF CHARGED PARTICLES IN A TRAVELING-WAVE FIELD

V. M. Mokhov and V. V. Kushin

UDC 621.384.6.01

According to the principle of phase stability, the accelerated particles in the field of a traveling wave group into bunches near the stable equilibrium phase which is unique in the cycle of rf oscillations. However, if the field phase varies in the direction of propagation of the wave, then, as Dreval' and Kushin [1] noted, there arises the possibility of a second stable phase, which leads to the formation of two stable bunches in every cycle of rf oscillations. In the present work, we investigated the conditions in which there arise two stable synchronous phases in the traveling wave whose amplitude and phase vary periodically in the direction of particle motion.

Suppose there propagates along the Z axis a wave in which the synchronous phase φ_S and the amplitude E_m vary along Z periodically with period L, taking the following values in each half-cycle:

$$\varphi_s=\varphi_0\pm\varphi_1,\ E_m=E_0\pm\Delta E_m=E_0(1\pm\varepsilon),$$

where

$$\varepsilon=\Delta E_m/E_0. \tag{1}$$

The equation for longitudinal oscillations for particles with mass m_0, charge e, and phase deviation from a synchronous particle $\Delta\varphi$ in a field with wavelength λ has the form

$$m_0\frac{d^2(Z-Z_s)}{dt^2}=F_1(\Delta\varphi)\pm F_2(\Delta\varphi). \tag{2}$$

Here

$$\begin{aligned}F_1&=eE_0\{[\cos(\varphi_0+\Delta\varphi)-\cos\varphi_0]\cos\varphi_1-\varepsilon[\sin(\varphi_0+\Delta\varphi)-\sin\varphi_0]\sin\varphi_1\};\\ F_2&=eE_0\{[\sin(\varphi_0+\Delta\varphi)-\sin\varphi_0]\sin\varphi_1-\varepsilon[\cos(\varphi_0+\Delta\varphi)-\cos\varphi_0]\cos\varphi_1\}.\end{aligned} \tag{3}$$

According to the method for averaging over oscillations in the form proposed by P. L. Kapitsa [2], the effective potential energy is given by

$$U_{\text{eff}}=-\int F_1\,d(Z-Z_s)+\frac{k^2F_2^2}{4m_0\Omega^2}, \tag{4}$$

where k is the coefficient of the first harmonic term in the expansion of the periodic alternating force $\pm F_2$; $\Omega=2\pi\dot{Z}_S/L$ is the frequency of this force. Here and later, the subscript s indicates the values for the synchronous particle.

For two minima of the potential function to exist in a cycle, it is necessary for its derivative to have in the cycle four different real roots. Taking into account that, for stepped modulation, $k=4/\pi$, $\Delta\varphi=2\pi\cdot(Z-Z_S)/\beta_S\lambda$ (here, $\beta_S=\dot{Z}_S/c$ and c is the velocity of light), we obtain the equation for finding the extrema of the potential function:

$$F_2\frac{dF_2}{d(\Delta\varphi)}-\frac{\pi^4}{4}\cdot\frac{eE_0}{B}F_1=0, \tag{5}$$

where

$$B=\frac{\pi eE_0\lambda}{m_0c^2\beta_s}\left(\frac{L}{\beta_s\lambda}\right)^2.$$

Translated from Atomnaya Énergiya, Vol. 34, No. 3, pp. 209-210, March, 1973. Original article submitted April 19, 1972.

When $\varphi_1 = 90°$, the particles pass through neighboring half-cycles in antiphase, but when $\varepsilon \neq 0$, owing to different field amplitudes in the half-cycles, the velocity increment of the particles in the cycle will be nonzero. In this case, the condition for the existence of two stable equilibrium phases is found in the following manner.

When $\varphi_1 = 90°$, taking into account Eq. (3), Eq. (5) becomes

$$\sin\frac{\Delta\varphi}{2}\cos\left(\varphi_0+\frac{\Delta\varphi}{2}\right)\left[\cos(\varphi_0+\Delta\varphi)+\frac{\varepsilon\pi^4}{4B}\right]=0. \tag{6}$$

The first two cofactors give extrema at $\Delta\varphi = 2k\pi$ and $\Delta\varphi = \pi-2\varphi_0 + 2k\pi$. The second minimum in the cycle arises only when there exist two real roots of the last cofactor of Eq. (6). The condition for the appearance of the second stable phase is determined from the inequality

$$\left|\frac{\varepsilon\pi^4}{4B}\right|<1. \tag{7}$$

If Eq. (7) is satisfied and $0 < \varphi_0 < \arccos(-\varepsilon\pi^4/4B)$, then U_{eff} has in the cycle maxima at $\Delta\varphi = -\varphi_0 \pm \arccos(-\varepsilon\pi^4/4B)$ and minima when $\Delta\varphi = 0$ and $\Delta\varphi = \pi-2\varphi_0$. Then, the maximum at the point $\Delta\varphi = -\varphi_0 + \arccos(-\varepsilon\pi^4/4B)$, separating these two minima, is located below the second maximum. Therefore, the potential well is common to the two minima and its width becomes significant. Thus, for instance, when $\varphi_0 = 30°$, $B = 5$, and $\varepsilon = 0.1$, the distance between the minima is $\pi-2\varphi_0 = 120°$, and the width of the common potential well reaches 300°.

Similarly, one can find the conditions for the existence of two stable equilibrium phases when $\varphi_1 = 0$ or $\varepsilon = \pm 1$. In these regimes, Eq. (5), takes the form

$$\sin\frac{\Delta\varphi}{2}\sin\left(\varphi_0\pm\varphi_1+\frac{\Delta\varphi}{2}\right)\left[\sin(\varphi_0\pm\varphi_1+\Delta\varphi)+\frac{\pi^4}{4B\varepsilon^2}\right]=0. \tag{8}$$

Here, one must choose the positive sign before φ_1 if $\varepsilon = 1$ is considered, and the negative sign before φ_1 if $\varepsilon = -1$. In cases where $\varphi_1 = 0$, it must be omitted from Eq. (8). For these regimes, the condition for the existence of two stable equilibrium phases takes the form

$$|B|>\frac{\pi^4}{4\varepsilon^2}. \tag{9}$$

If we eliminate the possibility of the roots of Eq. (5) coinciding, then conditions (7) and (9) will be sufficient, also, for the indicated cases. In the remaining regimes, the conditions for the existence of two stable equilibrium phases can be found by numerical solution of Eq. (2) on computers.

We note that the results of exact calculations of particle phase trajectories and their approximations by the averaging method in practice often agree well, not only for small, but also for moderate, values of phase-oscillation frequencies. This was noted in [1], in which a calculation was made of the positions of two stable equilibrium phases in one rf cycle for the case $\varepsilon = 0$, and also in [3], where such a coincidence was observed in an accelerator with variable-phase focusing up to the frequency at which the phase advance of longitudinal oscillations in a period of variation of the synchronous phase was 40-50°. We should note that, for good agreement of the results, the modulation depth of the envelope of the longitudinal oscillations must be small.

The criteria we have obtained show in which cases the particle beam moving synchronously with the traveling wave will be grouped into stable bunches whose repetition frequency will be twice the frequency of the traveling wave.

In conclusion, the authors take this opportunity to express their sincere appreciation to B. I. Bondarev, A. D. Vlasov, and L. Yu. Solov'ev for their valuable comments and assistance in the work.

LITERATURE CITED

1. I. D. Dreval' and V. V. Kushin, At. Énerg., 28, No. 5, 423 (1970).
2. P. L. Kapitsa, Zh. Éksp. Teor. Fiz., 21, 588 (1951); Usp. Fiz. Nauk, 44, 7 (1951).
3. I. D. Dreval' and V. V. Kushin, Zh. Teor. Fiz., No. 9, 1915 (1972).

PRODUCTION OF NEUTRONS BY COSMIC RAYS AT VARIOUS DEPTHS UNDERGROUND

G. V. Gorshkov and V. A. Zyabkin

UDC 539.125.5.03:537.59

In measuring small neutron activities care must be taken to reduce the intrinsic background of the detectors themselves due to the natural alpha activity of the structural materials, and the background due to the neutron flux at the earth's surface. This flux consists of neutrons from the atmosphere, neutrons produced by cosmic rays in materials surrounding the detectors, and neutrons from the natural radioactivity of the surrounding rocks.

In experiments at the earth's surface the background is commonly reduced by enclosing the detectors in shields of hydrogeneous materials. A paraffin shield 50 cm thick, for example, decreases the neutron flux by about a factor of 5 to $\sim 10^{-3}$ neutrons/cm^2 sec. A further increase in the shield thickness leads to a slower decrease in the flux at the detector because of the increased importance of neutrons produced by cosmic rays in the shield itself.

A further decrease in the background can be achieved by making measurements underground where the background is determined by the natural radioactivity of the surrounding rocks and the neutrons produced in these rocks by cosmic rays.

We have calculated the rate of production of neutrons in lead, cadmium, iron, and aluminum at depths up to 1000 m water equivalent the nuclear-active (w.e.) cosmic ray component, slow negative muons, and high-energy muons.

The calculated results were compared with measurements of the rate of production of neutrons in the elements mentioned at depths of 40, 80, 140, and 800 m w.e. below the earth's surface [1-3].

The following data were used in the calculations:

1) the rate of production of neutrons in lead at sea level is $8.7 \cdot 10^{-5}$ neutrons/g·sec [4];

2) the rate of production of neutrons at sea level in an element of atomic number A is approximately proportional to $A^{1/3}$ [5];

3) the mean range of the nuclear-active component in the earth is 200 g/cm^2 [5];

4) data on the muon spectrum at sea level in the vertical direction are taken from [6];

5) the angular distribution of muons of various energies at sea level is taken from [7-11];

6) the average number of neutrons $\bar{n}$ emitted by a nucleus which absorbs a slow negative muon is calculated from [12]

$$\bar{n} = \alpha A^{\beta},$$

where A is the atomic weight of the element, $\alpha = 0.292 \pm 0.050$, and $\beta = 0.337 \pm 0.025$;

7) the positive muon excess, the ratio of the number of positive to the number of negative muons, is approximately 1.25 [13], which corresponds to a ratio of negative to total muons of 0.445;

8) in the calculation of the rate of production of neutrons by high-energy muons the following were taken into account: electromagnetic processes leading to the production of neutrons in the penetration of muons through matter, namely the direct interaction of the electromagnetic field of the

Translated from Atomnaya Énergiya, Vol. 34, No. 3, pp. 210-213, March, 1973. Original article submitted August 3, 1972.

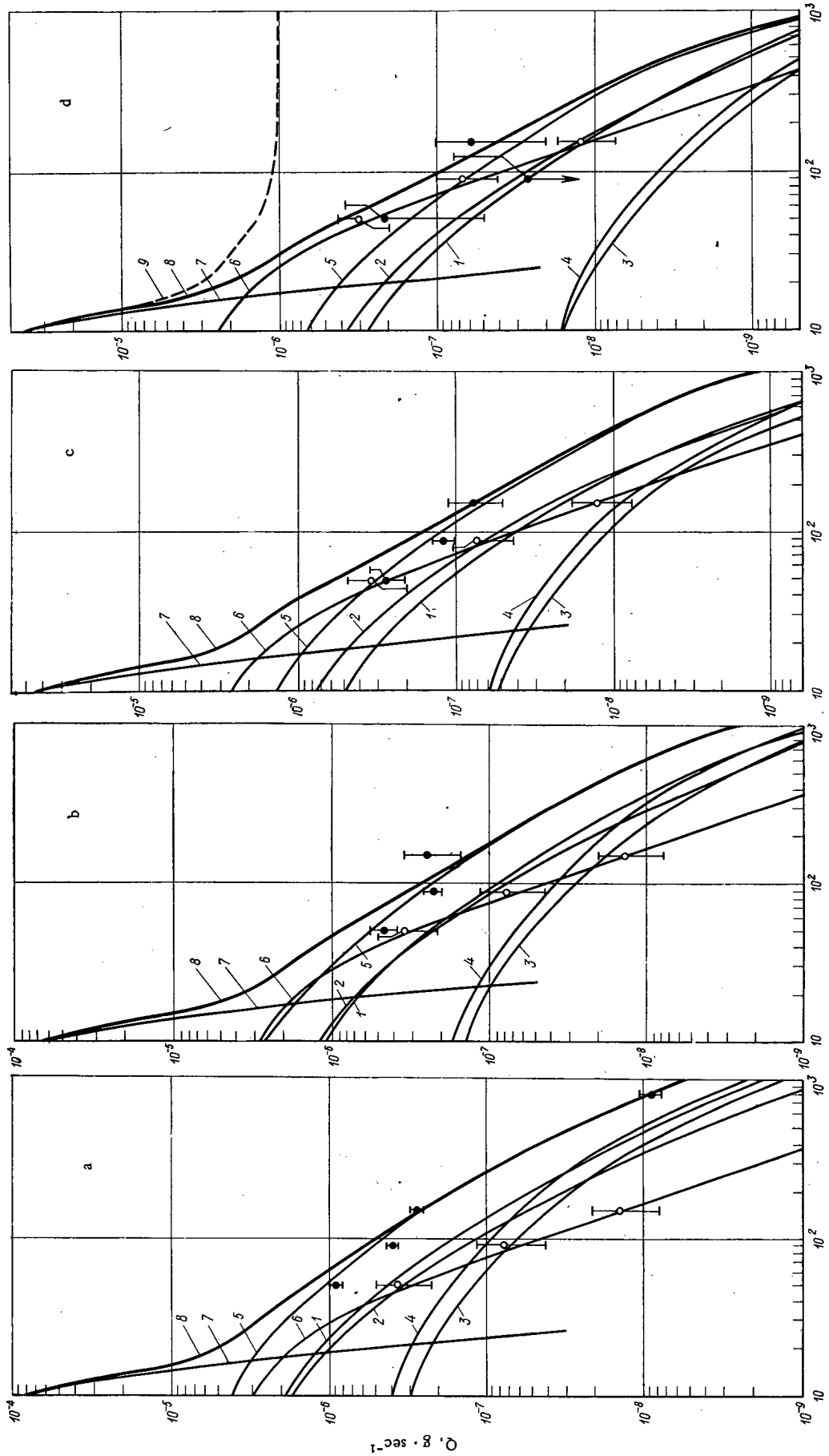

Fig. 1. Rate of production of neutrons in a) lead and b) cadmium; c) and d) aluminum as a result of various processes: 1) direct interaction of the electromagnetic field of a muon with a nucleus; 2) production of δ electrons by muons; 3) bremsstrahlung of muons; 4) production of muon pairs; 5) total rate of production of neutrons by high-energy muons; 6) production of neutrons by the capture of slow negative muons; 7) rate of production of neutrons by the nuclear-active cosmic ray component; 8) total rate of production of neutrons by cosmic rays; 9) rate of production of neutrons in granite by cosmic rays and as the result of the natural radioactivity of granite; experimental points are the results from [1-3] for the production of neutrons by high-energy muons (●) and slow negative muons (○).

muon with nuclei; the production of δ electrons; bremsstrahlung of muons; the direct production of muon pairs. The procedure for calculating the neutron yield from these processes is described in detail in [2, 3].

The results of the calculation are shown in Fig. 1a-d. These figures show the experimental data from [1-3] on the production of neutrons in lead, cadmium, iron, and aluminum by high-energy muons and slow negative muons at various depths. The figures show rather good agreement between the experimental and calculated values.

The rate of production of neutrons in rocks such as granite due to natural radioactivity is $\sim 10^{-6}$ neutrons/g·sec[5]. Since the average atomic weight and density of granite are close to the values for aluminum, the results of the calculation for aluminum can be used to estimate the rate of production of neutrons in granite by cosmic rays. Curve 9 of Fig. 1d shows that for rocks such as granite the neutron background in underground rooms will be practically completely determined by the natural radioactivity of these rocks for depths greater than ~100 m water equivalent.

LITERATURE CITED

1. G. V. Gorshkov and V. A. Zyabkin, Yadernaya Fizika, 7, 770 (1968).
2. G. V. Gorshkov and V. A. Zyabkin, Yadernaya Fizika, 12, 340 (1970).
3. G. V. Gorshkov and V. A. Zyabkin, Yadernaya Fizika, 13, 791 (1971).
4. A. Tobey and C. Montgomery, Phys, Rev., 81, 517 (1951).
5. G. V. Gorshkov et al., Natural Neutron Background of the Atmosphere and the Earth's Crust [in Russian], Atomizdat, Moscow (1966).
6. A. Aurela and A. Wolfendale, Ann. Acad. Sci. Fennicae A VI (Finland), No. 227 (1967).
7. J. Smith and N. Duller, J. Geophys. Res., 64, 2297 (1959).
8. G. T. Zatsepin and V. A. Kuz'min, Zh. Éksp. Teor. Fiz., 39, 1677 (1960).
9. J. Allen and A. Apostolakis, Proc. Roy. Soc., 265, 117 (1961).
10. K. Maeda, J. Geophys. Res., 69, 1725 (1964).
11. F. Ashton et al., Proc. Phys. Soc., 87, 79 (1966).
12. I. B. Bobodzhanov, Preprint OIYaI, 15-5839, Dubna (1971).
13. A. O. Vaisenberg, The Muon [in Russian], Nauka (1964), p. 375.

XXIII SESSION OF THE COMECON PERMANENT COMMISSION ON PEACEFUL USES OF ATOMIC ENERGY

V. A. Kiselev

In accordance with the work plan of the COMECON Permanent Commission on the peaceful uses of atomic energy, the XXIII session of the Commission was held in Wroclaw (Poland) November 28-December 2, 1972.

Participating in the Commission's session were delegations from Bulgaria, Hungary, the German Democratic Republic, Poland, Rumania, the USSR, and Czechoslovakia. Representatives of the Interatominstrument economic association on nuclear instrumentation were also invited.

Reactor science and reactor engineering, and nuclear power engineering, were discussed at the section, in areas covered by the Comprehensive Program for further deepening and improvement of collaboration and development of socialist economic integration of the COMECON member-nations and the related fulfillment of the resolutions passed at the XXVI session of COMECON and the Executive Committee of the COUN Council [on Mutual Economic Aid–COMECON].

The Commission also discussed particular topics pertaining to scientific and technical collaboration in the area of production and applications of isotopes, in the area of radiation engineering and radiation technology, topics relating to standardization, and other subjects of interest in the collaboration of COMECON member-nations in the utilization of nuclear power for peaceful purposes. Information on activities of coordination scientific-technical councils on fast reactors and reprocessing of spent fuel was also heard.

The Commission confirmed its 1973-1974 work plan and the 1973 work plan in the area of standardization.

Appropriate recommendations and solutions were accepted on all of the topics discussed.

Translated from Atomnaya Énergiya, Vol. 34, No. 3, pp. 215, March, 1973.

BUDAPEST CONFERENCE ON IMPLEMENTATION OF RADIATION PROCESSES AND RADIATION FACILITIES

V. P. Averniaov

A conference of COMECON member-nations on implementation of high-level radiation facilities and radiation technology in industry was held October 2-4, 1972, in Budapest. This was the first conference organized on the initiative of the new working body under the jurisdiction of PKIAÉ SÉV [COMECON Permanent Commission on the peaceful uses of atomic energy] – the Coordination Science and Engineering Council on Radiation Technology, KNTS-RT.

Over 80 specialists from Bulgaria, Hungary, the German Democratic Republic, Poland, Rumania, the USSR, and Czechoslovakia took part in the work of the conference, in addition to staffmembers of the COMECON Secretariat and the Interatominstrument international economic association on nucleonic instrumentation. Some 36 reports were heard on the most urgent topics concerning the development of industrial and pilot radiation facilities, and their operating history, on the production technology of new radiation-chemical processes, processes involving radiation sterilization of medical wares, and radiation processing of foodstuffs and agricultural products. All of the reports were of a decidedly and clearcut practical bent, and contained concrete examples, tested out in practice, of the utilization of high-level radiation sources under full-scale plant production conditions.

Some reports of appreciable interest were, for instance, one by W. Suckoff (East Germany) on facilities for radiating medical wares, one by J. Kalmán (Hungary) on the fabrication of self-contracting polyethylene tubing one by M. Pešek (Czechoslovakia) on wood-plastic polyester composite materials, one by A. Papazov (Bulgaria) on radiation processing of food products, and one by M. Petszak and Z. Bulgak (Poland) on the technological dosimetry of radiation processes, as well as other papers.

The papers presented by Soviet specialists on experience in implementating industrial technology of radiation-chemical processes, development of new designs of radiation facilities, providing dosimetric monitoring and radiation safety measures under industrial plant conditions, were heard with great interest. A lively discussion followed the presentation of V. M. Kodyukov's report on engineering cost trends in the development of radiation engineering and radiation technology, in which the dynamics of the growth of output levels in radiation production in various countries throughout the world were presented, and the opportunities open for further improvements in radiation technology and expansion of the scope of applications of radiation technology were discussed.

The conference demonstrated the high level and high-quality performance attained in the area of industrial realization of radiation technology in the COMECON member-nations, which is not inferior to the level and indices attained in the leading capitalist countries in this area. It was also pointed out that the scale and tempo of industrial implementation of radiation techniques and radiation-processing equipment in the national economies of the COMECON member-nations cannot be complacently accepted as satisfactory, and that this field in the peaceful uses of atomic energy requires still higher concentration of material resources and greater concentration of the efforts of scientists and engineers of the socialist countries.

The conference was well organized, and made an unquestionably useful contribution to the exchange of experience and up-to-date information between specialists of COMECON member-nations working on applications of ionizing radiations in the various branches of the socialist economy.

The papers delivered at the conference will be published as a collection of articles in Hungary in 1973.

Translated from Atomnaya Énergiya, Vol. 34, No. 3, p. 215, March, 1973.

COLLABORATION DAYBOOK

A conference of specialists on radiation sterilization of medical materials and wares, and on the development of unified regularatory documents in that area, was held at Baku, November 15-17, 1972. On the eve of the conference, November 13-14, a symposium was held to expedite discussion of methodological topics pertaining to the development of the appropriate regulatory documentation. The two panels in this symposium (radiation chemistry panel and medical biology panel) heard and discussed 25 scientific reports. Participating in the work of the symposium and the conference were specialists from Bulgaria, Hungary, the German Democratic Republic, Poland, Rumania, the USSR, Czechoslovakia, and the COMECON Secretariat.

On the basis of the results of the discussion following presentation of the papers at the symposium and conference, it became clear that the development of regulatory documentation common to all COMECON member-nations in the field of radiation sterilization of medical materials and wares is of enormous importance for the realization in practice of full-scale industrial processes of radiation sterilization.

The following unified regulatory documents agreed upon and accepted for application in the COMECON member-nations: "Summary of rules regulating the radiation sterilization of medical materials and wares in the COMECON member-nations"; "procedures for public health chemical testing of polymeric materials and wares subjected to sterilizing doses of radiation."

In addition, draft procedures for testing radiation sterilization products for pyrogenicity and toxicity were discussed; a draft of a unified scale of exposure dose dependence on the initial degree of contamination of medical materials and wares, a list of terms and concepts in use in the field of radiation sterilization, results of joint investigations conducted by Hungarian and USSR specialists in accelerated ageing of polymeric materials, and other related topics were also discussed.

The conference drew up a plan including measures geared toward further development of research in the field of radiation sterilization of medical materials and wares, and agreed upon an agenda for the forthcoming conference on specialists of COMECON member-nations on these topics, now scheduled for the latter half of 1973 in the USSR.

* * *

The fourth session of the Council of the Interatominstrument international economic association on nucleonic instrumentation was held in Warsaw, November 21-27, 1972. Chairing the session was I. Traikov, member of the Council and director of the Izotop association of factories in Bulgaria.

In line with the accepted agenda, the Council discussed plans for talks on specialization of production and scientific-research work, suggestions on coordinating collaboration in the field of foreign trade involving nucleonic instruments and devices. Suggestions on how best to organize technical servicing, maintenance and repairs of nucleonic instruments and devices fabricated by Interatominstrument members, and also on the organization of exhibitions and participation of Interatominstrument in international exhibitions and trade fairs, were discussed. The Council accepted for inclusion in the Interatominstrument catalog of products isotope sources which have now been included in the set of available nucleonic instruments and devices, and confirmed the work plan drawn up for the years 1973-1974.

Appropriate resolutions were adopted on all these topics.

Translated from Atomnaya Énergiya, Vol. 34, No. 3, p. 216, March, 1973.

The next regularly scheduled session of the Council will be held in April 1973, to deal with an agenda agreed upon beforehand.

The session took place in a businesslike atmosphere in a spirit of complete mutual understanding.

CONFERENCES

INTERNATIONAL CONFERENCE ON SAFETY ENGINEERING OF FAST REACTORS

Yu. E. Bagdasarov

A conference on engineering aspects of fast reactor safety was held in Karlsruhe (West Germany), October 9-13, 1972. Over sixty reports were delivered, on the following topics: experience in the design and operation of fast reactors; safety engineering and safe realiable operation; breakdown of fuel elements, boiling of sodium, and interactions between sodium and liquid fuel; mechanical effects of core breakdown; analysis of hypothetical accident situations; reaction of sodium with air and activity release. Over half of the reports dealt with the first two problems mentioned.

At the present time, BOR-60 experimental fast reactors (USSR), the Rapsodie fast reactor (France), the Dounreay (Britain), and the EBR-II (USA) fast reactors are already in successful service; a scientific-research program on the SEFOR facility (USA) has been concluded, relatively stable operation of the low-power Enrico Fermi reactor in the USA and KNK reactor (sodium-cooled thermal reactor) in West Germany is underway, and the modernization of the BR-5 fast reactor (USSR), whose power ratings are to be doubled, is nearing completion. Particular success has marked the performance of the BOR-60 fast reactor, with its maximum oxide fuel burnup of 10%.

The basic research findings obtained with the SEFOR reactor have included securing detailed data on the Doppler coefficient of reactivity and its components; it is now asserted that these data make it possible to calculate reciprocal reactivity effects (due to the Doppler effect) in the analysis of hypothetical accident situations, to within ± 20%. The properties of the fast reactor, quite satisfactory from the vantage point of reactor safety, were demonstrated on the SEFOR facility in experiments with supercritical reactor run-aways (up to 1.3 dollars/sec), during which the power level fell back, after an initial rise, because of release of feedback reactivity.

Following the well-known accident involving partial meltdown of fuel in two Enrico Fermi fuel assemblies in 1966, there has not been a single serious accident on any of the reactors in question. There have been some ordinary malfunctions; problems due to fuel fabrication flaws, insufficient experience in the field of sodium technology, and personnel judgement errors, have occurred.

Counted among the most typical types of malfunctions are those due to precipitation of sodium vapor and sodium vapor aerosols in narrow slit clearances of a gas void, a factor which adds difficulties to the correct performance of rotating mechanisms, and malfunctions due to errors in the design and installation of the electrical heating for the tubing, which lead to sizable unevenness in temperatures, errors in performing operations in the system designed for oil lubrication of sodium loop equipment (primarily loop pumps), which allow grease to get into the sodium and in which case special measures must be taken to get rid of the grease; equipment fabrication flaws.

The most important and crucial equipment, from the standpoint of reliable operation of fast reactors, is the steam generator with one-wall separation of sodium from water and steam. The performance of experimental steam generators at experimental reactors can be considered quite encouraging on the whole. After the design of the steam generator units serving the Enrico Fermi reactor had been improved (defective tubing replaced, reinforcements improved, throttle washers in the form of long short-diameter tubes installed), they have been functioning satisfactorily on the whole. The heat-transfer tube in the KNK reactor worked loose because of a factory defect at the site where the spacer was welded on; the tube was retracted; the steam generator is being prepared for recommissioning. A 30 MW module of a vessel type steam generator with coiled tubing, designed for the BOR-60 fast reactor, is giving successful performance; it has been in service for over 8000 h at parameters close to ratings.

Translated from Atomnaya Énergiya, Vol. 34, No. 3, pp. 217-219, March, 1973.

Several large prototype fast reactors are being built or put into service. The basic technological tests on the primary and secondary sodium-filled loops have been completed on the BN-350 fast reactor (USSR), and the physical startup is in progress. The loops of the Phenix reactor (France) are ready for their sodium charge, and physical startup is planned for the April-June, 1973 period. The PFR reactor (Britain) is at a similar stage. The BN-600 reactor is now under construction in the USSR. Large nuclear power stations built around fast reactors are being planned in several countries.

Close attention is being given to "routine" problems in the dynamics of the reactor and of the installation as a whole, to thermal shock, emergency cooldown, sources of gas accumulation in the loop, loop gas transport, and vibration problems. Some interesting results on determination of the heat regime of fuel elements when some amount of homogeneously dissolved gas is presented in the sodium have been obtained in the USA. For example, the temperature of the casing rises by about 10°C when the level of 20 vol.% gas is attained. At the same time, the changes in reactivity brought about by that amount of gas is sufficient for detection. In addition to computational studies of thermal shock, great significance is attached to direct experimental research on thermal shock affecting different type of process equipment on test stands. Such studies have been made on a 50 MW steam generator test rig at Renardier (France) and on a pump test stand at Interatom (West Germany). A 50°C/h or slower rate of sodium temperature change is deemed safe.

As earlier, close attention is being given to operational realibility problems and steam generator safety. The study of effects brought about when large amounts of water gain access to the sodium stream in accidents (as much as 12 kg/sec) is being pursued in West Germany and Japan, confirming the conclusions reached earlier elsewhere (including in the USSR) that such accidents do not involve "chain" reactions: failure of any one tube does not bring about failure of nearby tubes. During accident simulation experiments, it is not possible to achieve excessively protracted water leakage (over 4-5 sec) because of inadmissible contamination of the test stand by interaction products. This highlights the importance of lowering the accident parameters (pressure and temperatures at the site of the interaction and throughout the loop) long before the water feed is cut off. The fact that not a single case of damage to bellows type temperature expansion joints in a simulated joint under high pressures has been recorded is accorded great practical importance.

The consequences of small water leaks into the sodium stream are still not given the attention they deserve. Medium-level leaks (over 400 g/h) were investigated in experiments reported at the conference (West Germany). The results are similar to those published in the USSR and in the USA.

Considerable space was reserved for analysis of reliability and safety in the design of reactors, shielding and localizing devices capable of narrowing the possibility of accidents developing.

Virtual unanimity was reached at the conference on the following measures required for fast-reactor safety.

1. Emergency Cooldown. Any of the working subloops of the reactor must be capable of bringing about long-term heat removal with the aid of natural circulation; a special auxiliary source (storage battery, diesel generator) must be installed directly in the reactor building for emergency power supplies. Since the emergency power supplies figure as protection devices, the probability of malfunctioning must be taken into account in plant safety analysis. It is assumed that an auxiliary low-output subloop (~2% of rating) completely independent of the principal subloops must be provided. As a rule, this unit is a heat exchanger built into the reactor pressure vessel, and transmitting heat to the second sodium–potassium loop, and from it air, with natural circulation of the coolants throughout all the loops of the system. It has been proved that the failure probability of the emergency heat removal system is two orders of magnitude lower when such an auxiliary subloop is built in than when it is lacking.

2. Emergency Protection. Two absolutely independent emergency protection systems are required, each of them capable of bringing the reactor back to a subcritical state. The emergency protection systems as a whole, and their components, should be provided with automatic malfunction monitoring devices. Development of emergency protection systems based on new principles is crucial. A paper from the General Electric Co. (USA) is interesting in that light. Their new system is based on holding the scram rod at top position through the action of hydraulic forces generated by a special pump. Experiments have shown a response time of 0.5 to 1.5 sec.

3. Core Safety State Monitoring. This problem received relatively little attention at the conference. Nevertheless, we can sense unanimity on the need to detect a local emergency in time. Even though possibilities of monitoring with the aid of thermocouples at the exit of each fuel assembly are limited at low power levels, such monitoring is obligatory. Acoustic sensors still fail to satisfy requirements in determining sodium boiling noise. But the first successful results on utilization of acoustic systems to detect many other reactor phenomena were obtained at the Rapsodie reactor. A reactivity balance analyzer exhibiting impressively high reliability was installed at the Enrico Fermi reactor in 1970. It is stated that such a device would have been helpful in readily detecting the 1966 accident involving partial fuel meltdown.

4. Systems for Localizing Hypothetical Accidents. Despite the fact that an accident involving core meltdown, formation of secondary critical masses, and explosions is considered highly improbable, and due to the development of "ordinary" accidents with sequential failure of many protective systems, a virtually unanimous opinion has been formed on the part of foreign scientists on the need to provide protection devices to handle that case as well. Systems in question include the reactor pressure vessel, the surrounding structures, and the containment shell, which are to take up the impact of the explosion and confine sodium vapor, sodium vapor aerosols, fuel particles, and fission products.

The second half of the conference was devoted to results of a study of the topics under discussion, computational investigations of local accidents and limiting cases of accidents, and their mechanical effects on structures; work programs on fast-reactor safety and descriptions of experimental test stands and devices.

The experimental papers can be divided into three basic categories: 1) simulation of local accidents, meltdown accidents, and fuel element and core failure, mechanical effects of explosions on structural members, using water and metals (e.g., lead) to simulate fuels; 2) in-pile investigations of sodium streams; 3) in-pile experiments. We note the following data which are essential from the standpoint of accumulating factual material for a clearer grasp of the physical picture in the development of accidents. The hydraulic characteristics of a fast-reactor package are somewhat ambiguous: local sodium boiling over the entire cross section of the package can be accompanied by rapid (~1 sec) flashing of the sodium and destruction of the channels. That renders it extremely important to establish the fact of nonpropagation of a local blockage or obstruction in one or several fuel-element channels, or local sodium boiling over the entire cross section of the package. It has been shown experimentally that, in initial sodium superheat to 150°C, the resulting stream void grows to 3 cm in diameter and then collapses in 25 msec; the locally generated and disappearing voids bring about oscillations in the sodium flowrate and in the pressure within the fuel assembly, which can be recorded by instrumentation; overheating of the fuel element does not constitute a serious hazard. It has been stated (on the basis of calculations and comparison of empirical findings and experimental) that the influence zone of the local blockage of channels in individual fuel elements is small. Similar results were obtained in the in-pile experiments.

It has been established experimentally that local blockage of a channel results in destruction of the fuel element if the blocking material exhibits low thermal conductivity; the explosive nature of the destruction of the fuel element accompanied by rapid ejection of fuel into the coolant is a possibility only under conditions where heavy pressure is exerted on the cladding in the course of the accident. Direct experiments at the TREAT reactor (USA) have shown that even meltdown of 40% to 60% of the fuel in the element does not increase the initial diameter of the fuel rod substantially. On the basis of an analysis taking results of in-pile experiments into cognizance, it was found that meltdown of a single fuel element on account of erroneous overenrichment of the fuel does not cause the accident to propagate to nearby fuel elements. An abrupt increase in the diameter of the fuel rod in contact with sodium was noted in in-pile experiments, with an increase in the O/M ratio in the oxide fuel; increased swelling of the fuel was also reported, with an increase in the oxygen content in the sodium.

Results of numerous experiments and calculations of a hypothetical accident carried out in relation to specific reactor installations (PRF, Phenix, SNR, FFTF, etc.), show that the intervals in the initial disturbances gradually narrow down. These disturbances are typified by the following figures: maximum rate of reactivity insertion 25 to 100 dollars/sec; ratio of destructive mechanical energy to thermal energy released ~0.04 to 0.1; absolute values of mechanical energy ~50 to 100 MW sec.

Some attention was given, at the conference, to sodium leakage to the surroundings, to dissemination of sodium aerosols and aerosols of fission products in response to sodium combustion. Some of the papers

were presented with films as visual aids. A report on the corrosion rate of the wall of tubing when micro-leakages of sodium turn up was the most interesting of all. A graph of the dependence of the time to formation of inadmissible corrosion (with hazard of a major failure) on the initial sodium leakage was shown; at leakages ~4 g/h or more, the time is ~100 h; at smaller leakages, the time stretches (say, to 1000 h for leakages of $4 \cdot 10^{-2}$ g/h).

The reports presented at the conference will be published in February-March, 1973.

SYMPOSIUM ON THE CHEMISTRY OF THE TRANSURANIUM ELEMENTS

N. N. Krot and I. K. Shvetsov

A symposium on the chemistry of the transuranium elements, organized under the auspices of the Presidium of the Academy of Sciences of the USSR and GKAÉ SSSR, was held in Moscow, September 4 through September 8, 1972. This symposium attracted 100 Soviet radiochemists and 23 foreign scientists (from the German Democratic Republic, Poland, the USA, France, West Germany). Attention centered on discussions on redox reactions and different properties of simple and complex compounds of the transuranium elements. A good portion of the reports submitted dealt with laboratory and industrial methods for isolating and purifying transuranium elements. There were also some interesting theoretical communications of the end region of the D. I. Mendeleev periodic system and on scientific forecasting of the properties of superheavy elements. A total of 55 reports were read.

The symposium opened with remarks by Academician V. I. Spitsyn.

Review papers covering general topics in the chemistry of the transuranium elements were presented by V. I. Spitsyn, G. N. Flerov, N. B. Mikheev (USSR), G. Seaborg, O. Keller, and J. Peterson (USA).

G. Seaborg and G. N. Flerov took note of the isolation of isotopes of element 104 and element 105, assessing this as a great achievement. Research is now being pursued further on synthesis of element 106 and element 107, as well as superheavy elements from the theoretically predicted stability region of nuclides extending from Z = 110 to Z = 114. Targets of heavy elements were bombarded with accelerated xenon nuclei at Dubna, and an accelerator of heavy ions all the way up to uranium is scheduled for commissioning in the USA in the near future. In addition to attempts at synthesis, close attention is being given to theoretical calculations of possible electronic configurations of as yet undiscovered elements, and to predictions based on their physical and chemical properties. Searches for new elements occurring in natural materials are being continued both in the USA and in the USSR. An interesting report was made on the isolation of the long-lived isotope Pu^{244} ($T_{1/2} = 7.5 \cdot 10^7$ years) from ores. However, attempts to detect superheavy elements in nature still elude success.

Results of several research efforts on the transuranium elements conducted at Oak Ridge were reported in a paper by O. Keller. The staff of the ORNL has succeeded in growing a single crystal of a new compound, with septivalent neptunium, composition $LiCo(NH_3)_6Np_2O_8(OH)_2 \cdot 2H_2O$. X-ray structural analysis revealed that the neptunium atoms in this complex compound are surrounded by oxygen atoms forming a deformed octahedron with four short bonds and four long bonds. The octahedra are interlinked in long zigzagging chains. It was inferred from these results that septivalent neptunium exists in alkaline solutions in the form of $NpO_4(OH)_2^{3-}$ anions.

Photoelectron spectroscopy, useful in studying the properties of solid-phase transuranium elements, has won quite widespread popularity as a research technique in recent work at ORNL. The effectiveness of the method is illustrated by the results of an investigation of chemical bonds in fluorides of the actinoids. Work on developing and improving speedy methods for isolation and chemical identification of short-lived heavy isotopes is being continued. Among the promising methods in view are some based on ion exchange and vapor chromatography, such as had been proposed and utilized earlier at Dubna.

J. Peterson delivered a report on scientific and teaching activities carried out by the late Professor B. Cunningham, who passed away in 1971, and who made a major contribution to the development of micro research techniques and the study of the chemistry of actinoids in the USA. A paper submitted by V. I.

Translated from Atomnaya Énergiya, Vol. 34, No. 3, pp. 219-221, March, 1973.

Spitsyn rendered homage to the memory of Soviet scientists who were founders of radiochemistry and initiators of the study of the chemistry of the transuranium elements in the USSR (V. I. Vernadskii, V. G. Khlopin, I. V. Kurchatov, B. V. Kurchatov).

A review paper by N. B. Mikheev discussed the advantages and feasibility of cocrystallization and adsorption as techniques for studying the properties of trace amounts of the transuranium elements. These methods have been used by the author and colleagues to identify lower valency forms, and to study oxidative–reducing reactions involving the transcurium elements.

In recent years, the production of the far transuranium elements has increased measurably, which sets up favorable conditions for more profound investigations of the chemistry of these elements. In particular, it has become possible to isolate metallic berkelium, californium, and einsteinium, and to study their properties (J. Peterson, R. Beybarts, USA). Macroquantities of berkelium and californium have been useful in determining the stability constants of the monochloride and thiocyanate complexes of those elements. The polarographic method has been used to show that the potentials of Bk(IV)–Bk(III) and Cf(III)–Cf(II) vapors are close to the potentials of Ce(IV)–Ce(III) and Sm(III)–Sm(II) vapors, respectively.

The expansion and deepening of research on the chemistry of the transuranium elements has led to highly intriguing and unexpected results, particularly in the field of oxidative–reducing reactions. Relatively high stability of the bivalent state of these elements, starting with californium and continuing all the way to nobelium, has been established in work by Soviet and American scientists. Californium dibromide and californium diiodide have been isolated in the solid state, and have been identified by the x-ray structural method. An attempt to isolate the oxide of bivalent einsteinium by reducing Es_2O_3 with hydrogen failed to yield unambiguous results. The bivalent state of the elements Cf–Fm in aqueous-etholic solutions was identified by coprecipitation techniques. Standard redox potentials of M(III)–M(II) vapors for einsteinium and californium were found to be -1.55 ± 0.04 V and -1.60 ± 0.04 V, respectively. The potential for fermium lies somewhere between the potentials for europium and ytterbium. Experimental data on the redox properties of the remote transuranium elements are in satisfactory agreement with results predicted by L. Nugent (USA) on the basis of a study of the optical properties of those elements.

The first information on reduction of mendelevium to the univalent state was presented at the symposium (N. B. Mikheev, V. I. Spitsyn, and colleagues, USSR). Univalent mendelevium was identified by studying its coprecipitation with CsCl from ethanolic solutions in the presence of strong reducing agents.

In addition to investigation of the lower degrees of oxidation of the transuranium elements, there was considerable interest in data on the properties of those elements in anomalously high valency forms. Recently, the californium dioxide was isolated and its structure investigated (R. Beybarts, USA). A series of papers came out on the special features of the chemistry of neptunium and plutonium in the septivalent state. The experiments performed supported the inference that septivalent neptunium and plutonium bear no essential similarity with the elements in the seventh group in the higher degrees of oxidation (N. N. Krot, A. D. Gel'man, and co-workers, USSR). Data on the IR spectrophotometry of some compounds of septivalent neptunium (A. Yu. Tsivadze et al., USSR) are in satisfactory agreement with the results of above-mentioned x-ray research conducted at Oak Ridge. Electronic absorption spectra of alkaline solutions of septivalent neptunium and plutonium, of sexivalent americium, and of quadrivalent berkelium (D. Cohen, USA) were taken. It was found that sexivalent americium is reduced by water at a measurable rate, at room temperature in alkaline media. Quadravalent berkelium is found to be stable against attack by alkalis.

The attention of investigators has been steadily attracted to the pentavalent state of the actinoids in recent years. It has been shown that neptunium, plutonium, and americium form stable peroxide complexes in that form of valency (C. Meusicasse, France). Pentavalent americium, when in weakly acidic or neutral solutions, enters into a complexing reaction with oxalate, ethylenediaminetetraacetate, and diethylenetriaminepentaacetate ions. Pentavalent americium is rapidly reduced by organic complexing sequestrants under those conditions, partially to the pentavalent form and partially to the trivalent form (V. P. Shilov et al., USSR). Several new solid-state compounds of pentavalent neptunium have been isolated from solutions (M. P. Mefod'eva et al., USSR).

There has been considerable interest in the results of an investigation into the nature of chemical bonds in actinoid ions, using methods of IR spectroscopy (V. M. Vdovenko et al., USSR). It was shown that there exists some correlation between changes in the infrared spectra of these ions and the stability of their complexes with diverse ligands.

Some of the typical features of octahedral complexes of trivalent and quadrivalent actinoids with halides were discussed in a report by Yu. A. Barbanel' (USSR). These acido complexes form readily in aqueous-alcoholic solutions containing halide ions.

Acido complexes of trivalent actinoids with nitrate ions, chloride ions, bromide ions, iodide ions, and thiocyanate ions as ligands play an important part in solvent extraction by salts of tertiary and quarternary alkyl ammonium (E. P. Derevyanko et al., USSR). The efficacy of the solvent extraction process depends on the nature of the ligand and on the molecular structure of the extractant. There exists some correspondence between the distribution coefficients and the degree of covalency of the metal–ligand bonds in the complexes.

New concepts on the nature of the interaction between pentavalent neptunium and multiply charged cations, and its effect on the rate of redox processes, were dealt with as illustrated by the example of the reaction involving pentavalent neptunium and divalent iron, and quadrivalent neptunium and trivalent iron, in a report submitted by A. A. Frolov and A. G. Rykov (USSR).

The study of the kinetics of those reactions is of great importance in elucidating the mechanism underlying redox reactions of the transuranium elements. The results of such investigations in relation to reactions involving pentavalent and sexivalent neptunium and hydrazine, trivalent plutonium and quadrivalent uranium with nitric acid, and quadrivalent plutonium with Mn^{3+} and MnO_4^-, were mentioned in a report by V. S. Koltunov and colleagues (USSR). Extensive material on the kinetics of cation–cation reactions occurring with a change in the structure of ions, in the case of the transuranium elements, was presented in a report by A. G. Rykov (USSR). In reviewing this material, the author established some regularities in the variation of thermodynamical parameters of activation of the reactions, and proposed empirical equations for estimating the parameters.

The kinetics of redox reactions of uranium and neptunium in nonaqueous solutions were discussed in a report by L. M. Frolova et al. (USSR). G. M. Kazakova and V. N. Kosyakov did a comparison of the redox behavior of berkelium and cerium. The results obtained are important and valuable for developing techniques for isolating and purifying berkelium.

New data on the interaction of neptunium, plutonium, and americium with radiolytic products in aqueous media were presented in detailed reports by A. K. Pikaev and M. V. Vladimirova et al. (USSR). These data were used by the authors to validate the mechanism of radiation-chemical transformations of actinoid ions in various media.

K. Keller (West Germany) reported on the results of investigation of the synthesis of intermetallic compounds of the elements from thorium to californium with the noble metals. These compounds are formed as hydrogen acts on the oxides of the actinoids in the presence of finely pulverized platinum, palladium, iridium, and rhodium. They decompose, at an elevated temperature, into their constituent components. In that way, W. Müller et al. (West Germany) succeeded in isolating gram quantities of high-purity americium, which those authors then used in determining the heat of formation of Am^{3+}(aq) ions: 616.7 ± 1.2 kcal/mole.

Several papers dealt with discussions of the structure of solid compounds of the transuranium elements. In studying the structure and coordination numbers of metals in fluoride complexes with thorium and uranium extracted from aqueous solutions, R. Penneman (USA) detected a hitherto unknown compound for the actinoids $7NH_4F \cdot 2ThF_4 \cdot H_2O$, with a dimer unit cell in its lattice. L. V. Sudakov and I. I. Kapshukov (USSR) carried out an x-ray investigation of the phases present in the system curium–oxygen, which made it possible to refine and expand presently available information on oxygeneous compounds of curium. A study of the structure of chalcogenides of the actinoids (D. Dallier and R. Berget, France) revealed close similarity between those compounds and corresponding compounds of the lanthanoids. Their structure and properties depend essentially on the ionic radius of the metal.

Interesting papers among those dealing with separation and purification of the transuranium elements were, in particular, those discussing experience in full-scale industrial production of those elements. Solvent extraction by trilaurylamine from nitrate streams is widely relied on in France (A. Chenet) for separating quadrivalent neptunium and trivalent plutonium. This operation is sufficiently efficacious either for isolating neptunium from process wastes or for separating neptunium from irradiated neptunium targets. The trilaurylamine can also be used to advantage when isolating and purifying americium and curium.

A combination of ion exchange, extractive chromatography, and precipitation of bicarbonate of pentavalent americium and pentavalent potassium was resorted to at the European Institute of the Transuranium Elements (W. Müller et al., West Germany) in order to isolate gram quantities of pure americium and curium isotopes. Tricapryl ammonium nitrate and di-(2-ethylhexyl)-orthophosphoric acid (D2EHPA) were employed as extraction agents.

In order to isolate americium and curium from process wastes in the reprocessing of spent fuel elements from power reactors, coextraction of trivalent actinoids and lanthanoids using a synergetic mixture of D2EHPA and TBP has been recommended (G. Koch et al., West Germany). Separation of americium and curium from (rare-earth fission products can be achieved through back-extraction using solutions of complexing agents and lactic acid.

Group extraction with the aid of D2EHPA is being used at Oak Ridge in the first stage of separation of transplutonium elements. The next step in separation of transcurium elements from the bulk of the americium and curium is carried out by anion exchange from LiCl solutions. The elements are finally purified from curium to fermium on cation exchange resins, with the aid of ammonium α-hydroxyisobutyrate; the technique of high-pressure ion exchange is resorted to.

An extraction scheme based on DAMP and D2EHPA has been proposed in the USSR (V. N. Kosyakov, E. G. Chudinov, and I. K. Shvetsov) for the production of milligram amounts of californium. This scheme makes it possible to isolate transplutonium elements at a very high degree of purity. The scheme is based on the use of combined solvent extraction and chromatographic techniques distinguished by simplicity and reliability.

Methods for separating transplutonium elements, based on the utilization of higher valency forms of americium and berkelium, were discussed in a paper by B. F. Myasoedov (USSR). Excellent separation of trivalent curium from pentavalent americium has been achieved in solvent extraction by 1-phenyl-3-methyl-4-benzoyl-pyrosolon-5. Selective extraction of quadrivalent berkelium has been achieved through sorption on zirconium phosphate.

The sorptive behavior of the transplutonium elements in aqueous-organic solutions and the application of the results obtained in the development of methods for separating those elements were covered in a detailed paper submitted by L. I. Guseva et al. (USSR).

Some interesting results were reported by M. K. Chmutova et al. (USSR) from studies of solvent extraction of the transplutonium elements using synergetic mixtures of extraction agents capable of increasing and enhancing extraction and purification of the elements in a number of instances.

A report by G. V. Korpusov and colleagues (USSR) analyzes different extraction processes with optimum separation of trivalent transuranium elements, on the basis of which systems and conditions most suitable for practical use were selected.

Extensive theoretical material on solvent extraction of actinoids using neutral and acidic organophosphorus compounds and amines was presented in a report by A. M. Rozen and co-workers (USSR). These authors placed special attention on the extraction mechanisms and on the effect of the structure of the extraction agents on their extractive properties.

Vapor-phase chromatography has made an excellent name for itself in the isolation and identification of the remote transuranium elements. A report by J. Zvary et al. (Dubna) was devoted to applications of vapor-phase chromatography and its possibilities.

G. Yu. Baier et al. (USSR) reported on rapid electrolytic concentration and electromagnetic separation of isotopes. It was shown that mass separation of isotopes of the actinoids, including californium, takes place quite efficiently.

The concluding session of the symposium was devoted to the position of the transuranium elements in the periodic table, and extrapolation to superheavy elements (V. I. Spitsyn, A. N. Nesmeyanov, A. A. Chaikhorskii, USSR; G. Seaborg, R. Penneman, and G. Weiber, USA). It should be stressed that the problem of what position the transuranium elements occupy in the periodic table remains an open one. As for predictions of the properties of the superheavy elements, this question cannot be considered definitively solved either, without experimental confirmation of the actual existence of "islands of stability."

It should be stated, in conclusion, that the symposium held will contribute to the further development of the chemistry and technology of the transuranium elements.

SEPTEMBER 1972 SYMPOSIUM ON COLLECTIVE METHODS OF ACCELERATION

V. P. Sarantsev

A symposium on collective techniques of acceleration, devoted to a review of the research completed in the past year, was held in Dubna in September, 1972. This symposium was a demonstration of the steadily increasing interest in research on collective methods of acceleration both in the Soviet Union and in other countries. The symposium was organized by the countries of the socialist camp (by JINR and by the USSR Academy of Sciences), but was the most representative meeting of specialists on collective methods of acceleration. The symposium attracted 200 or so scientists from all the scientific-research centers of the world engaged in work in this area. Some sixty reports were heard.

In addition to prominent scientists, the participants also included highly qualified young specialists. This appears to be the decisive factor in determining progress in this direction of research.

The principal sections of the symposium scientific agenda were: electron storage ring accelerators; acceleration of charged particles in plasma and in electron beams; production and shaping of high-current electron beams. The largest number of papers on a single topic (about thirty) dealt with the first of these topics.

The symposium showed that the geographic picture of investigations into collective methods of particle acceleration has been expanded considerably. For the first time, research terms from Canada, France, and Japan showed up, as well as several new terms actively working in this area in the Soviet Union.

Electron storage ring accelerators. This topic is being tackled by many teams working in different countries (the level of the work being done varies). We need concern ourselves here only with the basic research.

Different modes of electron storage ring capture during the compression process have been investigated at Berkeley (USA) during the past year. Attention has been centered on the study of conditions under which radiation effects or other collective processes, leading to a restriction of the number of particles trapped in the compression process, failed to occur. Several theoretical contributions, in addition to the principal report, dwelt on these topics.

An extensive series of investigations of wall effects (range of wall resistivities 100 to 0.06 Ω/cm^2) and their influence on longitudinal beam instabilities has been carried out. The latest of these experiments employed a bubble chamber. A 15 μ thick stainless steel chamber was placed inside a ceramic chamber, in the usual procedure. This arrangement made it possible to trap a beam with an intensity of at least 10^{13} electrons, normally. The principal conclusion drawn is: the compression process must be carried out near walls with sufficient conductivity in order to trap a large number of particles. The same applies to the acceleration process.

Research at Garching (West Germany) has been centered on improving the beam parameters of the linear electron accelerator with the object of increasing the number of particles trapped in the compressor. Additional focusing devices capable of increasing the number of particles to $8 \cdot 10^{12}$ were introduced into the accelerator tube, and of those $5 \cdot 10^{12}$ particles were trapped in the compression mode; the ring radius was brought to 2.5 cm. Searches for more sophisticated compression systems are not being neglected either. Specifically, possibilities of a single-revolution compressor are being looked into. The circuit in such a system would function simultaneously as the vacuum chamber.

Translated from Atomnaya Énergiya, Vol. 34, No. 3, pp. 222-223, March, 1973.

A procedure for producing electron rings from a cylindrical beam immersed in a magnetic field is being developed at the University of Maryland (USA). To date this work has been done on a low-intensity linear accelerator, and the resulting storage rings do not contain large numbers of particles. A single-gap accelerator with a field emission cathode generating a cylindrical electron beam with 5 MeV particle energy and 20 kA beam current has been acquired in order to conduct these experiments. This type of current cylinder, 3 m in length because of deceleration in the growing magnetic field, is to be converted into a storage ring.

Work with electron storage rings is being pursued further at Karlsruhe. Experimental research in this area has commenced at Saclay (France) and in Japan.

Great interest was shown in the Soviet reports, in particular the report by staff of the Institute of Experimental and Theoretical Physics [ITÉF] entitled "On a collective high-current accelerator," which cited the basic arguments on the possibility of constructing a $\approx$ 1 GeV meson factory type collective accelerator. It was shown that even given a possible limitation on the rate of ring energy gain via coupling resonances of radial and axial oscillations of electrons and ions, there should be no great practical difficulty in building an accelerator with an average current ~1 mA and a high efficiency.

The largest number of reports submitted on different aspects of the design and acceleration of electron rings was forthcoming from JINR. Possible production of rings with 10^{14} electrons is under study at Dubna; preparations for relevant experiments have now been completed. The machine built for the experiments is expected to accelerate heavy ions (up to uranium ions) with an intensity far in excess of the intensity of existing heavy-ion accelerators. The special-purpose Silund electron accelerator is being used for this purpose, as well as an adherer chamber made of thin stainless steel. Assembly of these systems is now nearing completion. Variants of the accelerating systems are also under investigation.

Particle Acceleration in Plasma and in Electron Beams. The basic trends in research on particle acceleration in plasma and in electron beams coincide in many ways, even though the problems are different in nature. When we refer to particle acceleration in plasma, we have in mind, as a rule, acceleration in an electromagnetic wave excited by a high-power electron beam interacting with a plasma. This problems is being investigated in the most fundamental way at the Harwell Physics and Engineering Institute. The use of modulated electron beams has made it possible to excite electromagnetic oscillations with a narrow spectrum in the plasma. The intensity of the field in such a wave runs as high as tens of kilovolts per centimeter. Electrons have been accelerated in plasma waveguide, and acceleration of ions is on the cards. Work on increasing the power of the excited wave is in progress. Ya. B. Fainberg and associates rendered accounts of all of these research projects.

Another ion acceleration mechanism of interest is direct interaction between the high-density electron beam and ions of the surroundings. This trend commenced its development 12 years ago, when the team led by A. A. Plyutto at Sukhumi succeeded for the first time in detecting acceleration of ions in the production of an electrom beam from a plasma cathode. At that time, the phenomenon drew forth quite an array of competing explanations, but none of the acceleration mechanisms proposed in detail were ever verified. With the appearance on the scene of high-current electron accelerators, interest in these experiments revived. Several American teams discovered that when an electron beam is passed through a gas-filled drift chamber at low pressure an appreciable number of ions of that gas show up accelerated to anywhere from several millions to several tens of millions of electron volts, depending on the species of gas. The number of accelerated ions attained 10^{14} in a single pulse. As the present symposium showed, the process involved in that acceleration still eludes experimental control, and data obtained by different research teams are contradictory. We can only point out at this time that the acceleration lengths are small (units of centimeters), so that the strengths of the accelerating fields are great.

Several hypotheses explaining the acceleration process in principle were put forth. Crucial experiments are in the works, here and in other countries, to verify these hypotheses. That will evidently make it possible to build efficient accelerators with energies to 100 MeV and intensities to 10^{15} ions per pulse.

Production and Shaping of High-Current Electron Beams. Progress in building high-current electron accelerators is of great significance for the development of collective methods of particle acceleration. One important fact is the commissioning of facilities capable of generating electron beams with currents of tens of kiloamperes, and the start of experiments using those facilities. The Impul's accelerator with 30 kA current (FIAN, USSR), the Tonus machine with current 50 kA at Tomsk Polytechnic Institute and the

50 kA accelerator at NIIÉFA [Scientific-Research Institute for Electrophysical Equipment], were reported on at the conference. The first experiments performed on these machines provide grounds for hoping that they will provide an excellent equipment base for experiments related to collective methods of particle acceleration. New accelerators useful in shaping electron storage rings were also reported on. Accelerators of that type are being built at Dubna and at NIIÉFA.

A. Kolb gave an account of the most recent achievements in the construction of high-current accelerators in the USA, and particularly on some facilities which went into service during the past year. The largest of these machines are the Black Jack and Aurora. These machines are capable of generating electron beams with currents of 1 to 1.2 million amperes at 10 to 12 MeV energy. The Aurora accelerator can be used as a source of extremely high-density gamma radiation.

In addition to these basic trends, some new concepts in the design of accelerators utilizing the collective principle were also aired at the symposium. All of these ideas are in their initial stage of development, and therefore will be covered in brief.

A. A. Kolomenskii performed calculations on the design of the Gyrotron system. The general idea behind this system is that an electromagnetic field of a special type can be employed to impart a closed configuration to the electron beam, and to get the beam to rotate as a single entity. Ions can be trapped by such a beam. The trapped ions pick up energy as the beam rotates as a single entity and as the ions glide along the beam. Calculations show that acceleration in this mode is possible down to low γ values.

M. S. Rabinovich submitted a paper discussing some forgotten possibilities in acceleration: acceleration in electron streams and impact acceleration. With the vigorous development of high-current electron accelerators, this reminder is by no means superfluous, since work in that direction appears promising. The use of solutions – or unified nonlinear waves – for acceleration is another intriguing possibility. Investigations in that area hold forth promise of accelerating fields as high as 10,000 MeV.

N. Rostoker (USA) discussed the possibility of designing a Hipac type heavy-ion accelerator through the use of relativistic beams, which would render the problem of how to obtain the required electron densities in a torus easier.

The proposals referred to earlier on self-acceleration of electrons and the possible use of beam scanning were also discussed.

The symposium demonstrated that collective methods of particle acceleration are highly promising, and that the building of highly efficacious accelerators based on that principle is possible within the very near future.

SECOND INTERNATIONAL CONFERENCE ON ION SOURCES

A. S. Pasyuk

The second international conference on ion sources was held in Vienna, September 11-15, 1972. About 250 scientists from 25 different countries took part in the work of the conference. The biggest delegations were those from France, West Germany, the USA, Austria, and Britain. A delegation of ten (including Dubna delegates) came from the Soviet Union. Over a hundred reports, including eight tutorial review papers, were heard at the eleven panels of the conference. Soviet scientists presented five reports.

The purpose of the conference was to provide a forum for discussion of the latest achievements in the physics and technology of ion sources, and their steadily increasing and more versatile applications. While these topics have been on the agenda at conferences and symposia in the past, dealing with facilities making use of ion sources (e.g., accelerators, mass separators, thermonuclear fusion machines, etc.), special conferences on ion sources have begun to be organized starting with 1969.

The agenda of the Vienna conference covered wide ground. The principal topics under discussion were: high-intensity ion beams and neutral-particle beams of low energy; sources of multiply charged ions; sources for high-energy accelerators; sources of negative and polarized ions; mass-separator sources and low-intensity sources with a small ion energy spread.

Beams of fast hydrogen atoms (deuterium atoms) with equivalent currents upwards of 10 A and beam power upwards of 100 kW are required in order to accumulate and heat plasma in magnetic traps. In that case, in contrast to conventional limited-density focused ion current plasma sources, a plasma surface with a high and uniform density of ions (plasma surface on the order of tens of kV·cm units) must be shaped, a multiaperture accelerating system capable of distending and focusing high-power ion streams is needed. This problem received considerable attention at the conference. Quite a few reports were submitted by USA scientists. A good deal of progress has been made in this area at Berkeley, where a source with no externally applied magnetic field and with a large cathode emission surface, the cathode situated on the periphery of the discharge, has been developed. W. Cooper reported that about 15 A deuterium ion current has been extracted, at energy 20 keV, from a 13 cm diameter discharge chamber at 1000 A discharge current, with the aid of a multislit extractor. After the beam was recharged on gas issuing from the discharge chamber, an equivalent current of 8.6 A, 85% of the energy of which was accounted for by neutral particles, was passed through a 10×20 cm target at a distance of 3.3 m.

Interest in sources of multiply charged ions has been on a sharp increase in recent years. This owes to the development of research on the nuclear physics of heavy ions and the synthesis of remote transuranium elements in such countries as the USSR, USA, France, and Britain, and also to the expansion of work on implantation of ions in substrates, the development of research on disturbances and imperfections in the structure of crystals, the use of accelerated heavy ions in biological research. The special current interest in sources of multiply charged ions is attested by the scheduling of the first international conference on ion sources and accelerating systems of multiply charged ions in Gatlinberg (Tennessee, USA) in October of 1971.

Over 15 years ago, arc sources of multiply charged ions with either cold cathodes or a heated cathode were in use at accelerator facilities. A heated-cathode source developed at the I. V. Kurchatov Institute of Atomic Energy [IAÉ] under the supervision of L. A. Artsimovich has been in operation for about 15 years at Dubna cyclotrons. During that time, the source has been used under G. N. Flerov's supervision to generate and accelerate high-intensity beams of multiply charged ions, formed from either gaseous or solid substances up to xenon (multiply charged ions up to rhenium ions have been generated on a test stand).

Translated from Atomnaya Énergiya, Vol. 34, No. 3, pp. 223-225, March, 1973.

Currents of multiply charged ions obtainable from that source are many times greater than in cold-cathode sources. Heated-cathode sources are now coming into use in the USA, France, Japan, and Sweden. Two Soviet reports (by A. S. Pasyuk and B. N. Makov) dealing with research and development work on such a source were found to be of great interest at the symposium.

At the present time, scientists in the USA, West Germany, and France are actively pursuing theoretical and experimental research, and also engineering improvements, on sources of multiply charged ions using cold cathodes, and on the duoplasmatron. New concepts on the design of sources of multiply charged ions have appeared. Some of these concepts are based on the utilization of magnetic traps built into thermonuclear fusion machines. In addition, a procedure for laser generator of multiply charged ions is also in the development stage. But the development of all these new trends is still far from the stage of practical applications of those sources. Some progress made in the development of sources with magnetic traps was reported in a paper by C. Jacquot (Grenoble, France). The authors successfully observed completely stripped nitrogen atoms in the beam when the electron-cyclotron resonance was exploited to heat electrons. A. Perez (Limeille, France) reported observations of ions of 13-charge aluminum and 24-charge iron obtained with the aid of a laser. We note that completely stripped carbon, nitrogen, and oxygen atoms have been produced [1] at JINR in an electron-beam source. A laser has been employed in the USSR (MIFI) to generate multiply charged ions all the way to 25-charge cobalt [2]. Sources capable of generating completely stripped atoms are of great interest for synchrotron applications and when heavy ions have to be accelerated, and also for solving other research problems.

A review paper presented by T. Slaters (Brookhaven, USA) discussed the characteristics of ion sources for linear accelerators serving as injectors to proton synchrotrons. One interesting special feature of all these foreign ion sources is the use of oxide cathodes with lifetime greater than 3000 h at high current pulse width (to 500 μsec) and pulse repetition rates from 10 to 120 Hz. As a rule, duoplasmatrons are employed with a pulse expander, but the possible use of sources of other types is not excluded. For example, a Penning discharge source developed by K. Turner for the Brookhaven cosmotron, with 80 mA current, offers much greater brightness than the duoplasmatron. The lifetime of this source extends to 3000 h, the maximum current attained is 500 mA. D. Mueller (Los Alamos, USA) reported on research on a duoplasmotron using Pierce optics. The 250 kV accelerating column plays the role of both voltage divider and focusing device. C. Curtis (NAL, USA) reported on research, at Batavia, on a preinjector with a 750 kV Pierce column and proton current to 250 mA.

The new 200 MeV Linac linear accelerator at Brookhaven is now being employed, with a peak current 80 mA and beam emittance $1\pi \cdot cm \cdot mrad$, to generate beams of intensity $2 \cdot 10^3$ particles/pulse. The Linac is operating at a frequency of 10 Hz.

It may be pointed out that the performance characteristics of the duoplasmatron type ion sources developed at the Scientific-Research Institute for Electrophysical Equipment (NIIÉFA) and in use at linear accelerator-injector facilities in the Soviet Union are superior to comparable facilities in other countries. For example, one such source in operation at the Institute of Theoretical and Experimental Physics (ITÉF) produces about 1 A current at the injector entrance.

Reports discussed sources of polarized ions of hydrogen, deuterium, and lithium for tandem accelerator systems and for cyclic accelerators based on the familiar principles of the atomic beam method and the Lamb method. A method of high-frequency bunching of a beam extracted from a duoplasmatron has been developed at Los Alamos for a source based on the Lamb method. Negative polarized hydrogen ions in 60 nsec width pulses with a pulse repetition rate of 3 MHz can be generated at the output of this source. General Ionics Corp. (USA) is ironing out full-scale industrial fabrication of sources of negative polarized ions based on the Lamb method. Pulsed atomic beam ionizers are being investigated at Saclay (France), with the object of developing a suitable source for the Saturn installation. A variant with an oscillating electron beam has been judged the best to date. Discharge and ionization of the atomic beam are excited by pulses of a strong magnetic field. Extraction of the polarized ions takes place at right angles to the direction of the atomic beam; the pulses, lasting 500 μsec, repeat in 2 sec. The ionization efficiency is $1.2 \cdot 10^{-3}$ in an atomic beam of 10^{15} atoms/sec, making it possible to generate 200 nA polarized deutron current. The present goal is to develop a variant of the ionizer with current to 10 μA.

Reports were also presented on the traditional method of generating negative ions by the charge-transfer method. D. Osher (Livermore, USA) reported that a current of 50 mA negative deuterium ions

was obtained through charge transfer of 200 mA of positive ions on cesium vapor. At Munich (West Germany), passage of helium ions through calcium vapor used for charge transfer in a conventional charge-transfer source produced 600 nA negative calcium ions when the appropriate voltage across the electrodes was applied. The process by which they form is not entirely clear. Designs of sources capable of producing both positive and negative ions depending on the operating conditions are also of interest. Here we are also concerned with redesigned duoplasmatrons with separate feeds of heavy gas to the anode region and light gas to the cathode region. Interaction between heavy ions and the hot cathode can be minimized in that way. Beams of negative fluorine ions, negative chlorine atoms, etc., can be generated by direct pulling from an anode plasma. Oxygen ions have been obtained to 50 μA (Orsay, France).

Low-intensity sources of heavy ions have come into increasing use in recent years in nuclear spectroscopy research and in semiconductor engineering. A tutorial review paper presented by T. Sidenium (Denmark) contained some general recommendations on applications of such sources, which were arbitrarily divided into five distinct groups. A source developed by V. I. Raiko (Dubna, USSR) was cited as representative of the group of sources with an ionization surface. The efficiency of this source is about 100% for cesium, and 80% for neodymium. A report by V. I. Raiko on research and development work on that source was heard with keen interest. M. Bochet (Grenoble, France) reported that a modernized source with a beam of round cross section is being employed for ion alloying in a 150 keV accelerator. This device operates at temperatures to 300°C without an external magnetic field, and can bring about high enrichment of isotopes of refractory elements (tungsten, hafnium, niobium, et al.).

As pointed out earlier, the conference discussed not only the technology and applications of ion sources, but also theoretical aspects of the physics of the plasma in the sources, and the motion of ion beams. For example, tutorial review papers presented by J. Hasted (University of London, Britain) on ion–molecule reactions, by R. Lapostollier (CNET, France) on possible deterioration of beam quality on account of space charge effects, by K. Weismann (Marburg, West Germany) on plasma in an ion source, by J. Doliqueu (Grenoble, France) on neutralization of space charge in ion beams, were found highly interesting.

It was proposed that the proceedings of the conference be published in late 1972 or early 1973.

The next regularly scheduled conference on ion sources will be held in 1975, at Darmstadt (West Germany).

LITERATURE CITED

1. E. D. Donets et al., JINR Preprint R7-4412, Dubna (1968); JINR Preprint R7-4469, Dubna (1969).
2. Yu. A. Bykovskii et al., Zh. Éksp. Teor. Fiz., 60, 1306 (1971).

SACLAY OCTOBER 1972 INTERNATIONAL CONFERENCE ON ACTIVATION ANALYSIS

B. S. Kudinov

An international conference on activation analysis and an international colloquium sponsored by the National Scientific-Research Center of France (CNRS) on determinations of trace amounts of elements in high-purity organic and inorganic materials and in biological specimens, organized under joint sponsorship of CNRS and the French Commissariat de l'Énergie Atomique, were held at Saclay (France), October 2-6, 1972. The topics covered by the papers submitted to the conference and colloquium were largely similar, but the conference centered its attention more on the methodology of activation analysis, while the colloquium leaned more to applications of activation techniques and the results obtained. Papers which were similar in terms of technique were discussed at the conference and colloquium on different days or at different times of day, so that the participants in the gatherings were afforded opportunities to attend sessions of panels in either gathering that were of greatest interest to them. The colloquium schedule allowed more time for questions and discussion from the floor. About 350 specialists hailing from 30 countries took part in the conference, and presented 86 papers. Sixty-four papers were presented at a colloquium.

All of the papers can be grouped under the following headings: general topics in activation analysis; information processing techniques; activation by thermal neutrons and radiochemistry; activation by charged particles and by γ-photons; recording of prompt products accompanying nuclear reactions and ionization of atoms; activation by fast neutrons; applications of isotope neutron sources. From the vantage point of applications of activation techniques, we have to distinguish: microanalysis of surfaces; analysis of high-purity metals and semiconducting materials; utilization of activation techniques in biology, in earth sciences and in ecological research.

A report made to the plenary session on the opening day of the conference, and devoted to contributions made by nuclear techniques to analysis, was presented by V. Meincke (USA), who devoted a good deal of attention to the reliability of activation analysis in determinations of traces of elements below the level of 1 part per million, stressing the importance of assessing possibilities inherent in the method in the light of concrete examples. The reporter drew attention to the growing role played by analysis, with important decisions being taken on the basis of the results of materials analysis, and expressed the conviction that the principal problem facing activation analysis practice in the coming ten years would be extension of reliable trace analysis to the level of 1 part per billion.

The agenda reserved a considerable amount of space for determinations of trace impurities through the use of neutron activation analysis, primarily, but also radiochemical separations. This topic accounted for over a third of all the reports submitted to the conference, and over half of the reports at the colloquium. Some papers (J. Host, Belgium; M. Verheicke and J. Verplancke, Netherlands; J. Blouri et al., France) proposed schemata for determining a large number of impurities in a single specimen with separation of the elements into several large groups and the use of Ge(Li)-detectors. The most effective separation techniques were employed in the work: ion exchange, solvent extraction, extraction chromatography. The operations of radiochemical separation were automated in some of this work. In recent years, with enriched-fuel reactors going into service, it has become possible to improve the sensitivity of analysis of especially high-purity materials. E. Ricci (USA) reported on one such reactor, with thermal flux $5 \cdot 10^{14}$ neutrons/cm^2 $\cdot$ sec. The special features of analysis of materials presenting a large thermal neutron capture cross section were discussed in a contribution by I. P. Alimarin et al. (USSR).

The analysis of semiconducting materials, and purity monitoring of the initial single crystal in semiconductor technology, are being given close attention, as pointed out in an article by E. Szabó (Hungary) on

Translated from Atomnaya Énergiya, Vol. 34, No. 3, pp. 225-226, March, 1973.

the latest technological processes in this area, such as growing of films, controlled diffusion, ion implantation, etc. The mass of the specimen is within the 1 mg to 10 mg range in these cases, and measurement of the mean concentration of impurities shares interest with the study of impurity distributions. A paper by H. Raus et al. (Hungary) discussed the distribution of alloying elements and impurities in epitaxial silicon films, as determined by layer-by-layer dissolution of specimens following thermal-neutron activation. The sensitivity of this method is 10^{13} atoms/cm^3.

Methods for analyzing surface layers of solids by direct observation of the products of nuclear reactions were discussed in 18 of the papers. Elastic scattering of charged particles, recording of prompt γ-emission, secondary protons, and α-particles from nuclear reactions are being used in the study of impurity distribution, the total concentration of impurities on the surface of the solid, and analysis of isotope ratios. A paper by M. Bruel et al. (France) dealing with studies of the concentration profiles of boron and phosphorus in silicon and in ZnTe, by the method of nuclear reactions combined with ion polishing of the specimen, is of interest. The resolution in depth extends to 300 Å. Narrowly focused beams of charged particles make it possible to study the topography of the surface with resolution to 3μ (J. Pierce, Britain).

A paper submitted by R. P. Meshcheryakov et al. (USSR) described the use of the anomalously large cross section for large-angle scattering of α-particles of energies greater than 15 MeV on C^{12} and O^{16} nuclei in studies of the distribution of carbon and oxygen in the surface layers of metals.

The position of impurity atoms in the silicon crystal lattice was determined with the aid of the channeling effect, in work described by V. MacIntosh (Canada). A report by J. Amsel (France) in which various applications of the method of direct observation of nuclear reactions of metallurgy, electrochemistry, biology, and crystallography was heard with interest.

Analytical techniques based on activation by charged particles were discussed in 14 papers. Proton activation was used in some of the work to determine not only light elements, but also medium and heavy elements. Many of the reports discussed problems of technique pertaining to estimates of surface contaminations, removal of the matrix effect, improving the reproducibility of analyses, and so on.

Activation by γ-photons is being used both in many-element analysis of rock (V. V. Sulin, USSR; T. Kato et al., Japan), biological specimens, and air filters (J. Hilson and D. Williams, Britain), and in the determination of light elements (F. Nordman et al., France; I. M. Pronman et al., USSR). The last of these papers also reported on neutron activation determinations of oxygen in several pure metals. There was keen interest in a report on applications of a 30 MeV microtron in activation analysis (S. P. Kapitsa et al., USSR).

Possibilities of ultimate analysis of the composition of materials utilizing scattering of polarized nucleons were discussed in a report by A. S. Shtan' (USSR). That paper also discussed several variants of the neutron-resonance method of analysis.

The method of ultimate analysis using the characteristics of x-radiation accompanying ionization of atoms by charged particles was represented by four papers submitted to the conference.

Ge(Li)-detectors 40 cm^3 in volume or larger are being used widely in activation analysis, as is computerized decoding of spectra, and computerized processing of the results of analysis. Techniques for optimizing conditions of analysis, comparative characteristics of different detectors, sensitivity, accuracy, and precision in analysis, and computer processing of analytical data were discussed in 14 papers. We might note the papers by L. L. Pelekis et al. (USSR) on determinations of limits of detection in activation analysis, H. Yule (USA) on estimates of weak components in γ-ray spectra, both dealing with computerized techniques. The use of coincidence techniques is discussed in a paper by Z. Niese (East Germany). Utilization of short-lived isotopes enabled E. M. Lobanov et al. (USSR) to shorten the time required to complete analysis of pure materials appreciably. Problems confronted in determinations of impurities near the limit of detection were discussed in a paper by R. Dybczyanski et al. (Poland).

G. N. Flerov and I. G. Berzina (USSR) made use of a radiographic technique in determinations of boron, lithium, uranium, and thorium in rocks and minerals. The session devoted to activation techniques in geology displayed special interest in analysis of specimens of lunar rocks. A specially organized discussion compared the results of analysis of all of the lunar rocks obtained by various authors for analysis.

Activation analysis in biology was the topic covered in 15 of the reports. Verification of the accuracy of the analysis against standard biological specimens has been getting increasing attention in this area in recent work. Some of the problems involved in the fabrication and analysis of such specimens were discussed in papers by H. Bowen (Britain) and F. Laughler (USA). Determination of elements in the organism in vivo is important for diagnostics in some instances. Activation analysis is hardly the sole method capable of solving the problem. Some interesting results have been obtained in analysis of biological specimens by neutron activation, in work described by R. Riviere et al. (France), A. A. Kist et al. (USSR), P. Kotas et al. (Czechoslovakia), and by E. L. Andronikashvili et al. (USSR).

The need to monitor atmospheric pollution, pollution of continental waters and seas, and to study the concentration of toxic elements in various links in the food chain, is becoming increasingly obvious. The high sensitivity of activation analysis renders this technique suitable for use in solving many of these problems. This topic was reflected in seven papers. Activation by neutrons or by γ-photons is being used in analysis of contaminants collected by air filters, and a method based on recording characteristic x-radiation resulting from irradiation by charged particles is also useful. The neutron activation method is being used to monitor the content of heavy metals, mercury above all, in surface waters (A. Kolazkowski et al., USA) and in various aquatic organisms (V. Gwynn et al., USA).

The proceedings of the conference will be published in the periodical Radioanalytical Chemistry in the first half of 1973.

ON-LINE-72 INTERNATIONAL CONFERENCE ON COMPUTERIZATION TECHNIQUES

V. I. Prikhod'ko and A. N. Sinaev

The On-Line-72 international conference, organized by the On-Line association created expressly for sponsoring conferences and exhibits on computerization, was held in September, 1972, in Axbridge (England). On-Line-72 was the first major international conference devoted to the design and applications of computer systems operating with active human participation in real time, i.e., what have come to be known as interactive computer systems.

The conference drew about 1000 specialists from 17 countries, to hear over a hundred reports. In addition, the latest equipment in the field was exhibited, science films in popular style pertaining to the topics on the conference agenda were given showings, and discussions were held on the most important topics. The principal problem under discussion at the conference was the establishment of close contacts between users and designers of interactive data-processing systems.

The agenda of the conference covered the following principal topics:

1) design of interactive computerization systems: development of large systems, graphical displays, communication lines between remote parts of a system, special dialog languages, software for the systems and graphical displays, programs for checking the performance of the systems, etc.;

2) applications of interactive systems in science and industry: for mathematical and statistical calculations, in scientific research, in development and research work on electronic systems, in devising mechanical structures and systems, in architecture and civil engineering, in medicine, etc.;

3) use of interactive systems in social and humanitarian endeavors, as in large data processing systems, for editing and processing texts, in learning and training systems, etc.

The balance sheet of the conference shows that interactive computer systems have experienced vigorous growth and development in recent years, and have won great and widespread popularity in various fields of human activity. Systems of that type have been instrumental in greatly improving the effective use of electronic computers, and have opened up new paths for computer applications in new areas. Interactive computer systems have already won themselves a firm place in loading branches of science and industry, and have become commonplace tools. The human operator or user interacts with the electronic computer through interactive graphical displays on which the results of intermediate computer calculations are read out in lucid form (most often in the form of different graphs, schemata, or texts). Special devices make use of estimates of the intermediate computer readouts to keep feeding additional operational information back to the computer to determine the direction of the computer's further work on the problem.

Analysis of the reports presented to the conference shows that, despite the fact that interactive systems are being used in the most varied fields of applications, we can single out the range of problems being solved most efficaciously with the aid of interactive computer systems, and arrive at the typical structure of the system. Interactive computer systems are used most often in science and in industry to solve such problems as control of the progress of an experiment or production process, design and simulation of the performance of flowsheets, projects, and installations, recognition of patterns, mathematical analysis and statistical analysis.

The principal device in sophisticated interactive systems is the graphical display on a cathode-ray tube, with additional equipment available for generating standard image elements (vectors, symbols,

Translated from Atomnaya Énergiya, Vol. 34, No. 3, pp. 227-228, March, 1973.

circles, etc.) and a variety of devices for operational input of data to the electronic computer in the system. The display is usually hooked up to a desktop computer which is hooked up in turn to the large (principal) computer in the system, which operates in a multiprogramming mode, often at a remote location. The large electronic computer is used only for complicated calculations, while the small computer handles image regeneration functions, transformation of the data format, simple calculations, dialog with the operator, etc. This combination is acknowledged as an optimum one for most scientific and engineering applications, since it offers certain advantages over direct hook-up to the large computer.

In terms of the type of display units on the cathode-ray tube, the graphical displays used can be divided into three types: units with arbitrary access to any point on the display screen, television (frame or raster) units, and charge-shortage tube units. Close attention has been given to the arbitrary-access type display as the most versatile one. But displays with charge-shortage memory tubes are the most popular ones at the present time, since they are comparatively cheap and do not require continuous access to the memory locations in order to regenerate the image.

Software for interactive computer and data processing systems which plays a major role in determining the possibilities of the systems and their convenient use, received its share of attention. It includes both the intermediate language (e.g., BEISIC) intended for communications between the human operator or user and the electronic computer, and the generally accepted programming language (e.g., FORTRAN) used for programming specific programs. New variants of intermediate languages were proposed in some of the papers.

An introductory review paper by K. Hammer (USA) dealt with the role played by interactive systems at the present time, and the outlook for the development of such systems in the future. The most pressing problem at present is how to device large-scale computer systems for solving scientific and engineering problems and also for solving problems of general national interest. These systems harbor enormous potentialities which must be combined with simple operation so as to provide access to the system for all those who lack any special training in computer practice. At the present level of complexity of computerization, the problem of how to develop simple means and methods of communication between the human operator or user and the computer is a fundamental problem. It has been suggested that the problem of how to write information into a computer directly from the human voice of the user or operator will be solved by 1980.

We should take note of several papers presented by nuclear physics research centers. A report by D. Cardwell (Oak Ridge National Laboratory, USA) demonstrated the experience acquired to date in the use of large general-purpose digital computers installed at general-purpose computing centers, for research in the field of nuclear reactors and plasma physics. With the development of interactive data processing systems, only desktop and intermediate-size computers connected by telephone lines to large general-purpose computers should be used. These systems provide economy of means and more complete utilization of the possibilities inherent in large computers.

One of the papers, presented by CERN, reported on communication lines linking a central computing and data processing complex consisting of a combination of large CDC computers and systems still in experimental testing areas. The communications link was established through the CDC-3100 computer, to which a small HP-2116 computer was hooked up. Depending on the data transmission rate and distance required, several alternate types of communications lines, capable of handling anywhere from 300 to $4 \cdot 10^6$ bits/sec, can be selected.

Another CERN paper dealt with the development of a special computer language for the interaction between the human operator or user and the computer machine in solving problems in computational mathematics. This language is a combination of the GAMMA and AMTRAN languages already in use. The structure and syntax of the language, and its utilization in a GAMMA interactive system, are discussed.

An exhibit organized to run parallel to the conference drew participation from about 40 firms in capitalist countries. Small and intermediate computers, displays, interactive graphical systems, and also information of practically all existing recent prototypes of small computers fabricated by concerns in the USA or in Britain were represented. These computers are intermediate, in terms of their structure and the organization of their performance, between the third and fourth generations of computers. They make use of integrated circuitry of a medium degree of complexity, feature a semiconductor memory for microprogramming purposes, and the circuitry is designed to handle floating decimal point operations. The

modular structure of these computers makes it possible to select from a variety of configurations to match the requirements of the user. As a rule, the computers operate with 16-digit numbers, have a memory cycle shorter than 1 μsec, and a memory capacity equal to the 4K-32K; the communication rate on the direct access channel can be as high as $\sim 10^6$ words/sec. The computers are amenable to modularization with a complete set of peripheral and interfacing devices; the software for these computers is highly sophisticated.

Also worthy of attention are the latest developments in small computers in the PDP-11 series and the PDP-15 medium series (Digital Equipment, USA); small computers of the Nova and Supernova series (Data General, USA); the small HP-2100 computer and the intermediate HP-3000 computer (Hewlett Packard, USA); the 620-100 small computers and the 73 line of intermediate-size computers (Varian Data, USA); the Micro-16Y small computer (Digico, Britain).

The graphical systems were exhibited both by firms manufacturing small desktop computers and by firms specializing mainly in the production of display and readout units and modules and utilizing computers obtained from vendors. As a rule, the firms also take the responsibility of delivering the software along with the graphical display systems. The greatest amount of attention is merited by the following developments.

1. The Vectorgraphics-11 graphical readout system from the Vector General series (R. and H. Epplide Dynamics, Britain). The system incorporates a display unit with a cathode-ray tube presenting a large display screen, symbol and vector generators, a coordinate transformation module, various devices for writing in data into the computer (light pencil, alphanumeric and functional keyboards, etc.).

2. The IDIIOM graphical display system (Stabletron Ltd., Britain) with makeup and characteristics closely similar to those of the Vectorgraphics-11 system.

3. The 4002A and 4010 charge-storage tube displays (Tektronics USA). The latter is a simple keyboard module, while the former is a sophisticated system incorporating symbol and vector generators, a data write-in module, and so on.

Both types of displays allow hook-up of device capable of transferring a copy of the image onto paper in rapid time.

The proceedings of the conference were published by the conference organizing committee.

CONFERENCE ON X-RAY SPECTRAL ANALYSIS

S. V. Mamikonyan

An international conference on x-ray spectral analysis was held in Dresden (German Democratic Republic) in September, 1972. Specialists from Bulgaria, Hungary, East Germany, Poland, Rumania, the Soviet Union, and Czechoslovakia took part in the conference. The conference heard 55 papers dealing with the most salient problems in x-ray spectral analysis.

Most of the reports dealt with the development and practical applications of x-ray spectral equipment using x-ray tubes (crystalless tubes and tubes with analyzer crystal) or radioisotope sources. Reports presented by A. N. Mozhevich, N. I. Komyak, et al. (USSR) on crystal dispersion equipment for quantitative x-ray spectral analysis in which Soviet type FRS-2 and FRS-4 x-ray spectrometers, type KRF-I and KRF-II quantometers, type FRA-1M and FRA-4 analyzers, and by Yu. M. Gurevich et al. (USSR) on the analytical capabilities of instruments designed for x-ray luminescent analysis (the instruments discussed were types BARS-1 and BARS-2, also BRA-6 and BRA-7), and by W. Siemann (East Germany) on the results of applications of the VRA-2 x-ray spectral analyzer at a cement factory in Bernburg, were heard with great interest.

X-ray spectral analysis utilizing radioisotope sources was reported by S. V. Mamikonyan (USSR). This report offered, in addition to information on research work and practical work carried out in x-ray radiometric analysis in the USSR, information on the FRAD-1, KTN-1, AZhR-1, RPS4-0.1, RRShA-1, and other instruments fabricated in the USSR.

Attention was drawn to a special report presented by V. P. Varvaritsa (USSR) on a two-channel FRAD-1 x-radiometric analyzer with automatic stabilization of the spectrometer part, so that analysis can be carried out on the two elements simultaneously in media of complex composition.

Some interesting reports on practical applications of a dispersion-free x-ray spectral equipment were presented by T. Flerkowski et al. (Poland). This paper gave an account of the continuous determination of calcium oxide in dry product, determination of heavy elements in sewage effluents, and continuous determination of copper in pulp.

The conference agenda reserved a special place for topics pertinent to analysis of light elements. Great achievements in this area have been scored by specialists of the Central Institute of Isotopes and Radiations of the German Democratic Republic. We should note the paper presented by D. Müller and P. Morgensterne (GDR) on the CNO-analyzer, a device for x-ray spectral analysis of light elements utilizing α-particles for excitation. This instrument has been used successfully to solve full-scale industrial problems (determination of carbon in organic substances, determination of fluorine in feldspar, etc.). Also of interest was a report by K. Richter (GDR) on optimum operating parameters of through-flow proportional counters in the wavelength range from 1.5 Å to 30 Å. The design parameters and operating parameters of flow proportional counters (window geometry, energy resolution, gas composition, etc.) were optimized in terms of the needs of the prospective applications, in the report.

Certain advances have been attained in applications of protons to excite the characteristic radiation of light elements. This research has been carried on intensively at the Technical University in the German Democratic Republic under the supervision of S. Koch. A report on that topic was presented by V. P. Afonin et al. of the Soviet Union.

Several reports were devoted to the development of quantometers using semiconductor detectors. Cooling of the detectors was discussed, as well as computerized processing of the spectra. There was special interest in a report by P. Jugelt and H. Schmidt (GDR) on separation of close-lying lines through

Translated from Atomnaya Énergiya, Vol. 34, No. 3, pp. 228-229, March, 1973.

computer decoding of the spectra. The opportunities and limitations in separation of close lines with the aid of the method of least squares, using a standard spectrum, were discussed. An example of decording of 18 close-lying spectral lines was advanced. The research was conducted at the Branch of Isotope Engineering of the Technical University (Dresden).

Some of the papers dealt with research into methods and procedures of x-ray spectral analysis. Papers submitted by staffmembers of the Institute of Geochemistry of the Siberian Branch of the USSR Academy of Sciences were heard with great interest.

Some of the papers dealt with detectors of x-radiation. Some interesting accounts of research and development work on sealed proportional counters were given by K. W. Ostrowski (Poland).

A summary report on the work achieved at the conference was provided in the closing remarks by Koch. He pointed out that the proceedings of the conference reflect the substantial progress that has been made in x-ray spectral analysis in recent years, and stressed that one of the promising trends in x-ray spectral analysis involves further improvements and wider acceptance of semiconductor detectors and quantometers utilizing semiconductors and backed up by special-purpose computer devices.

S. Koch also reported that the proceedings of the conference were to be published in early 1973.

The participants of the conference suggested scheduling the next such conference sometime in 1974.

APPLICATIONS OF RADIOISOTOPE EQUIPMENT IN THE COAL INDUSTRY

R. S. Morusan

An All-Union school on the utilization of radioisotope equipment in coal mines and at coal processing plants of the Ministry of the Coal Industry was held October 22-25, 1972 at the Atomic Energy Pavilion in the Exposition of Achievements of the National Economy. The school session drew representatives from scientific-research institutes, base-level isotope laboratories, combines, mines, and coal dressing plants.

Over 2000 radioisotope devices for monitoring various production processes are now in service at enterprises in the nation's coal industry. Savings resulting from the use of these devices now total 1.5 million rubles annually. The demand on the part of mines and coal plants for these instruments increases year by year, and radioisotope equipment has become an inseparable part of the means of automation on stream in the coal industry. The geography of applications of radioisotope equipment is also expanding continually. In addition to enterprises in the Ukraine's coal industry, radioisotope devices are also gaining in popularity at enterprises in the Far East, in the Komi ASSR, at Karaganda, in the Rostov region, and in other coal mining regions of the country.

Radioisotope equipment is now beginning to be used in the design of new mine shafts and in the redesign of existing mine shafts, and in new and existing coal processing plants, through the efforts of such design and planning institutes as Dneprogiproshakht, Yuzhgiproshakht, Dongiproshakht, among others.

To date, radioisotope relay devices for monitoring distinct production processes which had previously not been monitored or which had been monitored only unreliably by other types of automation equipment are the predominant applications in the coal industry.

The most effective use of radioisotope devices for automation and process monitoring is in the operation of skip hoist facilities. These devices monitor progress in the loading and unloading of skip hoist cars, exact positioning of the skip car when it comes to a halt, arrival of the skip car under the loading chute, filling of metering structures, top and bottom fill levels in loading and receiving hoppers, and counts of loaded skip cars. As a rule, all of these radioisotope devices are incorporated in the automatic control system for the hoist installation and facilities.

Radioisotope devices are also being used in the technical complexes built at the surface areas of mine pits and in the coal receiving and loading complexes of coal processing plants, where they are employed to monitor clogging of transport chutes, top and bottom fill levels of storage hoppers and loading hoppers, filling of railway cars, automated selective filling of empty hoppers, pneumatic breakdown of coal pile-ups and conglomerations in hoppers, and locating the automatic couplers on railway cars in the classification yard.

Radioisotope devices also come in handy at other points in the production process. For example, they are used on suspension type cableways to monitor loading and reloading of cablecars, top and bottom fill levels in hoppers, and to keep counts and tallies of loaded cablecars.

At points where dump trucks back up, the arrival of the truck is monitored, the loading of the truck body, and the presence of muck, gangue, or rock in the storage-hopper are monitored. The water fill level is monitored in boiler plants and process water tanks, and feed of water to the boilers is automated, while the level of condensate and the feedwater level in feedwater tanks, the water level in process water tanks, the presence of coal in coal feed hoppers, are all monitored by radioisotope devices.

Translated from Atomnaya Énergiya, Vol. 34, No. 3, pp. 229-230, March, 1973.

Radioisotope equipment is also being used on railway waste piles to monitor the bottom and top fill levels of the loading hopper, the arrival of the skip car (buggy) and reloading operations; at coal processing plants for automation of the release of the host rock to jigging machines and discharge of sludge to sludge thickners.

In all of the processes enumerated above, the radioisotope relay devices perform reliable monitoring functions and can be recommended on that basis for more widespread industrial use, with impressive savings in engineering costs.

But radioisotope relay devices cannot be used indiscriminately to monitor basic production processes in coal mining and processing, or to monitor the quantity and quality of commercial coal and products of coal refining. Investigations carried out in our country and elsewhere have shown that it is possible to design devices utilizing ionizing radiations in order to measure ash content, mass, moisture content, and sieve composition of coal, and also for monitoring the composition and dust content of mine atmospheres. Savings from such devices monitoring basic production processes will be much greater than achievable through the use of radioisotope relay devices. The need for such devices increases with the implementation of automated computerized process control systems in the coal industry. Scientific-research institutes and other organizations serving the coal industry are busy developing new devices and new equipment.

Industrial tests on a radioisotppe gangue and coal sensor for automated control of coal combines to monitor the hypsometry of the coal strata are being run at the A. A. Skochinskii Mining Institute, which also developed the sensor.

The VSKZ-1 equipment for monitoring the ash content of run-of-mine coal on stream, and IM-1 equipment for on-stream mass measurements, are devices developed at the Donets Coal Scientific-Research Institute.

Tha base isotopes laboratory of the Ministry of the Coal Industry of the Ukrainian SSR has developed equipment for locating stories of multistoried lift cages at mine shaft heads, equipment for automatic monitoring by the load distribution between cables on a multicable hoist arrangement (radioisotope relay devices are used here to sense deflections of the cable), equipment for automating cleanout of mine shaft buggies in circular dumpcar tipples, etc.

CONFERENCES AND SEMINARS OF THE ALL-UNION ISOTOPE ASSOCIATION

A technical conference of representatives of the installation and repair organizations of the Kiev Inter-Republic Section of the All-Union Isotope Association, for the exchange of experience in the introduction of radioisotope instruments and methods for the control and regulation of industrial processes at production plants, was held in Kiev in June, 1972.

Participants included the directors and the engineering and technical staff of the Donets, Dnepropetrovsk, Voroshilovgrad, Sokal', and Vinnitsa Basic Isotope Laboratories (BIL) and the isotope laboratories of the Makeev and Zhdanov metallurgical plants.

Attention was devoted to the fruitful work of the BIL, the Special Administration for Radiation-Technology Installation and Repair, and the All-Union Isotope Association to promote the introduction of radioisotope technology into industry.

In order to broaden the use of radioisotope technology in industry, it was recommended that material on the exchange of experience in the application of radioisotope technology should be submitted on a systematic basis of journals in the field and to the collection "Isotopes in the USSR," and that novel solutions to the problems involved should be proposed to the All-Union Isotope Association.

* * *

A sectoral seminar on the use of radioactive isotopes in the construction of tractors and agricultural machinery was held in Rostov-on-Don in September, 1972.

Participants included representatives of scientific-research institutes, design institutes, and factories involved in the manufacture of tractors and agricultural machinery. They exchange experience on the application of radioisotope instruments and methods of the automating of technological processes in machine construction; in addition, they visited the "Rost-sel'mash" factory, where they familiarized themselves with the work involving radioisotope technology.

* * *

A technical conference on the use of radioisotope instruments at Ukrainian light-industry enterprises was held in Kiev in October, 1972, by the Kiev Inter-Republic Section of the All-Union Isotope Association in cooperation with the Ministry of Light Industry of the Ukrainian SSR.

The purpose of the conference was to acquaint managers with mass-produced radioisotope instruments being produced by Soviet industry for the control and automation of technological processes.

* * *

A seminar on the use of radioisotope technology and radioisotope methods in the structural-materials industry was held in Tashkent in November, 1972. The participants discussed a substantial volume of experience acquired in the utilization of radioisotope instruments at structural-materials enterprises.

In the reports and communications it was shown that radioisotope instruments make possible the successful solution of problems such as monitoring the level of granulated and pelletized materials;

Translated from Atomnaya Énergiya, Vol. 34, No. 3, pp. 230-231, March, 1973.

conveyor-belt signals and shutdown systems; counting the packed sacks; temperature regulation; and monitoring the condition of refractory linings in baking zones.

* * *

A conference for the exchange of experience in the use of radioactive and stable isotopes in various sectors of industry, in medicine, and in agriculture was held in Kiev in November, 1972, by the Kiev Republican Section of the All-Union Isotope Association. Participants in the conference included representatives of industrial plants of various sectors of our country's economy. Twenty-two reports and communications were heard and discussed at the conference.

* * *

A seminar on advanced experience for the study and dissemination of operating and repair experience in radioisotope technology, industrial-laboratory work, and technological safety codes, as well as for the development of recommendations on the application of radioisotope technology at Ukrainian ferrous-metal lurgy enterprises, was organized in November, 1972, by the V. I. Lenin Metallurgical Plant of Krivoi Rog in cooperation with the F. É. Dzerzhinskii Metallurgical Plant of the Dnieper.

Participants included directors of central industrial laboratories and plant control-and-measurement sections and representatives of the Kiev Inter-Republic Section of the All-Union Isotope Association, as well as scientific staff members of the Dneprodzerzhinsk Industrial Institute.

An interesting communication was delivered by V. A. Smolyak, Department Head at the Dneprodzerzhinsk Industrial Institute, on the introduction of the Neutron 3-1 radioisotope hydrometer into use for the monitoring and automatic regulation of moisture in coke at Ukrainian ferrous-metallurgy enterprises.

Communications on the work done with radioisotope technology at ferrous-metallurgy enterprises were delivered by representatives of factories and radioisotope laboratories.

THE KVANT-1 DIRECT-READING SIGNAL DOSIMETER

I. E. Mukhin, G. A. Glinskii,
and V. S. Karasev

1. The Kvant-1 dosimeter was developed at the Institute of Physics of the Academy of Sciences of the Ukrainian SSR and the Institute of General and Communal Hygiene of the Ministry of Health of the Ukrainian SSR in 1969 by the authors of the present report.

2. The Kvant-1 dosimeter (Fig. 1) is designed for the monitoring of individual doses of gamma rays and x-rays; it includes a scale for observing the dose accumulated during the working process, a device for giving signals proportional to the dose rate, and an alarm signal to be activated when the accumulated dose reaches a predetermined value.

3. Figure 2 shows a block diagram of the dosimeter. Connecting the line voltage 1 starts the operation of the high-voltage source 2, which delivers a high voltage to the radiation detector 3 (SI-3BG). When acted upon by negative gamma rays or by x-rays, the detector generates pulses in proportion to the radiation dose. Each detector pulse is transmitted to the scalar 4, consisting of a slowed-down blocking generator and a pulse normalizer, a ferrite magnetic assimilation cell with a rectangular hysteresis loop, and a triode. Each pulse of the scaler 4 triggers the control circuit of an electromechanical summer 5, which operates on the principle of an alarm-clock type of mechanism and an electromagnetic relay (RS-9). The frequency with which the electromechanical summer circuit is triggered serves as a signal indicating the radiation dose rate, and the pointer on the dial shows the accumulated dose of radiation. When the dose pointer reaches the alarm-signal pointer, a spring-actuated alarm sounds, warning personnel engaged in work involving radiation danger that the predetermined radiation dose has been reached. In order to make it possible to verify quickly on the job that the dosimeter is in working order, it is provided with a built-in automatic check of the entire electromechanical circuit, for use before operation. When the "Check" button is pressed, the high-voltage source is connected to the counter, and the pulses generated by it are counted and actuate the electromechanical summer; if the summer functions, this serves to confirm that the electrical and mechanical systems of the dosimeter are in working order.

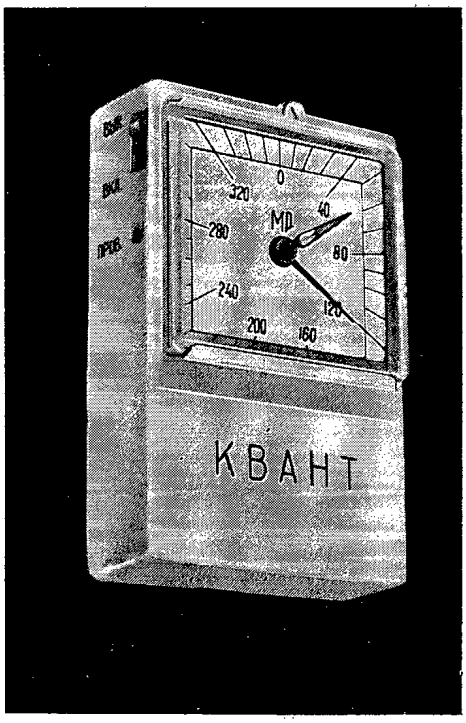

Fig. 1. External view of the Kvant-1 dosimeter.

The electrical circuit of the dosimeter consists of five triodes. Uninterrupted functioning of these triodes for 3000 h is ensured by five PTs-53 elements.

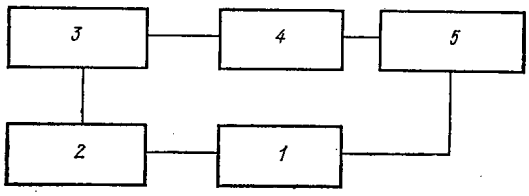

Fig. 2. Block diagram of the Kvant-1 dosimeter.

Translated from Atomnaya Énergiya, Vol. 34, No. 3, pp. 231-232, March, 1973.

The measurement error and the range of radiation energies are determined in practice by the parameters of the SI-3BG gas-discharge counter for radiation dose rates of up to 300 R/h.

Either "Krona" batteries or a D-0.1 storage battery can be used as the power source for the dosimeter. The dosimeter weighs 190 g and measures 85 × 55 × 23 mm.

Individual specimens of the dosimeter can be constructed at the experimental workshops of the Institute of Physics of the Academy of Sciences of the Ukrainian SSR at a cost of about 80-90 rubles.

breaking the language barrier

WITH COVER-TO-COVER ENGLISH TRANSLATIONS OF SOVIET JOURNALS

in mathematics and information science

Title	# of Issues	Subscription Price
Algebra and Logic *Algebra i logika*	6	$120.00
Automation and Remote Control *Avtomatika i telemekhanika*	24	$195.00
Cybernetics *Kibernetika*	6	$125.00
Differential Equations *Differentsial'nye uravneniya*	12	$150.00
Functional Analysis and Its Applications *Funktsional'nyi analiz i ego prilozheniya*	4	$110.00
Journal of Soviet Mathematics	6	$135.00
Mathematical Notes *Matematicheskie zametki*	12 (2 vols./yr. 6 issues ea.)	$185.00
Mathematical Transactions of the Academy of Sciences of the Lithuanian SSR *Litovskii Matematicheskii Sbornik*	4	$150.00
Problems of Information Transmission *Problemy peredachi informatsii*	4	$100.00
Siberian Mathematical Journal of the Academy of Sciences of the USSR Novosibirski *Sibirskii matematicheskii zhurnal*	6	$195.00
Theoretical and Mathematical Physics *Teoreticheskaya i matematicheskaya fizika*	12 (4 vols./yr. 3 issues ea.)	$145.00
Ukrainian Mathematical Journal *Ukrainskii matematicheskii zhurnal*	6	$155.00

Back volumes are available.
For further information, please contact the Publishers.

SEND FOR YOUR FREE EXAMINATION COPIES

PLENUM PUBLISHING CORPORATION
Plenum Press • Consultants Bureau
• IFI/Plenum Data Corporation
227 WEST 17th STREET
NEW YORK, N. Y. 10011

In United Kingdom
Plenum Publishing Co. Ltd., Davis House (4th Floor)
8 Scrubs Lane, Harlesden, NW10 6SE, England

breaking the language barrier

WITH COVER-TO-COVER ENGLISH TRANSLATIONS OF SOVIET JOURNALS

in physics

Title	# of Issues	Subscription Price
Astrophysics *Astrofizika*	4	$100.00
Fluid Dynamics *Izvestiya Akademii Nauk SSSR mekhanika zhidkosti i gaza*	6	$160.00
High-Energy Chemistry *Khimiya vysokikh énergii*	6	$155.00
High Temperature *Teplofizika vysokikh temperatur*	6	$125.00
Journal of Applied Mechanics and Technical Physics *Zhurnal prikladnoi mekhaniki i tekhnicheskoi fiziki*	6	$150.00
Journal of Engineering Physics *Inzhenerno-fizicheskii zhurnal*	12 (2 vols./yr. 6 issues ea.)	$150.00
Magnetohydrodynamics *Magnitnaya gidrodinamika*	4	$100.00
Mathematical Notes *Matematicheskie zametki*	12 (2 vols./yr. 6 issues ea.)	$185.00
Polymer Mechanics *Mekhanika polimerov*	6	$120.00
Radiophysics and Quantum Electronics (Formerly Soviet Radiophysics) *Izvestiya VUZ. radiofizika*	12	$160.00
Solar System Research *Astronomicheskii vestnik*	4	$ 95.00
Soviet Applied Mechanics *Prikladnaya mekhanika*	12	$160.00
Soviet Atomic Energy *Atomnaya énergiya*	12 (2 vols./yr. 6 issues ea.)	$160.00
Soviet Physics Journal *Izvestiya VUZ. fizika*	12	$160.00
Soviet Radiochemistry *Radiokhimiya*	6	$155.00
Theoretical and Mathematical Physics *Teoreticheskaya i matematicheskaya fizika*	12 (4 vols./yr. 3 issues ea.)	$145.00

Back volumes are available. For further information, please contact the Publishers.

SEND FOR YOUR FREE EXAMINATION COPIES

PLENUM PUBLISHING CORPORATION
227 WEST 17th STREET
NEW YORK, N. Y. 10011
Plenum Press • Consultants Bureau
• IFI/Plenum Data Corporation

In United Kingdom
Plenum Publishing Co. Ltd., Davis House (4th Floor)
8 Scrubs Lane, Harlesden, NW10 6SE, England

Declassified and Approved For Release 2013/09/15 : CIA-RDP10-02196R000400010003-7